



Structural inheritance in amagmatic rift basins: Manifestations and mechanisms for how pre-existing structures influence rift-related faults

Anindita Samsu^{a,b,*}, Steven Micklethwaite^c, Jack N. Williams^d, Åke Fagereng^e, Alexander R. Cruden^b

^a Institute of Earth Sciences, University of Lausanne, Lausanne, Switzerland

^b School of Earth, Atmosphere and Environment, Monash University, Melbourne, Australia

^c Sustainable Minerals Institute, University of Queensland, Brisbane, Australia

^d Department of Geology, University of Otago, Dunedin, New Zealand

^e School of Earth and Environmental Sciences, Cardiff University, Cardiff, UK

ARTICLE INFO

Keywords:

Rift basin
Rift-related fault
Structural inheritance
Pre-existing structures
Reactivation
Strain re-orientation
East African Rift System

ABSTRACT

In the context of rift basin formation, structural inheritance describes the influence of pre-existing structures on new rift-related structures, including faults. Pre-existing structures in the crust or upper mantle can determine where rift basins form. As these basins evolve, pre-existing structures in the rocks underneath the newly formed basin can also interact with the far-field strain or stress field, leading to variations in the orientations and kinematics of individual rift-related faults. Given that continental rifts commonly form in pre-deformed lithosphere, structural inheritance is likely to be the norm, not the exception. As such, structural inheritance has implications for reconstructing the paleotectonic history of rifts, investigating seismic hazards, and understanding the fluid transport and storage capabilities of natural fracture systems in the context of geo-energy and ore deposits.

The aim of this review is to provide a framework for recognising the various expressions of structural inheritance and their underlying mechanisms in amagmatic rift basins. We synthesise field and geophysical observations and the results of analogue and numerical models to: (1) demonstrate how different inheritance mechanisms (frictional reactivation vs. local re-orientation of the far-field strain and/or stress) can produce different geometric and kinematic relationships between pre-existing structures and rift-related faults; (2) classify these mechanisms in terms of hard-linked and soft-linked inheritance; and (3) show that different mechanisms can be activated at different depths by the same pre-existing structure. These insights can help us better interpret basement structures under the sedimentary cover of rift basins, which are not often well-imaged in geophysical data, and understand the multi-stage evolution of rift basins worldwide.

1. Introduction

Continental rifts commonly form in lithosphere with a pre-existing structural framework. Given the appropriate stress orientations, stress magnitudes, fluid pressures, and thermal gradients, pre-existing structures affect the development of rifts and rift-related structures (e.g., Wilson, 1966; Morley, 1995; Krabbendam and Barr, 2000; Schumacher, 2002; Chenin and Beaumont, 2013; Fossen et al., 2016; Schiffer et al., 2018, 2020). This **structural inheritance** (referred to as “rejuvenation” by Holdsworth et al., 2001a) operates at multiple scales in both frictional and viscous layers of the crust and in the lithospheric mantle (Fig. 1).

Lithospheric-scale (i.e., plate-scale) weaknesses up to thousands of kilometres in length, such as shear zones, sutures, and plumes or hot spots, span the frictional-viscous transition. These weaknesses can localise or segment entire rift systems, depending on their orientation with respect to the overall rifting direction; the influence of plumes or hot spots also depends on their location with respect to the propagating rift (McConnell, 1972; Daly et al., 1989; Versfelt and Rosendahl, 1989; Wheeler and Karson, 1989; Piqué and Laville, 1996; Doré et al., 1997; Holdsworth et al., 2001a; Miller et al., 2002; Gibson et al., 2013; Molnar et al., 2017; Peace et al., 2018b; Heron et al., 2019; Hopper et al., 2020; Amigo Marx et al., 2022). Lithospheric-scale weaknesses also modulate

* Corresponding author at: Institute of Earth Sciences, University of Lausanne, Lausanne, Switzerland.

E-mail address: anindita.samsu@unil.ch (A. Samsu).

the evolution of the lithosphere and the magmatic budget during rifting, in some cases up to the stages of continental break-up and passive margin development (e.g., Dunbar and Sawyer, 1989; Buiter and Torsvik, 2014; Petersen and Schiffer, 2016; Gouiza and Paton, 2019; Gouiza and Naliboff, 2021; Brune et al., 2023). The most prominent present-day example of plate-scale structural inheritance is the East African Rift System. Here, south of the Main Ethiopian Rift, the rift system bifurcates into western and eastern branches, which are co-located with pre-existing, relatively weak zones around Archean cratons (Fig. 2; structural inheritance in the East African Rift System is discussed in detail in Section 4.3).

At length scales of tens of kilometres or less, pre-existing structures influence the orientations, distributions and growth of basin-bounding and intra-basinal rift-related faults, as well as the geometry and internal architecture of rift basins. For example, reactivated faults or fabrics in the brittle crust may be active during the early basin-forming stage, thereby controlling the location and shape of sediment depocentres (Fig. 3) (e.g., Morley et al., 2004; Deng et al., 2020). Some rift-related faults can be misoriented with respect to inferred plate motion directions, caused by the presence of pre-existing fabrics that strike obliquely to the far-field extensional strain (e.g., Morley et al., 2004; Lyon et al., 2007; Wilson et al., 2010). Complex fault patterns can reflect the evolving interplay between faults that form within locally perturbed stress fields around pre-existing structures, and those that are not influenced by inheritance (Delvaux et al., 2012; Hodge et al., 2018; Muirhead and Kattenhorn, 2018) (Fig. 3a).

These diverse observations of pre-existing structures influencing rift basin formation and faulting suggest that structural inheritance is a common process occurring across multiple length and time scales in rift basin settings. However, regarding the mechanisms by which pre-existing structures define the architecture of basin to sub-basin scale faults, many studies pay particular attention to frictional **reactivation** – defined as frictional sliding occurring along existing planes. Such reactivation occurs in the upper crust and is evident in structures that have accommodated displacement during multiple discrete (i.e., intervals >1 Ma) deformation phases (*sensu* Holdsworth et al., 1997). Previous workers have documented the impact of reactivation of lithological

contacts (Ashby, 2013; Holdsworth et al., 2020; Wedmore et al., 2020a), faults or fault zones formed during previous extensional or contractional events (McCaffrey, 1997; Holdsworth et al., 2001b; Hansen et al., 2011; Lovecchio et al., 2018; Tamas et al., 2022a, 2022b), older rift fabrics (Whipp et al., 2014; Bladon et al., 2015; Duffy et al., 2015; Deng et al., 2017a; Henstra et al., 2019; McHarg et al., 2019; Phillips and McCaffrey, 2019; Deng et al., 2020; Wang et al., 2021b), and metamorphic fabrics within shear zones (Kirkpatrick et al., 2013; Bird et al., 2014; Phillips et al., 2016; Fazlikhani et al., 2017; Kolawole et al., 2018; Peace et al., 2018a; Heilman et al., 2019; Vasconcelos et al., 2019; Wedmore et al., 2020b).

The focus on reactivation has resulted in the common synonymous use of the terms “structural inheritance” and “reactivation”; in some cases, the two terms are used interchangeably (e.g., Corti et al., 2007; Manatschal et al., 2015). “Structural inheritance” is a useful, general, and descriptive term that broadly covers all influences of pre-existing structures on younger geological features. However, reducing structural inheritance to reactivation in the context of rift basins research is problematic, as it does not acknowledge other mechanisms by which pre-existing structures influence rift-related deformation. It also suggests that there is limited or no influence of pre-existing structures in areas with no evidence of reactivation (as defined by Holdsworth et al., 1997).

A number of field and modelling studies point to the re-orientation of strain (Corti et al., 2013b; Philippon et al., 2015; Hodge et al., 2018; Samsu et al., 2021) and stress (Bell, 1996; Morley, 2010; Tingay et al., 2010a) as mechanisms of structural inheritance that are distinct from reactivation. Through strain or stress re-orientation, pre-existing structures can influence deformation localisation and distribution without exhibiting significant (i.e., observable) signs of repeated slip or displacement on the pre-existing structures themselves. These mechanisms, which are more subtle than reactivation, may be more common in rift basins than the existing body of literature on structural inheritance suggests.

By distinguishing between structural inheritance mechanisms, we can better infer the different implications that they have for the kinematics and connectivity of rift-related faults. For example, consider pre-

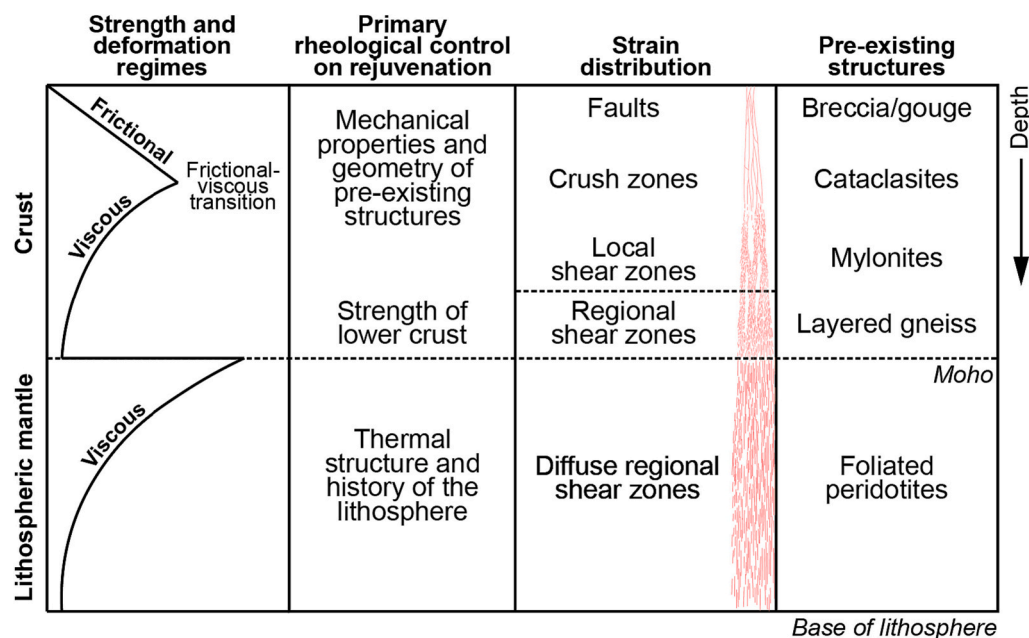


Fig. 1. Schematic strength profile of the “typical” continental lithosphere, including the frictional-viscous transition, as well as the primary rheological controls on “rejuvenation” (i.e., structural inheritance), strain distribution, and types of rocks or fabrics that act as pre-existing structures at different lithospheric depths. Modified after Sibson (1977) and Holdsworth et al. (2001a, 2001b).

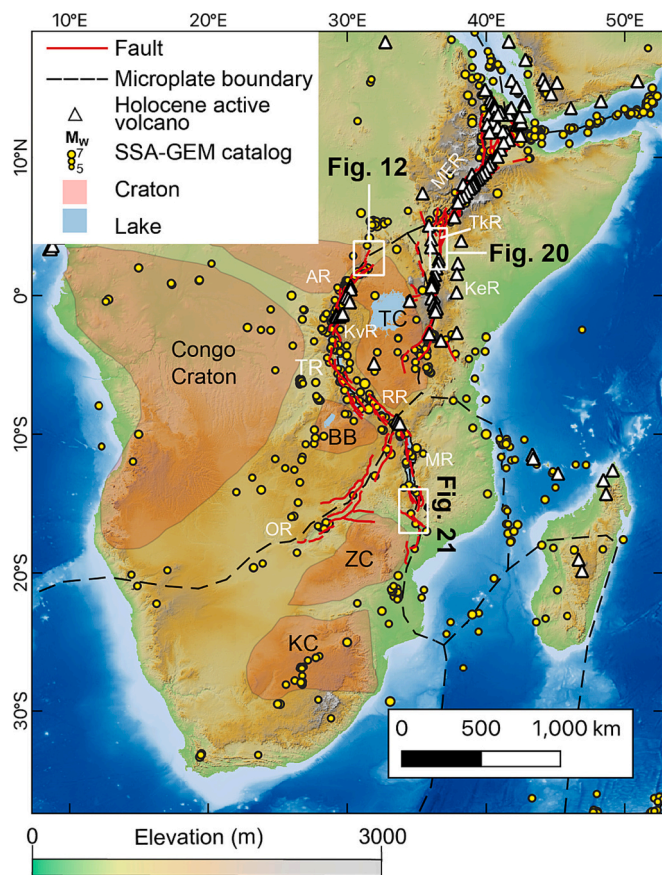


Fig. 2. Map of plate-scale structural inheritance in the East African Rift System showing the distribution of active faults (Hodge et al., 2018; Daly et al., 2020; Styron and Pagani, 2020), microplate boundaries (Stamps et al., 2021; Wedmore et al., 2021), Holocene volcanoes (Global Volcanism Project, 2013), earthquakes ($M_w \geq 5$, 1875–2015 from the Sub-Saharan Africa Global Earthquake Model (SSA-GEM) catalogue; Poggi et al., 2017), and the locations of Archean-Paleoproterozoic cratons (Van Hinsbergen et al., 2011). MER, Main Ethiopian Rift; TkR, Turkana Rift; KeR, Kenya Rift; AR, Albertine Rift; KvR, Kivu Rift; TR, Tanganyika Rift; RR, Rukwa Rift; MR, Malawi Rift; OR, Okavango Rift; TC, Tanzanian Craton; BB, Bangweulu Block; ZC, Zimbabwe Craton; KC, Kaapvaal Craton. Underlain by GTOPO30 Digital Elevation Model (DEM).

existing structures at mid- to lower-crustal depths (such as shear zones) that strike obliquely to the regional extension direction. When these pre-existing structures are reactivated, they normally experience oblique slip and can be hard-linked to younger, overlying, rift-related faults that are influenced by them (Fig. 4a). However, a pre-existing mid- to lower crustal structure that does not experience significant reactivation can still re-orient the local extension direction, without necessarily being hard-linked to the younger rift-related faults (Fig. 4b).

A more complete picture of different inheritance mechanisms at the basin to sub-basin scale can help to clarify the mechanical controls on basin evolution and open opportunities to: (i) uncover the characteristics of buried structures that are commonly poorly resolved in geophysical surveys; (ii) better understand the structural evolution of basins at rifted margins; and (iii) provide additional constraints on plate reconstructions. Understanding the potential effect of pre-existing structures on younger fault networks also has implications for seismic hazards assessment (e.g., Fonseca, 1988; Wedmore et al., 2020b; Hecker et al., 2021), geothermal energy (e.g., Schumacher, 2002; Bertrand et al., 2018; Dávalos-Elizondo and Laó-Dávila, 2023), mineral exploration (e.g., Rowland and Sibson, 2004), and CO₂ and spent nuclear fuel storage (e.g., Barton and Zoback, 1994; Andrés et al., 2016).

2. Scope and terminology

In this review, we summarise the multifaceted ways in which pre-existing structures control fault system geometry during rift basin formation in magma-poor rifts. **Pre-existing structures** refer to structures that already existed prior to the current rifting event. In the context of this review, we consider the crust to be rheologically layered with a thermally controlled transition that separates an upper frictional and lower viscous regime (*sensu* Handy et al., 2007; Fig. 1). Hence, pre-existing structures will include discrete discontinuities (e.g., the contact between a dyke and surrounding host rock, Table 1a; a fault or fault zone, Table 1b; the boundary between two rheologically distinct terranes, Table 1e), pervasive strength anisotropies (e.g., penetrative metamorphic or rift fabrics from previous collisional or extensional events, Table 1c and d), and lithospheric-scale weaknesses in the viscous lower crust or lithospheric mantle (Table 1f and g). The influence of these different types and scales of pre-existing structures is discussed in Section 3.1. In a few cases, we specifically discuss the influence of pre-existing “basement” structures on rift-related faults in the sedimentary “cover” (e.g., case studies on the influence of pre-existing intra-basement shear zones on rift faults; Section 3). Here we refer to **basement** as an assemblage of igneous or metamorphic rocks directly underlying the sedimentary cover; this terminology is commonly used in the petroleum and geothermal energy industries. The sedimentary **cover** is defined as basin fill related to the current rifting event (or earlier rifting events in the context of multiphase rifts).

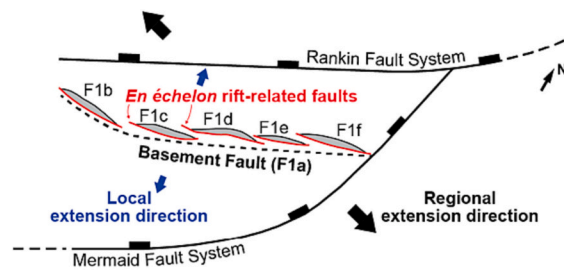
We explore mechanisms that lead to “misorientation” of rift-related faults at the basin to sub-basin scale, which can vary depending on the characteristics of the pre-existing structures (e.g., orientation, geometry, size, and rheology). Here, the term **misorientation** is used to contrast the orientation of a rift-related fault to that of an “optimally oriented” normal fault formed under Andersonian fault mechanics (Anderson, 1905; Section 3.4). In the context of this contribution, an optimally oriented fault is one that strikes orthogonal to the regional extension direction and has a moderate dip. An example of a misoriented fault, which strikes obliquely to the far-field extension direction due to an underlying pre-existing weakness, is illustrated in Fig. 4.

Pre-existing structures that are moderately dipping and orthogonal to the regional extension direction (i.e., optimally oriented) can influence fault growth (Section 3.1.5). However, it is difficult to evaluate if a rift-related fault has been influenced by structural inheritance in these cases, as the fault could have formed in that orientation in the absence of a pre-existing structure (Smith and Mosley, 1993). By the same argument, structural inheritance from optimally oriented structures should not lead to marked variations in fault geometry relative to faulting of intact crust. Hence, we mainly consider pre-existing structures that are “oblique” (with respect to the far-field extension direction) and/or gently or steeply dipping.

In this review, we focus on the development of rift basins dominated by faulting rather than magmatic structures. Although spatial links between continental breakup and major flood basalt provinces have been recognised for several decades (e.g., Morgan, 1971; Courtillot et al., 1999), requiring some interplay between rifting and magmatism, it varies between case studies whether magmatism controls or is controlled by the structure of the rift. For example, some recent volcanic structures in the East African Rift System in Ethiopia are aligned with pre-existing structures that are oblique to the rift axis (Lloyd et al., 2018; Franceschini et al., 2020), implying that magma transport was controlled by inherited structures. In those examples, and in most other examples reviewed by Buiter and Torsvik (2014), rifting starts before magmatism, and magmatic activity is regionally focussed within thinned lithosphere, and locally controlled by a combination of new and inherited structures. Although we recognise that magmatism can modulate the occurrence and timing of reactivation of pre-existing structures (e.g., Muirhead and Kattenhorn, 2018), we focus here on the development of rift basins and rift structures prior to any important

a Influence of pre-existing basement fault on rift-related faults & sediment depocentres (Deng et al., 2020)

Stage 1: Reactivation of basement fault



Stage 2: Continued reactivation of basement fault & formation of new faults

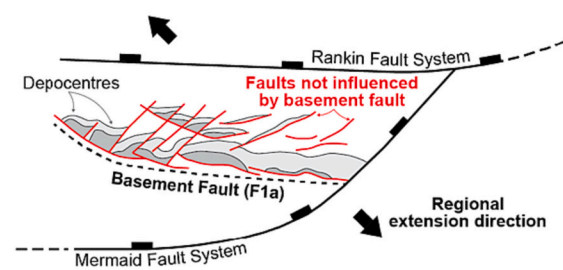
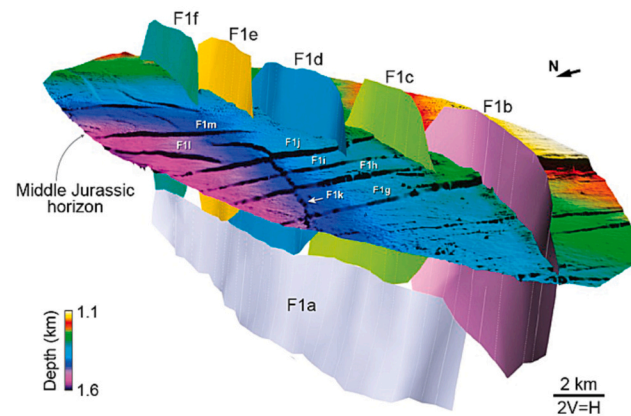
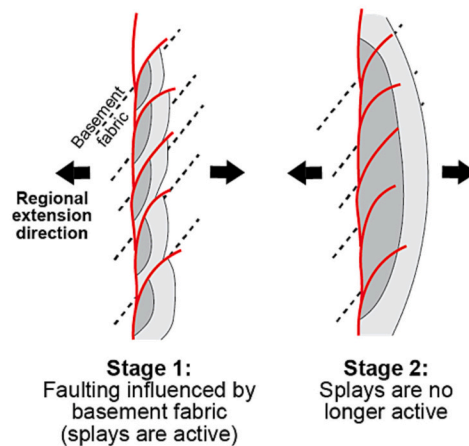
**b Linkage between basement fault & en échelon faults 3D visualisation of faults (Deng et al., 2020)****c Faults influenced by penetrative basement fabric (Morley et al., 2004)**

Fig. 3. Basin to sub-basin scale examples of pre-existing faults influencing rift-related faulting and the formation of sediment depocentres. (a) In the Dampier Sub-basin (NW Shelf of Australia), reactivation of a pre-existing basement fault (F1a) led to the formation of rift-related faults in the overlying cover, with an *en échelon* arrangement in map view. As rifting progressed, reactivation of the pre-existing fault continued, but a new set of faults formed in the cover, with strikes that are orthogonal to the regional extension direction. (b) 3D visualization of faults in (a) at the Middle Jurassic level, interpreted from seismic reflection data. Faults F1b-f may be linked to the reactivated basement fault F1a at depth. (c) Schematic illustration of penetrative basement fabrics that are reactivated at the early stage of rifting and later become less active, based on observations from Suphan Buri and South Pattani basins (Thailand). (a-b) modified from Deng et al. (2020), (c) modified from Morley et al. (2004).

effects that may be related to magmatic activity. We speculate that the structural associations identified in this review may become conduits for future rift-related magmatism, but an in-depth discussion of this topic is beyond the scope of the present contribution.

3. Examples and insights from nature and models

In this section, we summarise the spatial, geometric, and kinematic relationships between pre-existing structures and rift-related cover faults, based on observations from geophysical data and outcrops. Analogue and numerical models allow us to study rift and basin-forming processes over geological timescales in 2D and 3D, complementing observations from natural rifts (e.g., Allemand and Brun, 1991; Brun, 1999; Corti, 2012; Brune et al., 2017; Molnar et al., 2020; Maestrelli et al., 2022; Zwaan and Schreurs, 2022). Modelling also gives us the flexibility to examine the influence of various model parameters both separately (e.g., rheological layering, obliquity, geometry of inherited weakness) and together (Zwaan et al., 2016, 2021a, 2021b; Zwaan and Schreurs, 2017). The modelling approach is especially useful for distinguishing between the relative contributions of oblique rift kinematics and inherited structures in shaping rift basins, as each on its own can create a transtensional system, resulting in rift-related faults that are oblique to the inferred paleo-extension direction.

The models we discuss here demonstrate inheritance-driven

obliquity, where the model includes pre-existing weaknesses that strike obliquely to the bulk extension direction. This setup is distinct from boundary-driven obliquity, where bulk extension is oblique to the model boundaries (e.g., Tron and Brun, 1991; Keep and McClay, 1997; Autin et al., 2010). Most of the analogue models we highlight are simplified, multi-layer, crustal or lithospheric-scale experiments comprising a brittle upper crust, ductile lower crust, and in some examples a ductile lithospheric mantle. In this case, “ductile” is defined as exhibiting spatially continuous deformation at the scale of observation, and the ductile materials simulate deformation in the viscous layers of the lithosphere, although the rheology may be different (Wang, 2021). Pre-existing structures in analogue models are implemented as two rheologically distinct blocks, discrete weak zones, or pervasive anisotropy (see Table 2 for an overview). Based on these models, we discuss the impact of lithospheric or crustal strength variations and inherited weaknesses – with different strike orientations – on deformation localisation, deformation partitioning, and the local 3D strain field.

3.1. Recognising inheritance: Spatial and geometric relationships between pre-existing structures and rift-related faults

3.1.1. Map view relationships

Structural inheritance in rift basins is typically recognised through two observations in map view: “spatial co-location” and “geometric

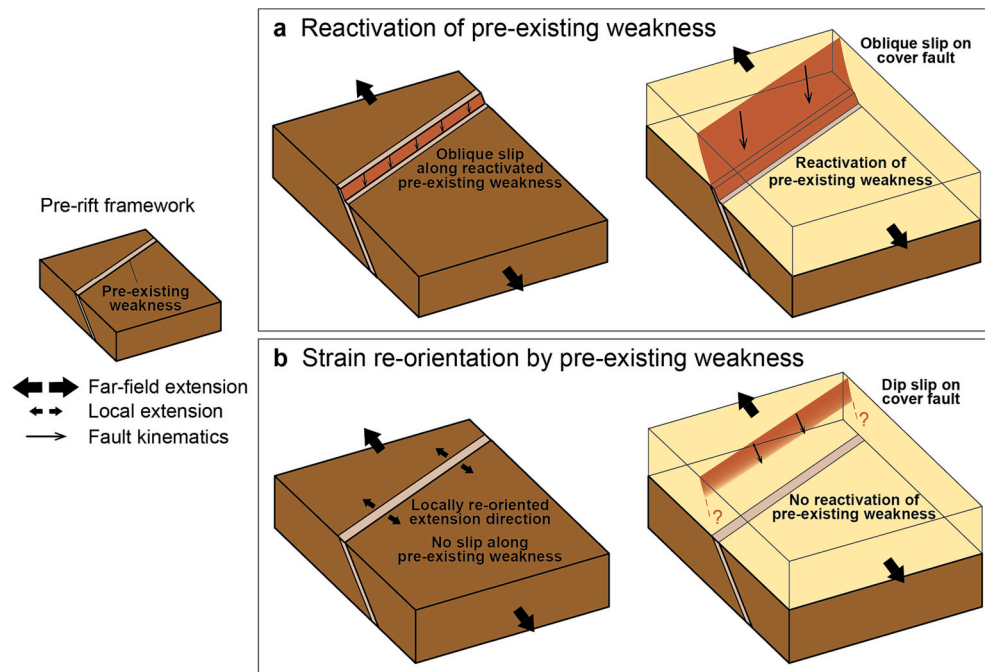


Fig. 4. A pre-existing weakness that strikes obliquely to the far-field extension direction can influence the orientation and kinematics of a rift-related, normal fault; as result of this interaction, the rift-related fault is “misoriented” with respect to the far-field extension direction. Different inheritance mechanisms can have different impacts on fault kinematics and linkage between the rift-related fault and pre-existing weakness, despite the two exhibiting geometric similarity in map view in both scenarios. Reactivation of the pre-existing weakness (a) is commonly associated with oblique slip along the pre-existing weakness and rift-related fault (e.g., Morley, 1995; Corti et al., 2007), in addition to hard linkage between the two structures (Phillips et al., 2016). A second mechanism through which the pre-existing weakness can influence rift-related faulting is local re-orientation of the far-field strain (b), which may result in dip-slip kinematics along the rift-related fault (Corti et al., 2013b; Philippon et al., 2015).

similarity” between rift-related faults and pre-existing structures (Fig. 5) (e.g., Laó-Dávila et al., 2015; Fazlikhani et al., 2017; Dawson et al., 2018; Collanega et al., 2019; Wedmore et al., 2020b; Bosworth and Tari, 2021). **Spatial co-location** refers to the occurrence of rift-related faults above or in the vicinity of a pre-existing structure. **Geometric similarity** (*sensu* Holdsworth et al., 1997) is characterised, in map view or cross-section, by rift-related fault traces that trend parallel to pre-existing structures; or, more rigorously in 3D, by rift-related faults that have the same strike and dip directions as pre-existing structures (Fig. 6a and b).

A growing body of work provides compelling evidence that rift-related deformation in the active East African Rift System broadly follows Proterozoic age structures, with some younger rift basins also co-locating with basins that formed during a previous Mesozoic rifting event (e.g., McConnell, 1967; Versfelt and Rosendahl, 1989; Castaing, 1991; Kolawole et al., 2021a; Wedmore et al., 2022). The multi-scale impacts of structural inheritance on rift-related structures in the East African Rift System is discussed in detail in Section 4.3. Below we highlight several other geographic areas in which structural inheritance has been recognised through the spatial co-location and geometric similarity between pre-existing structures (e.g., crustal shear zones) and rift-related faults (see Table 1 for more examples):

- **New Zealand:** The strike of the Terrane Boundary Fault in the Great South Basin (offshore South Island), which formed during Late Cretaceous extension (i.e., Gondwana break-up), is parallel to the Devonian–Cretaceous Terrane Boundary Shear Zone (Mortimer, 2004) that separates the Median Batholith and Western Province terranes. Seismic reflection data show that the Terrane Boundary Fault links with the crustal-scale (or potentially lithospheric-scale; e.g., Muir et al., 2000; Mortimer et al., 2002) Terrane Boundary Shear Zone at depth (Phillips and McCaffrey, 2019) (Fig. 7). Farther north in the Taranaki Basin (offshore North Island), the Terrane Boundary

Shear Zone and an adjacent boundary between the Median Batholith and Eastern Province terranes coincide spatially with the traces of the Cenozoic Cape Egmont and Taranaki fault systems (Muir et al., 2000).

- **North Atlantic:** The Lærdal-Gjende fault system is co-located and hard-linked with the Devonian Hardangerfjord Shear Zone, which is associated with a major Moho offset (Færseth et al., 1995; Fossen and Hurich, 2005; Fossen et al., 2014) (Fig. 8). Similarly, Permo-Triassic basin-bounding rift faults offshore the north coast of mainland Scotland exhibit geometric similarity with deep crustal reflectors in the underlying crystalline basement (Wilson et al., 2010 and references therein).
- **Northeastern Brazil, south Atlantic:** From aerial imagery and in the field, Kirkpatrick et al. (2013) and Vasconcelos et al. (2019) observed km-scale traces of Mesozoic rift faults, which trend parallel to Precambrian Brasiliano shear zones and crustal-scale anomalies interpreted from magnetic and gravity data.

Plate-scale structural inheritance (also known as **tectonic inheritance**; Wilson, 1966; Thomas, 2006; Audet and Bürgmann, 2011; Buiter and Torsvik, 2014; Petersen and Schiffer, 2016) is demonstrated by the spatial co-location of younger rift systems with pre-existing crustal or lithospheric-scale weaknesses (Fig. 2). While not the focus of this review, tectonic inheritance exerts a first-order control on where rifts – and therefore rift basins and rift-related faults – form in the first place. Rift initiation and propagation exploits pre-existing mechanical (including thermal) weaknesses, so that rifts commonly follow the trends of older rifts and/or highly deformed orogenic belts at craton boundaries (Table 1f). For example, most Phanerozoic rift basins in Africa are located within Proterozoic orogenic belts that may be linked to deep-seated weaknesses in the lithospheric mantle (Daly et al., 1989; Versfelt and Rosendahl, 1989; Tommasi and Vauchez, 2001; Table 1g).

Table 1
Various types and scales of pre-existing structures, their influence on younger rifts and rift structures, and examples of where such interactions occur.

Pre-existing feature	Scale	Mechanism	Observation(s)	Examples
<i>Rheological boundary (crustal-scale)</i>				
a Dyke-host rock contact	Meters	Reactivation	Geometric similarity	Lower Shire Graben, southern Malawi Rift (Wedmore et al., 2020b); NW Scotland (Holdsworth et al., 2020)
<i>Discrete structure or fabric</i>				
b Fault or cemented fault zone	Meters	Reactivation Stress perturbation	Geometric similarity Local stress re-orientation near pre-existing structure	North Sea Rift (Deng et al., 2017a); Colorado Basin, offshore Argentina (Lovecchio et al., 2018) North Sea Rift (Bell, 1996; Yale, 2003)
<i>Pervasive strength anisotropy</i>				
c Metamorphic foliation within shear zone	10s of km	Stress perturbation Reactivation	Complex fault pattern due to 3D transtensional strain Geometric similarity	North Sea Rift (Reeve et al., 2015; Osagiede et al., 2020); East African Rift (Morley, 2010 and references therein) Northern Thailand (Morley et al., 2004); North Sea Rift (Færseth et al., 1995; Phillips et al., 2016; Fazlikhani et al., 2017); offshore New Zealand (Muir et al., 2000; Collanega et al., 2019; Phillips and McCaffrey, 2019); onshore New Zealand (Villamor et al., 2017); East African Rift System (Laó-Dávila et al., 2015; Dawson et al., 2018); East Greenland Rift System (Rotevatn et al., 2018); onshore and offshore Norway (Fossen and Hurich, 2005; Fossen et al., 2014; Fossen et al., 2016)
d Rift fabric	10s of km	Reactivation	Normal fault sets with strikes that are oblique to each other	Barmer Basin, NW India (Bladon et al., 2015); Horda Platform, North Sea (Whipp et al., 2014; Duffy et al., 2015); Bohai Bay Basin, eastern China (Wang et al., 2021b); Great South Basin, offshore New Zealand (Phillips and McCaffrey, 2019); Northern Carnarvon Basin, Western Australia (McHarg et al., 2019); NW Shelf of Australia (Deng et al., 2020)
<i>Rheological boundary (lithospheric-scale)</i>				
e Terrane boundary	10s of km	Barrier to fault propagation	Splaying of fault as it propagates towards stronger crustal block	Great South Basin, offshore New Zealand (Phillips and McCaffrey, 2019); Sudan Rift System (Daly et al., 1989)
<i>Lithospheric weakness</i>				
f Orogenic structures, including shear zones (i.e., terrane boundary, suture zone, orogenic belt, mobile belt); pre-existing rifts	10s–1000s of km	Strain localisation	Rift localisation along pre-existing weakness; rift segmentation when pre-existing weakness is at a high angle to regional extension direction	North Atlantic (Wilson, 1966; Piqué and Laville, 1996; Doré et al., 1997; Buitter and Torsvik, 2014; Petersen and Schiffer, 2016; Schiffer et al., 2018, 2020); South Atlantic (Krabbendam and Barr, 2000); East African Rift System (McConnell, 1972; Daly et al., 1989; Versfelt and Rosendahl, 1989; Wheeler and Karson, 1989; Smith and Mosley, 1993; Ring, 1994; Theunissen et al., 1996; Morley, 2010; Kolawole et al., 2018; Muirhead and Kattenhorn, 2018; Wedmore et al., 2020a); Gondwana break-up along Pan African mobile belts (Sykes, 1978); Karoo Rift Basins (Daly et al., 1989); Baikal Rift (Petit et al., 1996); West Greenland Rift System (Heron et al., 2019); offshore southern Norway (Færseth et al., 1995; Phillips et al., 2016); onshore New Zealand (Rowland and Sibson, 2004); offshore New Zealand (Muir et al., 2000; Mortimer et al., 2002; Phillips and McCaffrey, 2019); Australian Southern Margin (Miller et al., 2002; Gibson et al., 2013)
g Pervasive anisotropic crystalline fabric within lithospheric mantle	10s–1000s of km	Strain localisation	Rift localisation	North, Central & South Atlantic (Vauchez et al., 1997; Tommasi and Vauchez, 2001)

Table 2

Various ways in which natural pre-existing crustal and mantle/lithospheric heterogeneities are implemented in analogue models. Several numerical modelling studies, in which the impacts of similar types of heterogeneities were investigated, are referenced in the last column. “Discrete” and “pervasive” denote the distribution of the heterogeneities at the scale of the model.

Relevance to natural feature	Influence on deformation	Implementation in analogue model	Reference(s)	Comparable numerical models
Crustal heterogeneity (discrete)				
Fault or fault zone in upper crust Shear zone in upper crust	Fault orientation & kinematics Fault orientation & kinematics	Zone of dilation in granular layer Ductile weak zone in granular layer Cylindrical PDMS seeds at granular-ductile layer interface	Corti et al. (2007) Brun and Tron (1993); Osagiede et al. (2021) Zwaan et al. (2016, 2020, 2021a, 2021b); Molnar et al. (2019, 2020)	Deng et al. (2017b, 2018)
Shear zone in lower crust	Fault orientation & kinematics; transfer zone width & orientation	Ductile weak zone in ductile layer Velocity discontinuity (rigid basal plates) Velocity discontinuity (rigid basal plate or plastic sheet separated by rubber sheet)	Sokoutis et al. (2007); Corti (2004, 2008); Corti et al. (2013b) Acocella et al. (1999) Withjack and Jamison (1986); McClay and White (1995); Wang et al. (2021a)	
Pre-existing rift (thinned crust & strong lithospheric mantle) Two rheologically distinct blocks	Orientation & distribution of linkage structures between rift segments Fault spacing & propagation	Thin granular upper crust and ductile lower crust layers Adjacent blocks with different ductile layer viscosities or thicknesses	Brune et al. (2017) Corti et al. (2013a); Beniest et al. (2018); Samsu et al. (2021)	Brune et al. (2017) Phillips et al. (2023)
Crustal heterogeneity (pervasive)				
Fabric in upper crust	Fault orientation, length & kinematics	Zone of dilation in granular layer Brushed plaster at model base underneath granular layer Pre-existing rift fabric from first rift phase in a two-phase rifting experiment	Bellahsen and Daniel (2005) Chattopadhyay and Chakra (2013); Ghosh et al. (2020) Henza et al. (2010, 2011); Wang et al. (2021a)	
Fabric in ductile crust	Fault spacing, orientation, kinematics & propagation	Laterally alternating weak/normal zones in ductile layer	Samsu et al. (2021)	
Mantle heterogeneity (discrete)				
Shear zone in lithospheric mantle, terrane boundary, suture zone, orogenic belt, or thermally weakened zone in lithospheric mantle	Strain (rift) localisation; border fault orientation, length & kinematics; basin asymmetry & subsidence	Velocity discontinuity (basal plastic sheet) Weak zone in lithosphere/lithospheric mantle	Tron and Brun (1991); Brun and Tron (1993); Michon and Merle (2000); Michon and Sokoutis (2005); Corti et al. (2007); Zwaan et al. (2021a, 2021b) Agostini et al. (2009); Molnar et al. (2017, 2018, 2019)	Tommasi et al. (2009); Tommasi and Vauchez (2015); Petersen and Schiffer (2016)
Pre-existing rift basin	Barrier to fault propagation; fault localisation at edges	Strong zone in lithosphere/lithospheric mantle	Autin et al. (2013)	

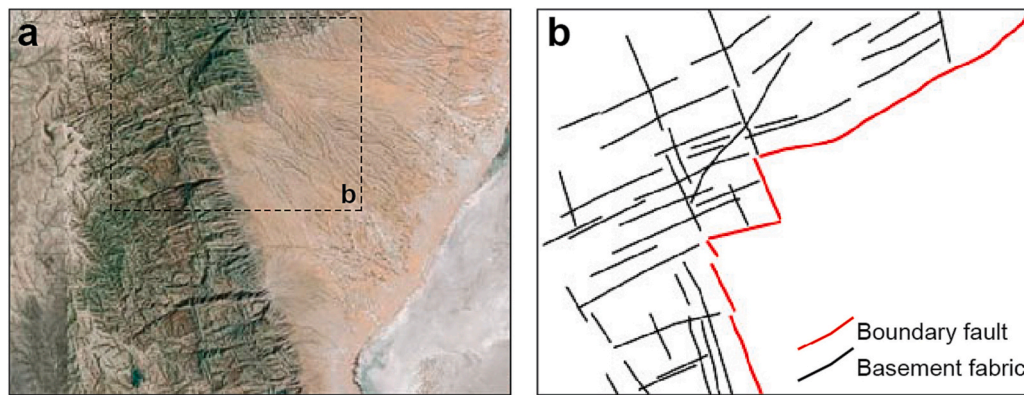


Fig. 5. Example of map-view spatial co-location and geometric similarity between pre-existing fabrics and basin-bounding, rift-related faults in the Chew Bahir Basin, southern Ethiopia. This interaction resulted in an angular or zigzag fault pattern. (a) Satellite image and (b) traces of faults and basement fabrics from Corti (2009). A similar zigzag fault pattern has been observed in other parts of the EARS (e.g., Lake Tanganyika, Lezzar et al., 2002; Malawi Rift, Hodge et al., 2018).

3.1.2. Cross sectional relationships

Geophysical data can provide insight into the geometric relationships between pre-existing structures and rift-related faults at depth, complementing map view observations. Phillips et al. (2016) illustrated three types of two-dimensional (2D) cross-sectional relationships between a pre-existing structure and younger, rift-related faults – “exploitative, merging, and cross-cutting” relationships – based on seismic reflection data from offshore southern Norway (Fig. 6). These relationships were identified from pre-existing, basement weaknesses (i.e., shear zones) and rift-related faults that have the same strike and dip direction. They used kinematic analyses of mapped faults to determine the history of fault activity and infer whether pre-existing shear zones were reactivated as the younger faults formed.

Phillips et al. (2016) showed that an **exploitative** relationship is characterised by a throughgoing structure that links a pre-existing structure and rift-related fault. Based on the physical linkage between shear zone-internal reflectors and younger rift-related faults, they inferred that the rift-related faults initiated in relatively weak mylonitic rocks (within broader shear zones) and propagated upwards into the sedimentary cover. A similar observation of such an exploitative relationship was made by Collanega et al. (2019) in the Taranaki Basin (offshore North Island, New Zealand), except that it was the damage zone above a pre-existing fault that was reactivated. These two case studies suggest that reactivation (of a discrete, pre-existing structure) is the underlying mechanism behind an exploitative relationship between a pre-existing structure and rift-related fault (Fig. 6a).

Merging and cross-cutting relationships (Fig. 6b) differ from an exploitative relationship in that the rift-related fault nucleates above the pre-existing structure and propagates downwards until they intersect. In a **merging relationship**, the rift-related fault nucleates within the hanging wall of the basement structure and – because of its steeper dip – merges at depth with the more gently dipping basement structure (Phillips et al., 2016). In a **cross-cutting relationship**, the rift-related fault may inherit the strike and dip direction of the basement structure but offsets it at depth. For example, the Mesozoic rift-related Dombjerg Fault (East Greenland Rift System) locally strikes parallel to the more gently dipping Caledonian Kildedalen Shear Zone but offsets it farther down-dip (Rotevatn et al., 2018). Phillips et al. (2016) attribute merging and cross-cutting relationships to strain re-orientation by a pre-existing basement structure that has been reactivated (Fig. 6b).

3.1.3. Subtle indicators of inheritance impacting fault orientation

The influence of basement heterogeneities has also been invoked in areas where geometric similarity is not observed, but instead: (i) the strikes of coeval normal faults vary within a relatively small area (on the order of several km) (e.g., Morley, 2010; Reeve et al., 2015) (Fig. 9), (ii) normal fault strikes are oblique to the strikes of basement structures and

not perpendicular to the inferred regional extension direction (Fig. 6c and Fig. 10) (Samsu et al., 2019), and/or (iii) fault strikes vary across areas that overlie different basement terranes (see Fig. 2 in Wilson et al., 2010). In the absence of evidence of reactivation, which is normally inferred from geometric similarity and other kinematic or chronostratigraphic indicators (Holdsworth et al., 1997), variable rift fault strikes that are oblique to pre-existing structures may indicate the subtle influence of basement rocks with fabrics that are oblique to far-field rifting directions.

In the brittle part of the crust, local perturbations of the regional stress field can be attributed to lateral variations in the elastic properties of rocks (Bell, 1996 and references therein). Deviation from the far-field or regional stress trajectories occurs because the principal stresses are deflected when they cross an interface between two materials with contrasting elastic properties (e.g., Zhang et al., 1994; Morley, 2010; Zang and Stephansson, 2010) (Fig. 11). Stress perturbations around a pre-existing weakness or discontinuity (e.g., a fault or damage zone) have been observed in photoelastic, numerical, and rock deformation experiments. In the field, they are reflected by curving of joints near a pre-existing fault (Cruikshank and Aydin, 1995; Muirhead and Kattenhorn, 2018; Samsu et al., 2020) or variable strain axes and kinematics of secondary, smaller-scale fault populations around a larger fault (Riller et al., 2017; Maerten et al., 2002).

We can invoke basement influence on rift-related faults in the overlying cover by considering stress coupling between the two units. Bell (1993, 1996) proposed that stress orientations in a sedimentary unit can “exhibit the signature” of underlying rocks, if there is no intervening weak unit that acts as a mechanical detachment. He refers to this coupled system as an “attached stress regime” (Fig. 11c) and draws on an example from the Labrador Shelf (offshore eastern Canada), where the in-situ maximum horizontal stress measured from borehole breakouts is similarly oriented to the focal mechanism P-axis of a 1971 earthquake with an epicentre located in the basement. In an attached stress regime, we can infer that any deflection or deviation of the far-field stress within the basement rocks would be transferred onto the directly overlying sedimentary unit(s) and accommodated by new brittle structures (i.e., faults and other fractures) during rifting. Such mediation of stresses from basement to cover is apparent in the Lake Rukwa area of the East African Rift System. Here, Morley (2010) suggested that the NW-SE trending Precambrian basement foliation has locally rotated the regionally dominant N-S maximum horizontal stress, resulting in similar NW-SE trends for the present-day maximum horizontal stress direction (Delvaux and Barth, 2010; Delvaux et al., 2012) and Cenozoic rift-related faults. In contrast, where a mechanically weak unit (e.g., shale-dominated unit, salt, or low-angle fault) is present between basement and cover rocks, the in-situ maximum horizontal stresses tend to show more variable orientations (“detached stress regime” in

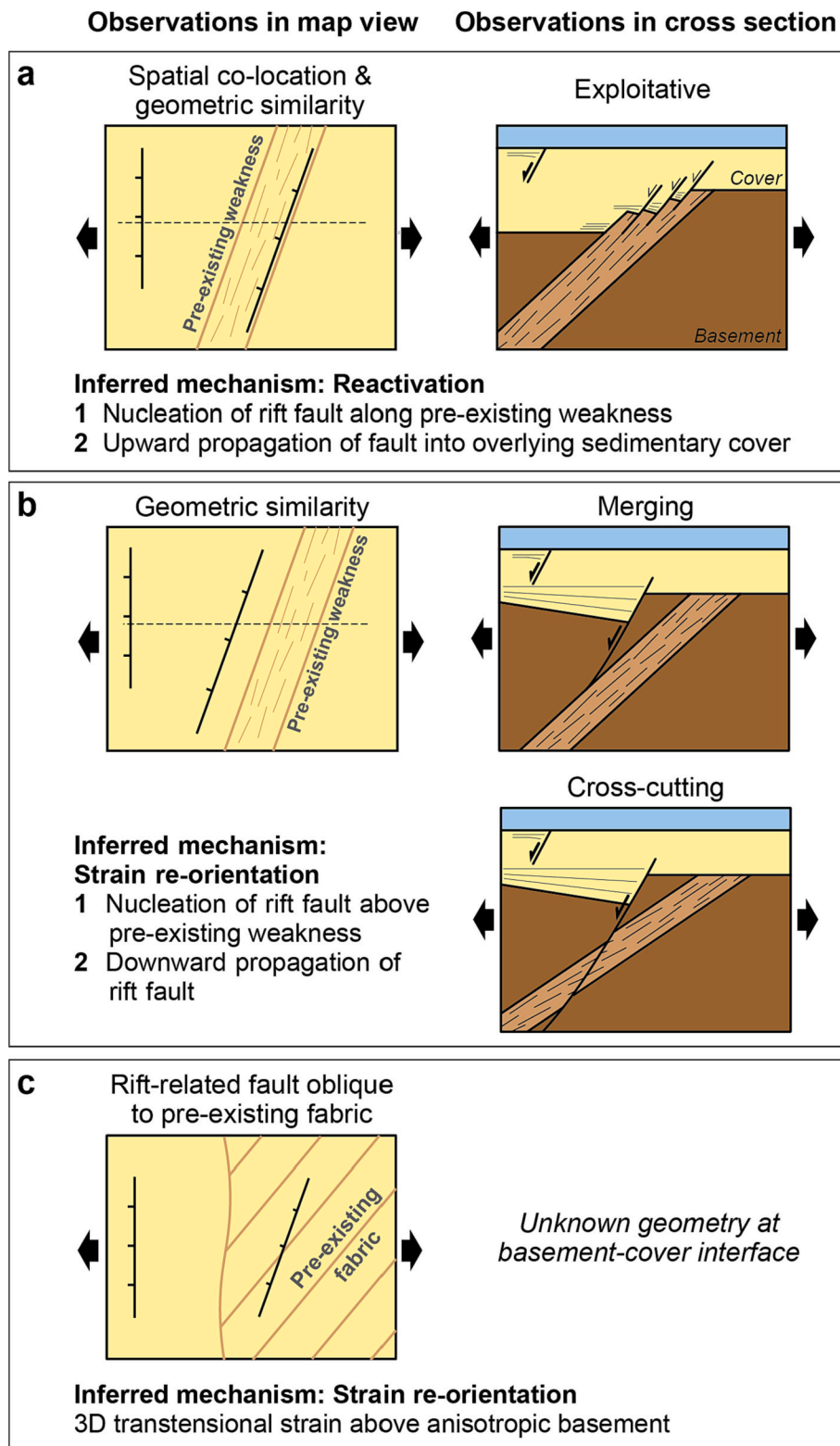


Fig. 6. Geometric relationships between pre-existing structures and overlying rift-related normal faults in map view and cross section (exploitative, merging, and cross-cutting relationships after Phillips et al., 2016). The inferred inheritance mechanisms behind these relationships are reactivation (a) and strain re-orientation (b and c). Thick arrows indicate the inferred regional extension direction during rifting.

Fig. 11c).

3.1.4. Basement strength variations impacting fault propagation and distribution

Lateral variations in the strength of basement rocks control the

propagation and distribution of rift-related normal faults. For example, the NW-trending Southern Sudan Rift terminates abruptly against the NE-trending Central African fault zone, which follows the trace of the steep Late Proterozoic Fouban Shear Zone (Daly et al., 1989). Farther south, the northern tip of the western branch of the East African Rift

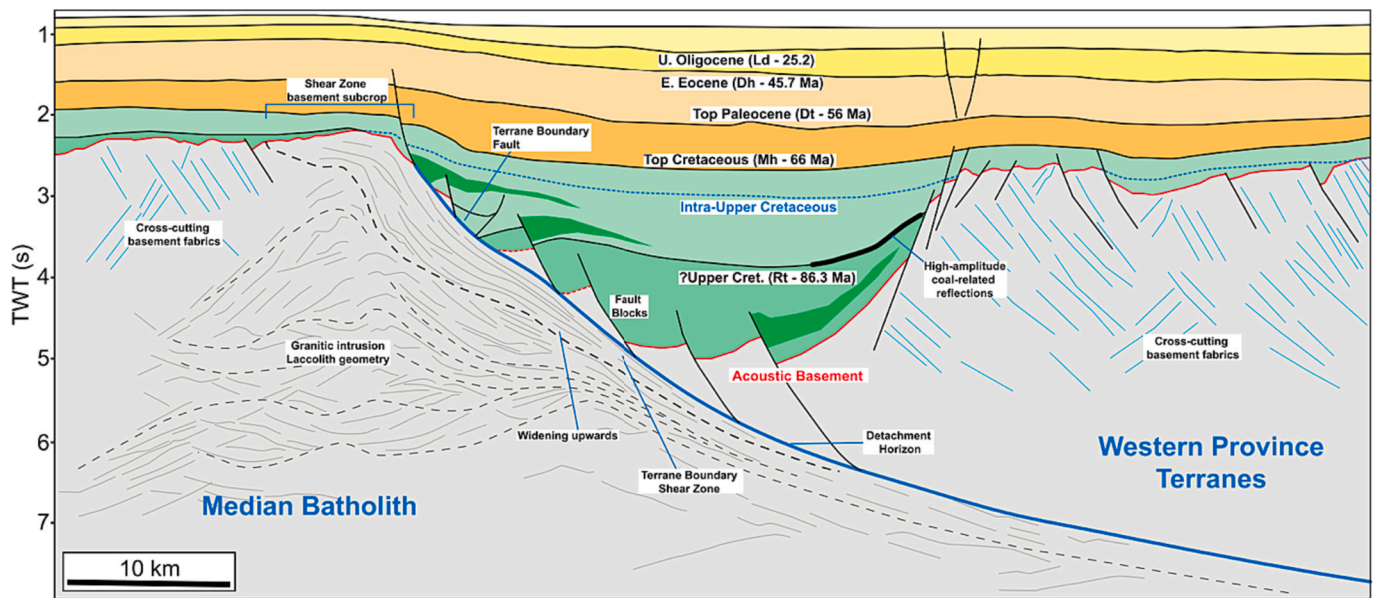


Fig. 7. Interpreted seismic reflection profile across the Great South Basin, offshore South Island of New Zealand (from Phillips and McCaffrey, 2019), showing hard linkage between the pre-existing, Devonian–Cretaceous Terrane Boundary Shear Zone and the Late Cretaceous, basin-bounding Terrane Boundary Fault.

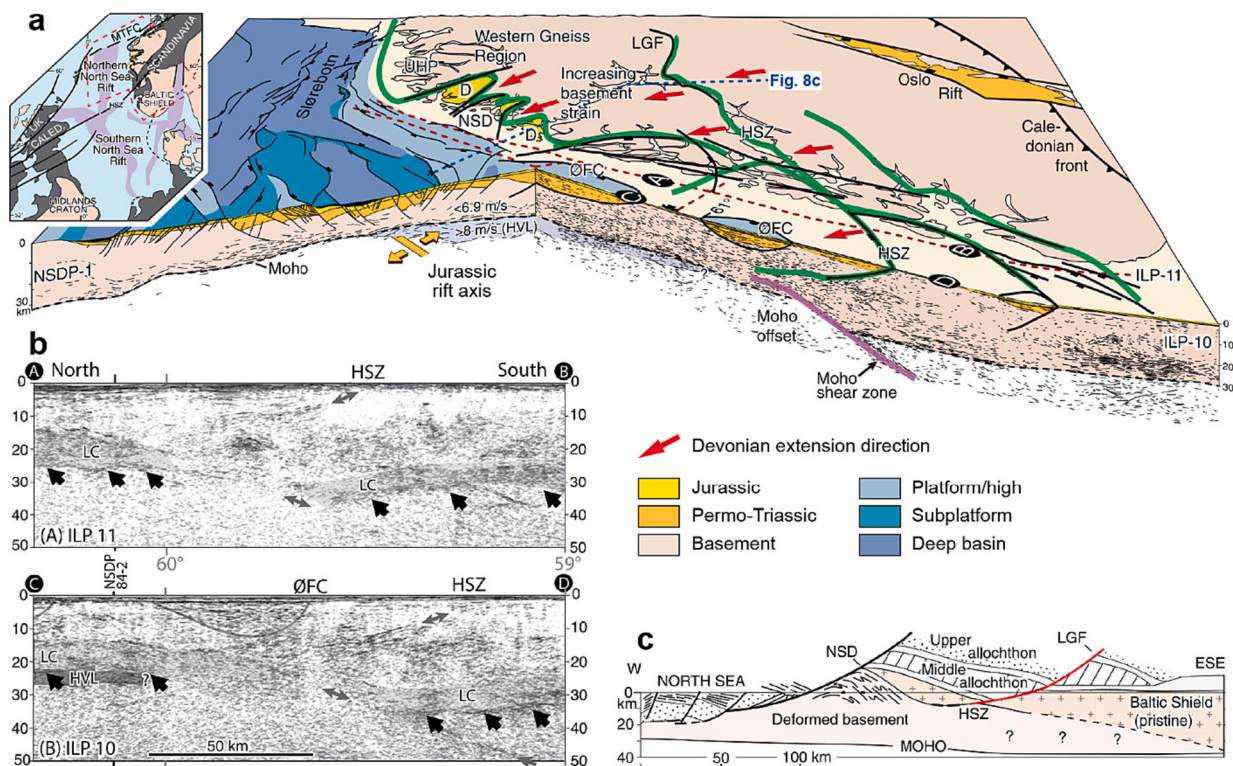


Fig. 8. (a) 3D view of northern North Sea Rift based on interpretation of deep seismic data along seismic lines NSDP-1, NSDP-2, ILP-10, and ILP-11 (Fossen et al., 2014). Here, the Lærdal-Gjende fault system is spatially co-located and hard-linked with the pre-existing, Devonian Hardangerfjord shear zone, which is also located above a major Moho offset. Green lines = major ductile Devonian shear zones; black lines = brittle faults; red arrows = Devonian extension direction; orange arrows = Permian-Triassic extension direction. D = Devonian; HSZ = Hardangerfjord shear zone; LGF = Lærdal-Gjende fault; MTFC = Møre-Trøndelag fault complex; NSD = Nordfjord-Sogn detachment; ØFC = Øygarden fault complex; UHP = ultra-high pressure; HVL = high-velocity layer. (b) Seismic sections A-B and C-D in (a) (Fossen et al., 2014). Black arrows = reflective Moho; gray arrows = shear zone locations. (c) Schematic cross section through the Caledonides (Fossen et al., 2014; modified from Milnes et al., 1997). See (a) for location. (For interpretation of the references to colour in this figure legend, the reader is referred to the web version of this article.)

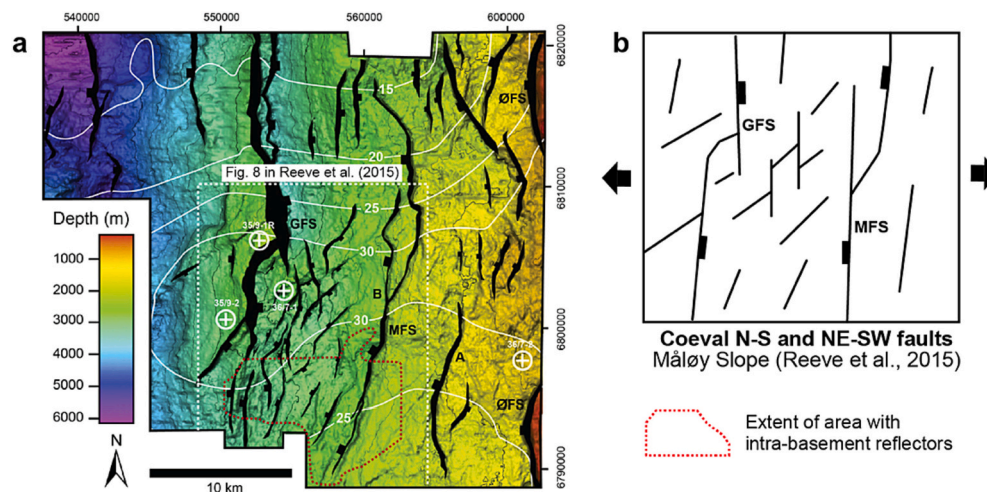


Fig. 9. Example of roughly coeval (i.e., within 10 Ma time window) N-S and NE-SW striking normal fault faults, which were active during Jurassic–Cretaceous E-W directed extension in the Måløy Slope, northern North Sea. NE-SW faults are interpreted to have formed under the influence of the underlying NE-SW striking fabric during an early phase of E-W extension. (a) Top basement depth below sea level in the study area of Reeve et al. (2015). Red dashed line indicates the areal extent of a pre-existing, NE-SW striking, intrabasement fabric interpreted by Reeve et al. (2013). (b) Simplified map of the main N-S striking fault set and smaller N-S and NE-SW trending faults (modified from Reeve et al., 2015). Numbered white lines in (a) are Bouguer gravity anomaly contours (in mGal) (from Smethurst, 2000). White crosses and circles indicate borehole locations and numbers in Reeve et al. (2015). GFS = Gjøa Fault System; MFS = Måløy Fault System; OFS = Øygarden Fault System. (For interpretation of the references to colour in this figure legend, the reader is referred to the web version of this article.)

System (trending NE at this locality) terminates against the NW trending, Mesoproterozoic Aswa Shear Zone (Katunwehe et al., 2015; Saalmann et al., 2016) (Fig. 12).

At the basin scale, the propagation of a normal fault can be inhibited by a relatively strong basement block when the lateral boundary between the weak and strong units is at a high angle to the fault strike. In the Great South Basin (offshore South Island, New Zealand), Phillips and McCaffrey (2019) documented two styles of normal faulting near the Terrane Boundary Fault, which separates the dominantly sedimentary Western Province from the dominantly plutonic Median Batholith. Within the hanging wall of the Terrane Boundary Fault, a large-displacement normal fault within an Upper Cretaceous sedimentary unit splays into a system of low-displacement segments as it approaches a structural high in the mainly granitic basement.

Analogue and numerical models similarly demonstrate strain partitioning in heterogeneous lithosphere during rifting. In a multi-layer model, strain distribution during extension is attributed to the coupling between the brittle and ductile model layers, which depends on the applied strain rate and mechanical layering (i.e., thermal structure) of the model lithosphere (Kuszniir and Park, 1986; Cowie et al., 2005; Wijns et al., 2005; Sokoutis et al., 2007; Zwaan et al., 2021b). This strain distribution determines where basin-bounding faults and accommodation space are created during rifting. Extension of two laterally juxtaposed crustal domains of different integrated strengths (i.e., a weaker basement next to a stronger basement) results in earlier strain localisation and more widely spaced and higher displacement faults in the weaker domain (Phillips et al., 2023; Samsu et al., 2021). When the domain boundary strikes perpendicular to the extension direction, greater strain localisation above the weaker domain leads to rift margin asymmetry (Corti et al., 2013a; Beniest et al., 2018).

3.1.5. Pre-existing weaknesses impacting fault growth

It is now generally observed that the growth of individual normal faults follows a two- to three-stage process: (1) the full fault length is established relatively early in an individual fault's history; (2) after the full length is established, displacement accrual occurs with no further fault lengthening; and (3) possible lateral tip retreat (e.g., Walsh et al., 2002; Jackson and Rotevatn, 2013; Nicol et al., 2017; Rotevatn et al., 2018; Lathrop et al., 2021, 2022). During the first stage of fault growth, lateral propagation of normal faults may be restricted by pre-existing

structures that are oriented at a high angle to the fault propagation direction (Tranos et al., 2019; Kolawole et al., 2022). Faults that acquire their full length at low displacement (i.e., constant fault length growth model) have been linked to the exploitation of geometrically similar, pre-existing crustal weaknesses (i.e., reactivation; Nicol et al., 2005; Vétel et al., 2005; Paton, 2006; Whipp et al., 2014; Rotevatn et al., 2018; Williams et al., 2022), with foliation-parallel normal faults reaching lengths >40 km within a few earthquake cycles (Hecker et al., 2021). However, rapid normal fault lengthening is also observed where there is no evidence for faults following pre-existing weaknesses, and so structural inheritance is not necessarily a prerequisite for this growth mechanism (Rotevatn et al., 2019; Lathrop et al., 2022). Hence, rapid lengthening of optimally oriented normal faults is only equivocal evidence for structural inheritance, as these faults may have grown this way without the influence of a geometrically similar pre-existing structures.

3.1.6. The scale of observation determines how we recognise inheritance

When structural inheritance occurs, its expression may not be recognisable at all scales. The activation of >1 km-long or km-wide weaknesses in lower levels of the crust can result in rift-related faults that are spatially co-located and geometrically similar with the reactivated weaknesses (Fig. 13a and b). However, rift-related faults show a more complex geometry at the sub-km scale (Fig. 13c and d). Outcrop observations suggest that the influence of crustal-scale basement weaknesses is less prominent at the meters scale, which has been attributed to the increasing complexity of fault zone architecture as faults accommodate greater amounts of strain (Kirkpatrick et al., 2013). While fault initiation is controlled by grain-scale anisotropy, the coalescence of fault segments and the development of fault core rock (i.e., cataclaste and fault gouge) with increasing displacement results in complex networks of subsidiary brittle structures (Childs et al., 2009; Kirkpatrick et al., 2013; Deng et al., 2017b; Williams et al., 2022). The main fault zone therefore maintains an orientation that is parallel to the pre-existing weakness, while secondary faults deviate from the main fault trend, cross-cutting local foliation in some places (Fig. 19c; also see Figs. 3 and 4 in Hodge et al., 2018). These scale-dependent manifestations of basement-involved inheritance can only be recognised using a multi-scale approach.

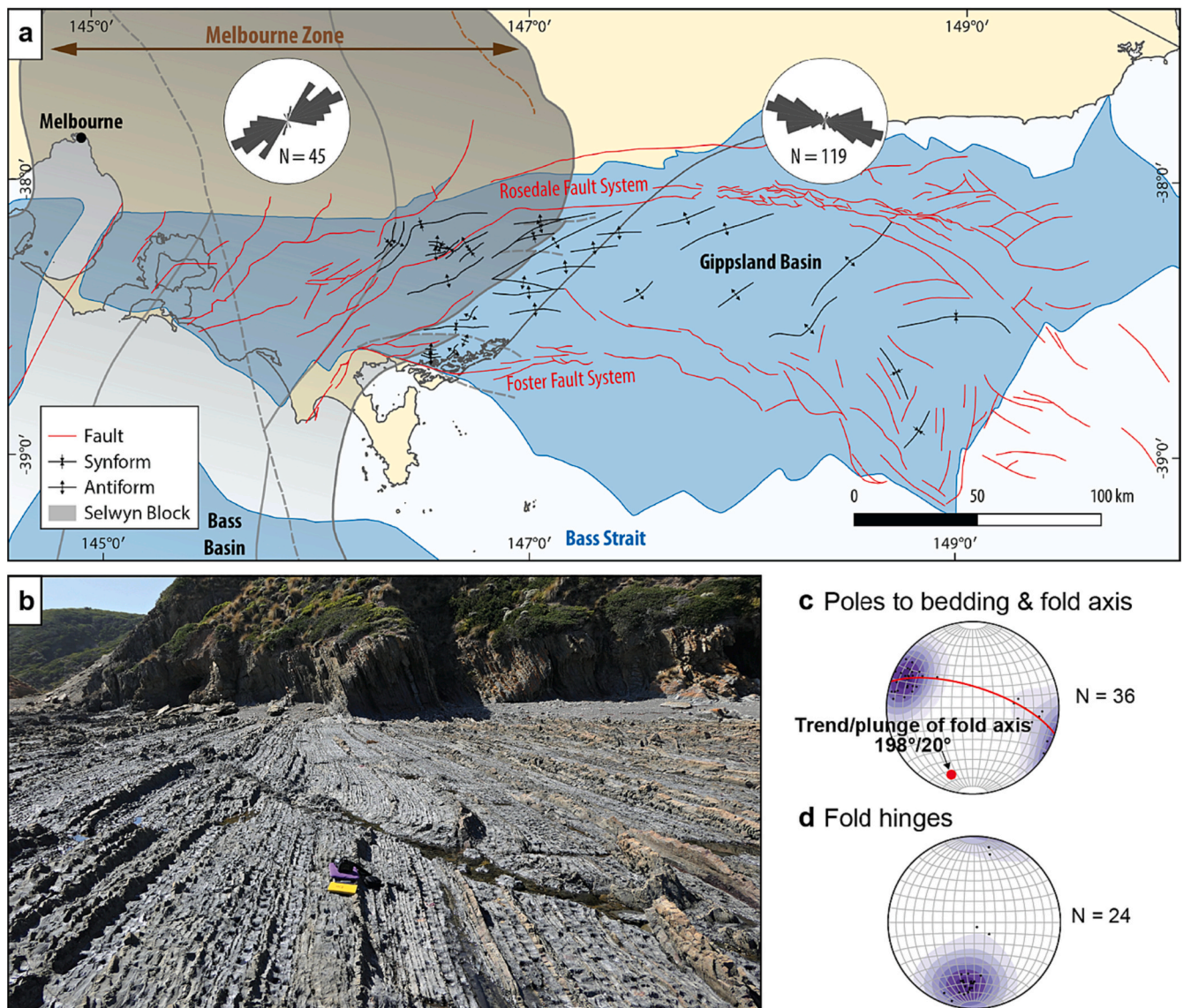


Fig. 10. (a) Cretaceous faults (in red) in the Gippsland Basin (Australian Southern Margin), with rose diagrams showing that faults strike NE-SW in the western onshore portion and WNW-ESE in the eastern offshore portion. These rift-related faults are interpreted to have formed during broadly N-S extension (Samsu et al., 2019 and references therein; map from Samsu et al., 2021). The western onshore part of the basin is underlain by the Paleozoic Melbourne Zone, which is characterised by folded turbidites with a NNE-SSW striking fabric in the study area, and the Neoproterozoic-Cambrian Selwyn Block (Cayley et al., 2002; McLean et al., 2010). (b) Photograph of folded turbidites of the Melbourne Zone. Equal area stereonets show poles to bedding and the fold axis (b) and fold hinges (c). (b-d) are modified from Samsu et al. (2020). (For interpretation of the references to colour in this figure legend, the reader is referred to the web version of this article.)

3.2. Factors modulating the orientations of rift-related faults and their linkage with pre-existing structures

There are a number of factors that determine the degree and mechanism of structural inheritance, which in turn determine the geometric relationship between rift-related faults and the pre-existing structure (Section 3.1). Based on analogue and numerical experiments, these factors are: (i) the obliquity of the pre-existing structure with respect to the bulk extension direction, which is defined as the angle α measured between the strike of the weakness and the orthogonal to the extension direction (e.g., Agostini et al., 2009), (ii) the geometry and size of the pre-existing structure, and (iii) its strength relative to surrounding rocks, which may depend on depth (i.e., the rheology of the host layer). Further, the influence of penetrative anisotropies (Section 3.2.2) can be distinct from that of discrete structures.

The depth of a pre-existing weakness controls the amount of strain localisation in the brittle upper crust. A weakness in the lithospheric

mantle will distribute strain over a wider area than a shallower weakness in the lower crust (Sokoutis et al., 2007). Further, an oblique weakness situated in a deeper level of the lower crust results in distributed, *en échelon* shearing, while a shallower weakness of the same orientation results in more localised faults that are geometrically similar to the weakness (Osagiede et al., 2021).

A hierarchy of inheritance is apparent in models where discrete weaknesses of variable orientations are present in more than one layer and compete to localise strain. Weaknesses in the strong upper crust and lithospheric mantle layers are preferentially (re)activated over a weakness in the lower crust, if the lower crust is relatively weak (Chenin and Beaumont, 2013; Molnar et al., 2020). When weaknesses are present in both the upper crust and lithospheric mantle, their relative contributions to strain localisation are determined by the degree of mechanical coupling between the two layers. This coupling depends on kinematic boundary conditions (e.g., rate of divergence) and the thickness and strength of the intervening, potentially weak, lower crust (Zwaan et al.,

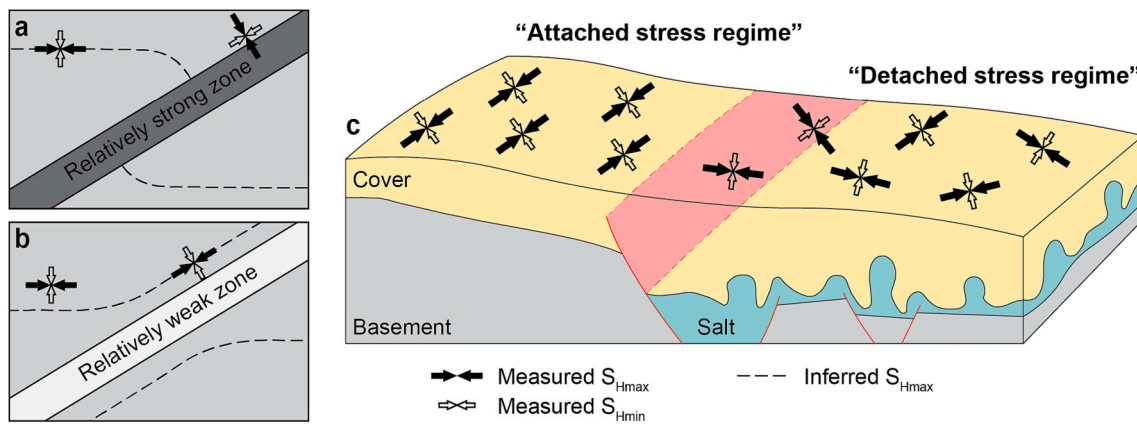


Fig. 11. Map view illustration of the re-orientation of maximum horizontal stress (S_{Hmax}) near a mechanically strong (a) and weak (b) zone (modified after Bell, 1996). S_{Hmax} trajectories are perpendicular to the trend of a strong zone and parallel to the trend of a weak zone. (c) Stress coupling between basement and cover rocks occurs in an “attached stress regime” (*sensu* Bell, 1996). Stress decoupling occurs when there is an intervening, mechanically weak layer (e.g., evaporites, overpressured shales, and low-angle faults). All panels modified after Bell (1996).

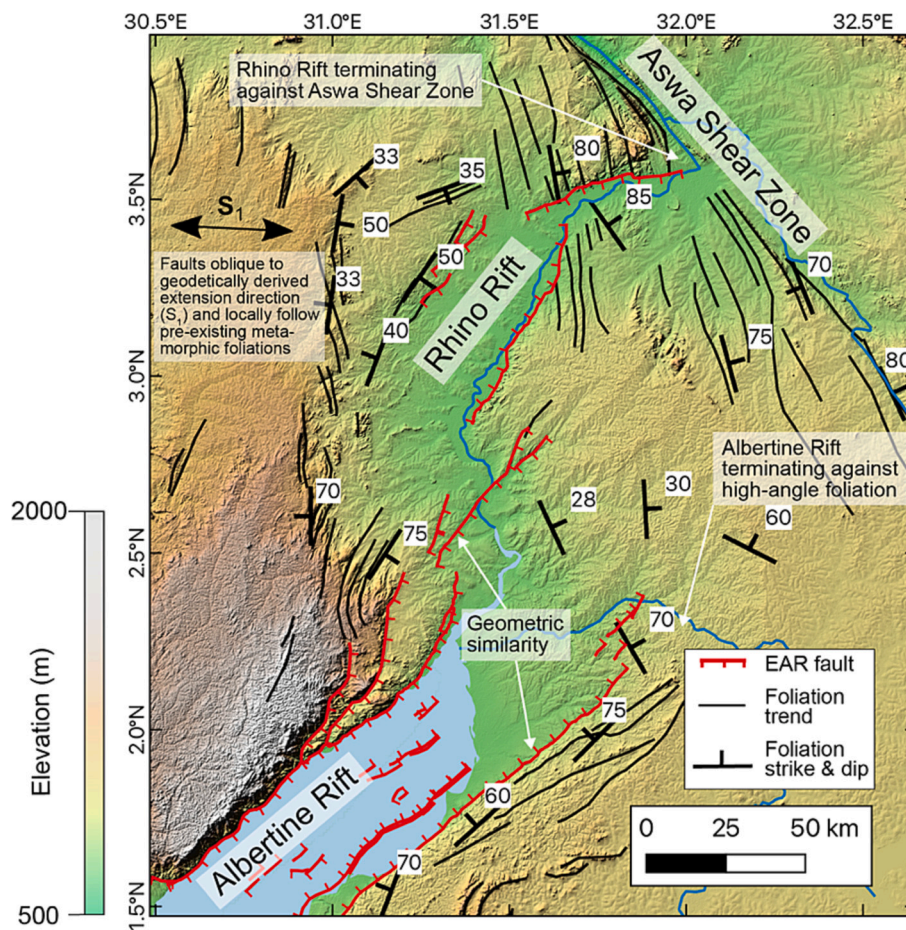


Fig. 12. Basin-scale structural inheritance in the Albertine and Rhino rifts. Fault and foliation mapping from Katumwehe et al. (2015), Karp et al. (2012), Westerhof et al. (2014), and Kolawole et al. (2021a). Regional extension azimuth after Saria et al. (2014). The geological interpretation map is underlain by 30 m resolution Shuttle Radar Topography Mission (STRM) DEM (Sandwell et al., 2011).

2021b).

3.2.1. Obliquity of discrete pre-existing weaknesses

Discrete, pre-existing weaknesses in the brittle upper crust influence the orientations, kinematics, growth, and linkage of rift-related faults in different ways, depending on their strike (Brun and Tron, 1993;

Bellahsen and Daniel, 2005; Corti et al., 2007; Chattopadhyay and Chakra, 2013; Ghosh et al., 2020; Maestrelli et al., 2020; Zwaan and Schreurs, 2020; Zwaan et al., 2021a, 2021b) (also see Table 2). Weaknesses that are at a high angle to the bulk extension direction ($\alpha < 30^\circ$) are reactivated in a normal sense, exhibiting mainly dip-slip kinematics and accommodating most of the extensional strain. Weaknesses that are

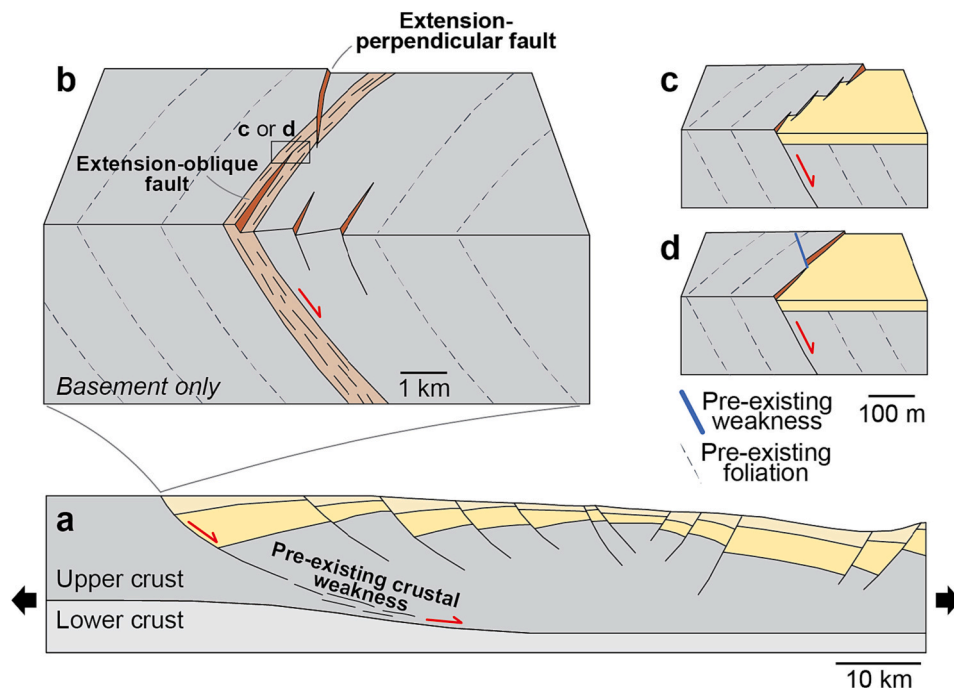


Fig. 13. A pre-existing crustal weakness can influence rift-related cover faults at a range of scales. Tectonic or plate-scale inheritance contributes to rift localisation (a), while basin to sub-basin scale inheritance results in spatial co-location and geometric similarity between pre-existing structures (e.g., basement shear zones and foliation) and rift-related normal faults (b). At the outcrop scale, some minor faults can deviate from the main fault and crosscut pre-existing foliation, reflecting the complex architecture of a fault zone (c) or reactivation of other pre-existing structures, such as dykes (d). Thick arrows indicate the inferred regional extension direction during rifting.

at a lower angle to the bulk extension direction are reactivated with a greater strike-slip component of movement; these typically give rise to secondary, extension-oblique faults that link the primary, extension-perpendicular faults (Bellahsen and Daniel, 2005; Osagiede et al., 2021). In general, the reactivation of discrete, pre-existing weaknesses that are hosted in the brittle upper crust results in geometric similarity between some of the rift-related faults and the pre-existing weaknesses.

Pre-existing weaknesses in the ductile parts of the lithosphere also influence the orientations and arrangement of rifts and rift-related faults. When the ductile weakness is oriented at a high angle to the extension direction ($\alpha < 45^\circ$), it guides the map-view strike of rift segments (Corti, 2008; Agostini et al., 2009; Tommasi et al., 2009; Tommasi and Vauchez, 2015; Petersen and Schiffer, 2016; Molnar et al., 2020). In contrast, a ductile weaknesses that is oriented at a low angle to the extension direction ($\alpha > 45^\circ$) determines where rifts are segmented and transfer zones form. In the brittle upper crust, faults form *en échelon* patterns of faults at the lateral boundary between the underlying ductile weakness and normal-strength lithosphere (see border faults in Fig. 14). For both low- and high-obliquity rifts, the strike of these faults is between the main rift trend (i.e., the trend of the linear weakness) and the bulk extension direction (Agostini et al., 2009; Corti et al., 2013b). The obliquity of these faults with respect to the far-field extension reflects the relative contributions of extension perpendicular to the rift trend and shear parallel to the rift trend (Withjack and Jamison, 1986). Early interpretations based on fault orientations alone suggested that these faults have oblique-slip kinematics (Agostini et al., 2009), which is a response to transtension under the imposed bulk extension boundary condition. Similar studies later showed that the extension-oblique faults actually display dip-slip kinematics (Corti et al., 2013b; Philippon et al., 2015), highlighting local slip re-orientation that is associated with the underlying ductile weakness. These insights from modelling support the interpretation of extension-oblique faults with dip-slip kinematics in some natural settings, including in the Main Ethiopian Rift (Philippon et al., 2015 and references therein), the Baikal Rift (Petit et al., 1996), and the Rukwa Basin in the East African Rift System (Delvaux et al.,

2012). They also imply that strain re-orientation – an inheritance mechanism that is different to reactivation – can occur when a pre-existing ductile weakness is oblique to the far-field extension direction.

3.2.2. Oblique penetrative anisotropies

Penetrative anisotropies can be considered as an area comprising alternating strong and weak zones (e.g., a pre-existing metamorphic fabric or a system of parallel rift-related faults from a previous rift phase). Penetrative anisotropies (oblique to the far-field extension direction) in the ductile layer can re-orient the far-field strain over a wide area, creating a complex pattern of extension-oblique faults in the brittle upper crust over the entire anisotropic domain. This form of inheritance was demonstrated in a crustal-scale analogue experiment by Samsu et al. (2021), in which the orthorhombic fault pattern above an anisotropic ductile lower crust (with the anisotropy oriented 45° to the imposed extension) is distinct from normal faults that developed above a homogeneous ductile lower crust in the adjacent domain. The anisotropic lower crust contains strength contrasts between the strong and weak zones that make up the anisotropy. The strong and weak zones resist extension to different degrees, so that the difference in the rate of thinning between these zones results in shearing at the strong-weak interfaces. This process results in localised re-orientation of the 3D strain field (i.e., non-coaxial deformation, where the strain ellipses are rotated) and therefore non-Andersonian faulting above the anisotropic domain.

At the basin scale, strain re-orientation is evidenced by laterally variable fault patterns above different blocks that contain different variably-oriented pre-existing fabrics (e.g., North Coast Transfer Zone, Scotland; Wilson et al., 2010). At the outcrop scale, strain can also be partitioned due to mechanical heterogeneities in faulted rocks. For example, in the Carboniferous Northumberland Basin (northeast England), minor faulting in the hanging wall of the reactivated 90-Fathom Fault is partitioned into an extension-dominated regime in dolostones and wrench-dominated transtension in quartz-rich sandstones (De Paola et al., 2005). This lithological control on fault kinematics has been

Weak zone (WZ) orientation

Fault pattern

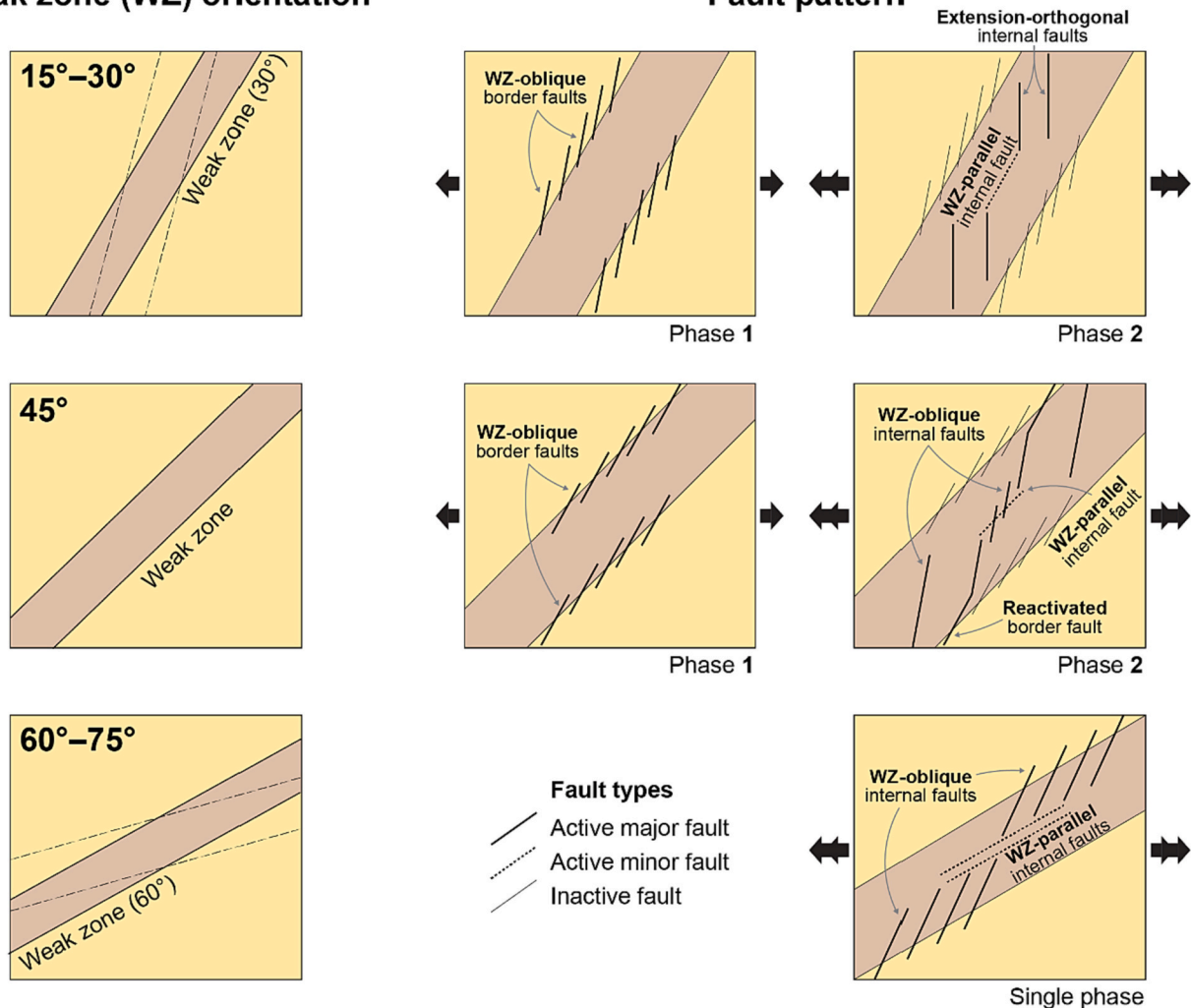


Fig. 14. Map-view summary of analogue experiments showing differences in the evolution and pattern of rift-related faults above a ductile weak zone (WZ) that is oblique to the imposed extension direction (modified after Agostini et al., 2009). Thick black arrows indicate the extension direction. Major faults are oblique to the extension direction and weak zone irrespective of weak zone obliquity.

attributed to differences in the Poisson's ratio of different rock types. This idea suggests that contrasts in the mechanical (in this case, elastic) properties of rocks contribute to strain re-orientation.

Both crustal-scale models and basin to outcrop-scale field observations suggest that during rifting, strain re-orientation operates at a range of length scales in response to sufficient contrast in the mechanical properties of the extended heterogeneous medium. Future experiments involving anisotropies with various orientations, different widths/thicknesses and strength ratios of the alternating strong-weak zones, and different kinematic boundary conditions, will increase our understanding of the influence of ductile and brittle fabrics on rift-related faulting.

3.2.3. Depth and size dependence

The depth dependence of inheritance influences the type of linkage between pre-existing structures and younger rift-related faults in the overlying units. Rift-related faults in deeper sedimentary units, for example, are hard-linked with and geometrically similar to reactivated structures in the underlying basement (Fig. 15). In contrast, shallower faults are perpendicular to the regional extension direction but form an *en échelon* arrangement parallel to the pre-existing structures (Fig. 3b) (Collanega et al., 2019; Deng et al., 2020; Phillips et al., 2022); these shallow faults are soft-linked by relay zones in map view (Giba et al., 2012). As faulting progresses, the shallow faults may become laterally

linked at the surface (Deng and McClay, 2021). Vertical linkage between deep and shallow fault segments creates an up-sequence rotation of fault strike to define a sigmoidal fault geometry in 2D (cross section) and a twisted fault surface in 3D (Fig. 15b). An intervening, mechanically weak unit would in theory decouple stress and strain between the basement and cover units (Section 3.1.3). However, when this intervening weak unit is relatively thin, vertical linkage between pre-existing and new faults may mainly be controlled by the displacement and geometry of the pre-existing structures (e.g., the presence of relay ramps between same-generation, pre-existing faults) (Phillips et al., 2022).

Collanega et al. (2019) documented the depth-dependent upward propagation of rift-related faults, observed from seismic reflection data from the Taranaki Basin. Here, Plio-Pleistocene rift-related faults nucleated either from intrabasement shear zones (possibly Mesozoic in age; Muir et al., 2000) or within damage zones above Late Miocene reverse faults. Collanega et al. (2019) suggested that the upward propagation of these faults into the overlying cover during rifting was controlled by the obliquity of the shear zone with respect to the regional extension direction. Shear zones that strike perpendicular to the extension direction are hard-linked to rift-related faults that extend into the upper levels of the cover. In contrast, shear zones that strike more obliquely to the extension direction are hard-linked to rift-related faults that are restricted to the lower levels of the cover.

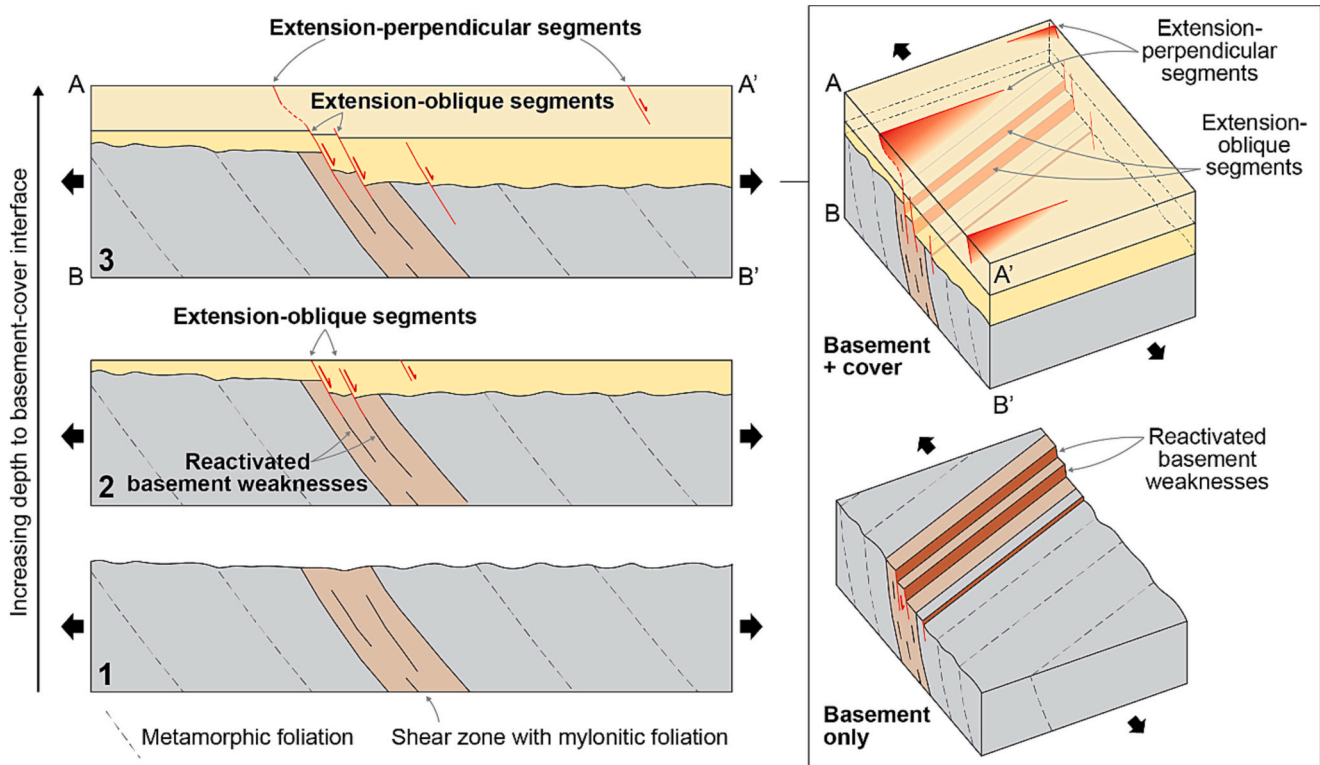


Fig. 15. Conceptual illustration of the depth-dependent influence of pre-existing weaknesses in metamorphic basement rocks, based on observations by Collanega et al. (2019). Numbers 1–3 indicate the progression of rifting and increasing thickness of cover rocks. Faults near the basement-cover interface are geometrically similar with and rooted in the reactivated basement weaknesses (e.g., shear zone, metamorphic foliation). Shallower faults are perpendicular to the regional extension (black arrows), suggesting that they are influenced to a lesser degree by the pre-existing weaknesses.

Another component that modulates the influence of an oblique pre-existing weakness is its size (e.g., its thickness measured normal to the margin of the structure). Collanega et al. (2019) inferred that rift-related faults nucleating at a thick, pre-existing shear zone (with a map-view width of ~ 1 km and $15\text{--}20^\circ$ dip) propagated further upwards to shallower depths compared to rift-related faults that nucleated at a thinner shear zone (with a map-view width of 100 m and $20\text{--}30^\circ$ dip). Analogue experiments also show that the dimensions and orientations of a pre-existing weakness variably influence fault localisation and kinematics (Osagiede et al., 2021). A thick oblique weakness may be more influential than a thin one due to the larger volume of reduced integrated strength near and within the weakness.

3.3. Multiphase rifting: The influence of first-phase faults on second-phase faults

In multiphase rifting, the extension direction in the second rift phase can be different to that of the first rift phase. Analogue models show that where the strike of first-phase normal faults is optimal for reactivation, these “pre-existing” faults can influence the fault system geometry of the second rift phase (e.g., Keep and McClay, 1997; Bellahsen and Daniel, 2005; Henza et al., 2010; Chattopadhyay and Chakra, 2013; Ghosh et al., 2020). It has also been observed in natural multiphase rifts that faults from the first rift phase can undergo oblique reactivation, while new faults also form with strikes perpendicular to the new extension direction. Second-phase faults may abut first-phase faults, transferring strain to a locally reactivated segment of the first-phase fault (i.e., “trailing fault”; Nixon et al., 2014). The first- and second-phase fault sets form a zigzag geometry in map view (Wang et al., 2021a). Analogue experiments by Henza et al. (2011) suggest that the amount of displacement on first-phase faults influences the lengths of second-phase faults and their connectivity with the first-phase faults (Fig. 16). In

addition, the size and distribution of first-phase faults appears to control strain localisation during second-phase faulting (Bailey et al., 2005).

Natural examples serve to highlight the nuances of structural inheritance in multiphase rifts, where factors other than fault geometry, such as thermal weakening, may influence whether faults are reactivated during subsequent rifting phases. During multiphase rifting in the northern North Sea, N-S striking faults that formed during the Permo-Triassic phase of rifting on the Horda Platform are co-located with regions affected by previous Devonian extension, with the faults possibly soling out into Devonian shear zones (Bell et al., 2014). However, these Permo-Triassic faults were not subsequently reactivated during later Middle Jurassic rifting, even though their N-S strike would have been favourable for reactivation during E-W to NW-SE extension (Bell et al., 2014; Fazlikhani et al., 2021). Instead, early Jurassic thermal doming of the North Sea resulted in lithospheric thermal weakening, which favoured the nucleation of new faults in the North Viking Graben to the west of the Horda Platform. However, subsequent rifting in the Late Jurassic–Early Cretaceous reactivated faults that formed during the first Permo-Triassic rifting phase. Here, reactivation was diachronous, with faults closest to the North Viking Graben reactivating first (Bell et al., 2014).

3.4. Geomechanical considerations on the reactivation of non-optimally oriented faults

One of the mechanisms of structural inheritance that we discuss in this review – reactivation – requires some degree of movement on pre-existing planes of weakness (e.g., pre-existing faults, shear zones, pervasive fabrics, or lithological contacts). For strain re-orientation, it is less clear whether such movement is required and in which situations; nevertheless, strain re-orientation has been observed to occur in conjunction with reactivation. In this section we review the wide range

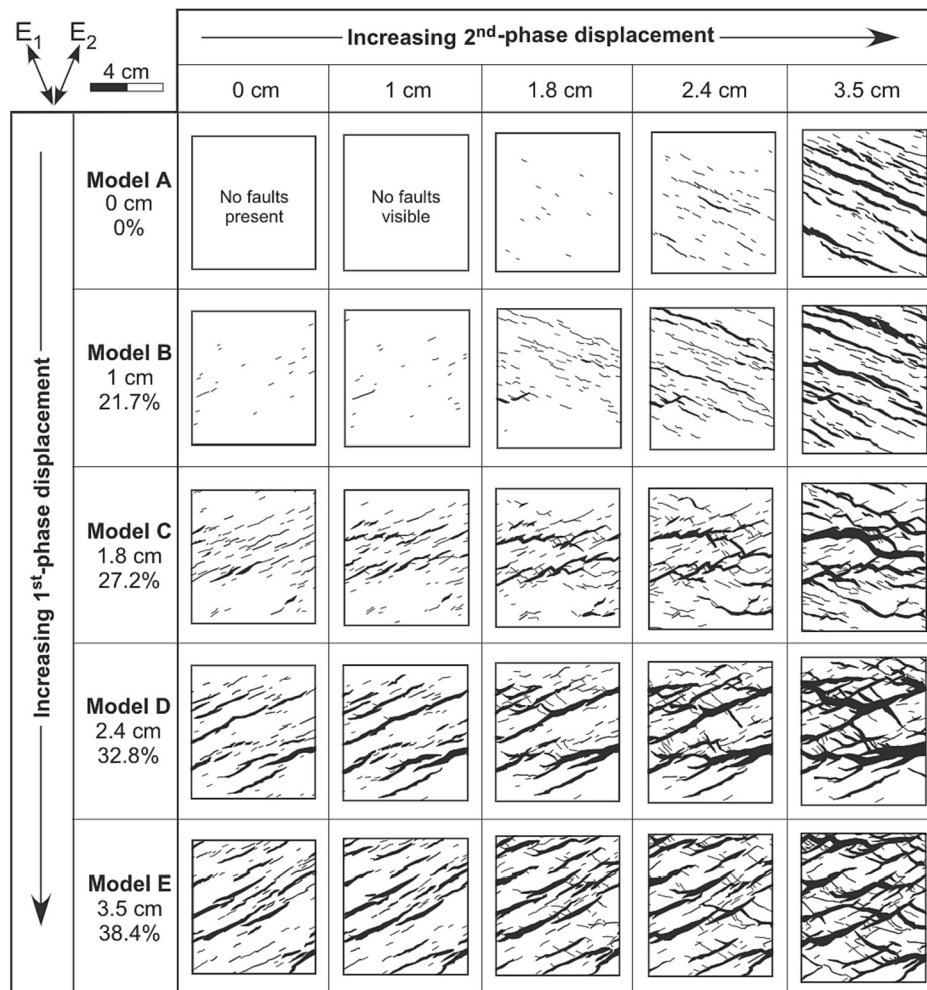


Fig. 16. Analogue experiments of multiphase rifting in wet clay, showing the influence of fault displacement during the first and second rift phases on fault length and connectivity (Henza et al., 2011).

of conditions under which pre-existing planes of weakness are expected to undergo frictional failure and potentially contribute to inheritance.

The tendency for frictional slip to reactivate planes of weakness (as opposed to the nucleation of new faults in intact rock; Byerlee, 1978; Butler et al., 1997; Holdsworth et al., 1997, 2001b) is governed by the local stress state, the orientation of the planes of weakness (Jaeger and Cook, 1979; Morris et al., 1996; Lisle and Srivastava, 2004), and the effective frictional strength of these weaknesses relative to that of surrounding intact rock (Section 3.4.1). Reduced effective frictional strength in pre-existing planes of weakness has been attributed to both pore fluid pressures in excess of hydrostatic fluid pressure, and lower cohesion or frictional coefficient due to grain-scale features such as: (a) interconnected zones of phyllosilicates or clays that provide low-friction sliding surfaces (Byerlee, 1978; Holdsworth, 2004; Collettini et al., 2009b, 2019); (b) grain boundary alignment and compositional banding (e.g., in gneisses; Shea and Kronenberg, 1993; Kirkpatrick et al., 2013); and (c) high grain boundary porosity and/or low intergranular cohesion in non-foliated rocks (e.g., non-cohesive cataclases; Sibson, 1977).

For a rift basin forming in an idealised Andersonian normal fault stress regime (Anderson, 1905) with a vertical maximum principal compressive stress (σ_1), the fault population will be dominated by normal faults that strike perpendicular to the horizontal minimum principal compressive stress (σ_3) and dip 58–68° (Collettini and Sibson, 2001). Much of our understanding of the geomechanics of inheritance in rift settings relates to deviations from this idealised scenario, in which pre-existing structures either strike obliquely to σ_3 and/or have a dip \neq

58–68° (e.g., Etheridge, 1986; Ranalli and Yin, 1990; Massironi et al., 2011; Williams et al., 2019). Here, we examine 2D and 3D approaches (Sections 3.4.1 and 3.4.2, respectively) to understand how slip occurs along pre-existing planes of weakness that are not optimally oriented for frictional reactivation.

3.4.1. Influence of frictional strength and fluid pressure on basement structures

In the case of a pre-existing plane of weakness that strikes orthogonal to σ_3 , the plane of weakness contains the intermediate principal compressive stress (σ_2). Therefore, assuming pure dip-slip, a 2D analysis can provide insights into the conditions required for reactivation, depending on the dip of the plane of the weakness. This analysis follows Sibson (1985), who defined an effective stress ratio required for slip to occur:

$$R = \frac{\sigma'_1}{\sigma_3} = \frac{(1 + \mu_s \cot \theta)}{(1 - \mu_s \tan \theta)} \quad (1)$$

where μ_s is the static coefficient of friction, which is a measure of the friction between two cohesionless stationary surfaces that are in contact (Byerlee, 1978), and σ'_1 and σ_3 are the maximum and minimum effective principal stresses ($\sigma'_1 = \sigma_1 - P_f$ and $\sigma_3 = \sigma_3 - P_f$; where P_f is the pore fluid pressure). θ is the angle between the plane of weakness and σ_1 .

The approach in Eq. 1 hinges on the application of a simple linear failure criterion for cohesionless faults (Amonton's Law) containing σ'_2

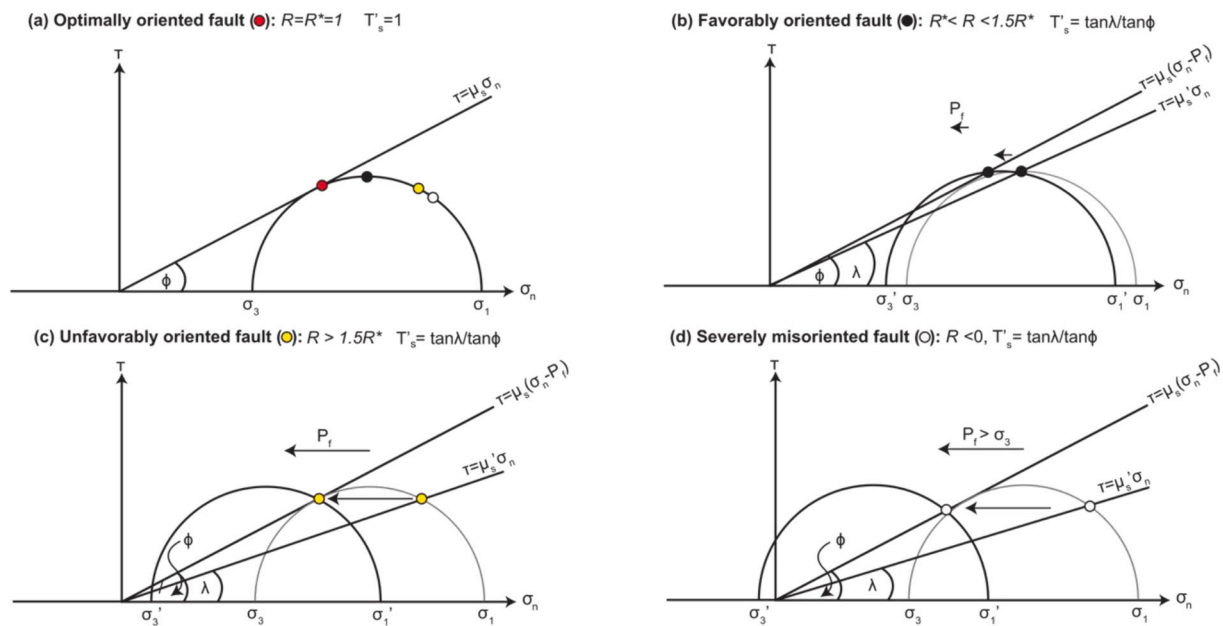


Fig. 17. Mohr diagram plots of shear stress (τ) versus normal stress (σ_n) for reactivation analysis of cohesionless faults that contain σ_2 . (a) The orientation of four faults with different reactivation potential as quantified by their stress ratio ($R = \sigma_1'/\sigma_3'$) and normalized slip tendency (T'_s ; Lisle and Srivastava, 2004). For the case of the optimally oriented fault ($\theta = 30^\circ$), R is denoted R^* and $T'_s = 1$. In (b)–(d), R and T'_s are schematically depicted for the reactivation of (b) favourably oriented, (c) unfavourably oriented, and (d) severely misoriented fault. In cases (b)–(d) a reduction in frictional strength (μ_s) and/or increase in pore fluid pressure (P_f) is required for fault reactivation. Modified after Williams et al. (2019).

(the intermediate effective principal stress). Alternative failure criteria can be applied that incorporate the important effect of σ_2' (e.g., Extended Griffith, Drucker-Prager; Murrell, 1963; Haimson, 2006); nevertheless, the analysis provides a useful base case. For example, it can be used to identify three non-optimal failure regimes (Sibson, 1990; Leclère and Fabbri, 2013; Fig. 17 and Fig. 18a), which can be compared against the R factor for an optimally oriented surface ($R = R^*$; Fig. 17a): (1) “Favourably oriented” surfaces have dips that deviate from the optimal orientation for failure by $<15^\circ$ (e.g., $1-1.5R^*$, Fig. 17b). (2) “Unfavourably oriented” surfaces have higher R values (e.g., $R > 1.5R^*$) with dips misoriented by up to $25-30^\circ$ from the optimal orientation (Fig. 17c). (3) “Severely misoriented” surfaces are ones that require pore fluid pressures that are greater than σ_3 to reactivate (i.e., R is negative, Fig. 17d).

A second outcome of Eq. 1 is the significant influence of friction on the reactivation potential of pre-existing planes of weakness in basement rocks. Laboratory measurements have yielded static friction coefficients as low as 0.2 for wet phyllosilicate and clay-rich fault gouges (Moore and Lockner, 2004; Numelin et al., 2007), compared to 0.5–0.85 for most other Earth materials tested in wet and dry conditions (e.g., Byerlee, 1978; Jaeger et al., 2007). This means that for structures rich in graphite, phyllosilicates, or clays (especially illite-smectite, chlorite, talc, biotite, and pyrophyllite), such as pre-existing faults, the range of dips that are optimally or favourably oriented for failure expands considerably. Pre-existing faults with coefficients of friction as low as 0.3 are therefore able to reactivate, even if their dips are as low as 25° (e.g., low angle normal faults; e.g., Collettini et al., 2009a, 2009b; Healy, 2009; Massironi et al., 2011; Demurtas et al., 2016; Singleton et al., 2018) or nearly subvertical, without requiring elevated fluid pressure (Fig. 18b).

Pore fluid factor diagrams (Fig. 18c; Cox, 2010) are a useful alternative graphical method and can be used to assess the role of friction, fluid pressure, and stress on the potential for frictional sliding of basement structures at a given depth. Based on this approach, Cox (2010) suggested that for the more unfavourably oriented normal faults (e.g. $\sim 30^\circ$ dip) with a typical frictional strength ($\mu = 0.75$), there is only a narrow range of differential stress in which it is possible for slip to occur,

and that elevated pore fluid pressures are a pre-requisite. However, using the same approach, Fig. 18c shows that when basement structures with low frictional strength are present, there is a wider range of stress conditions under which they are capable of sliding, with or without the presence of elevated fluid pressures. Fig. 18b also implies that sliding on these lower friction structures can occur over a range of fault dip angles. These pre-existing weaknesses are likely to be the first structures to begin sliding at the inception of rifting and therefore have the potential to become important controls on subsequent basin geometry.

3.4.2. Extension of geomechanical analyses to 3D and implications for sedimentary basins

A 3D approach is required to examine the mechanics of structural inheritance when pre-existing basement structures strike obliquely to σ_3 (i.e., the plane of weakness does not contain σ_2) (Williams et al., 2019). For example, “slip tendency analysis” (Morris et al., 1996; Lisle and Srivastava, 2004) provides a method to estimate the potential of a cohesionless plane of weakness to activate under any stress state (Fig. 17). More recently, Leclère and Fabbri (2013) introduced a 3D solution for the effective stress ratio, R , for reactivation that accounts for cohesion and does not assume an Andersonian stress regime. Relatively few studies have used this 3D approach to investigate the reactivation potential of pre-existing structures that strike obliquely to the regional extension direction. Williams et al. (2019) applied the 3D solution of Leclère and Fabbri (2013) to the southern Malawi Rift to show that weaknesses with a non-optimal strike ($>50^\circ$ to the trend of σ_3) can still reactivate. In their example, pre-existing faults with a favourable dip of $\sim 50-60^\circ$ can be reactivated if they are slightly weaker than intact rock ($\mu \sim 0.55-0.65$ vs. $\mu \sim 0.7$), or have an elevated but small pore fluid factor (pore pressure over normal stress $\sim 0.1-0.3$) compared to dry intact rock. Hence, a wide range of orientations and fluid pressure conditions are likely under which relatively weak basement surfaces can be reactivated.

The geomechanical considerations above enable us to be more specific about the conditions in which inheritance is likely to occur. Basement rocks comprising metamorphosed and deformed carbonaceous shales have the potential to contain graphite-rich planes of weakness

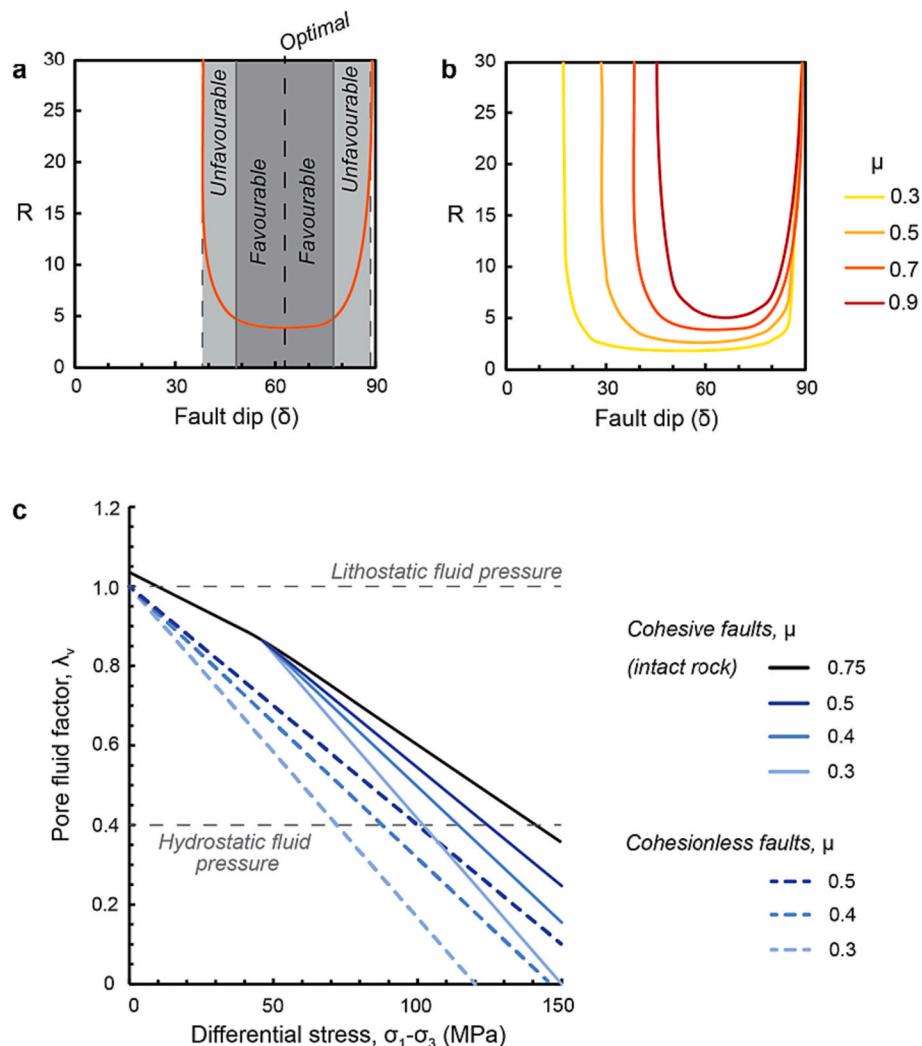


Fig. 18. (a) Stress ratio (R) required for frictional reactivation vs. fault dip for a cohesionless normal dip-slip fault ($\mu_s = 0.7$) in an Andersonian stress regime. Shown are the dip angles for the optimal fault orientation for (re)activation and the range of fault dips that are favourably oriented for failure. Also shown is the range of unfavourably oriented fault dips that require elevated fluid pressures to fail. (b) Reactivation potential for faults with low coefficients of static friction. The potential for failure of favourably oriented faults extends over a much wider range of dips. (c) Pore fluid factor-stress diagram (Cox, 2010), for normal dip-slip faults (10 km depth) that are optimally oriented for each value of static friction coefficient. Basement stress states increasing from near hydrostatic fluid pressure and low differential stress have the potential to reactivate pre-existing structures with lower coefficients of static friction, relative to intact rock, over a wide range of stress and fluid pressure conditions.

(implying low $\mu_s = 0.2-0.4$). Likewise, crystalline basement subjected to hydrothermal alteration or containing hydrated ultramafic rocks (ophiolites or Archean greenstone) may host phyllosilicate- and talc-rich zones of weakness. The 3D reactivation analysis could also be used in multiphase rifts to test whether faults that formed in the initial phase of rifting are reactivated in subsequent rifting phases with different extension directions. However, caution should be applied in this case, as local changes in stress and crustal rheology may mean that a fault's orientation relative to far-field stresses is not the only indicator for whether it will reactivate in later rifting events (Bell et al., 2014).

It is also well established that many sedimentary basins develop elevated pore fluid pressures below a critical depth due to compaction disequilibrium and other mechanisms (Suppe, 2014; Zhang, 2019). Given that basinal fluids are known to infiltrate into the basement (Yardley et al., 2000; Gleeson et al., 2003), there are situations in which basement rocks may be saturated in hydrothermal fluids at elevated pressure. As such, elevated fluid pressures and low friction planes of weakness are common in basement rocks, implying that structural inheritance during basin formation should be the norm rather than the exception.

4. Discussion

4.1. Reactivation and strain re-orientation are the two distinct structural inheritance mechanisms that influence rift-related faulting

2D and 3D observations from outcrops, geophysical data, and analogue and numerical models provide insight into the interactions between pre-existing and younger rift-related structures, as summarised in Section 3. From this synthesis, we suggest that two mechanisms underpin the control of pre-existing structures on rift-related fault orientations and geometries: **reactivation** and **strain re-orientation** (Fig. 19). Notably, both mechanisms can be active during the same rift phase, either along different pre-existing structures (with different orientations) within the same basin, or along the same pre-existing structure at different depths.

In the context of this discussion, (frictional) reactivation implies slip along a pre-existing weak surface in the brittle crust. During rifting, a pre-existing basement weakness can be a nucleation site from which a new fault propagates into the overlying cover (e.g., Phillips et al., 2016; Collanega et al., 2019) (Fig. 6a). Strain re-orientation refers to non-

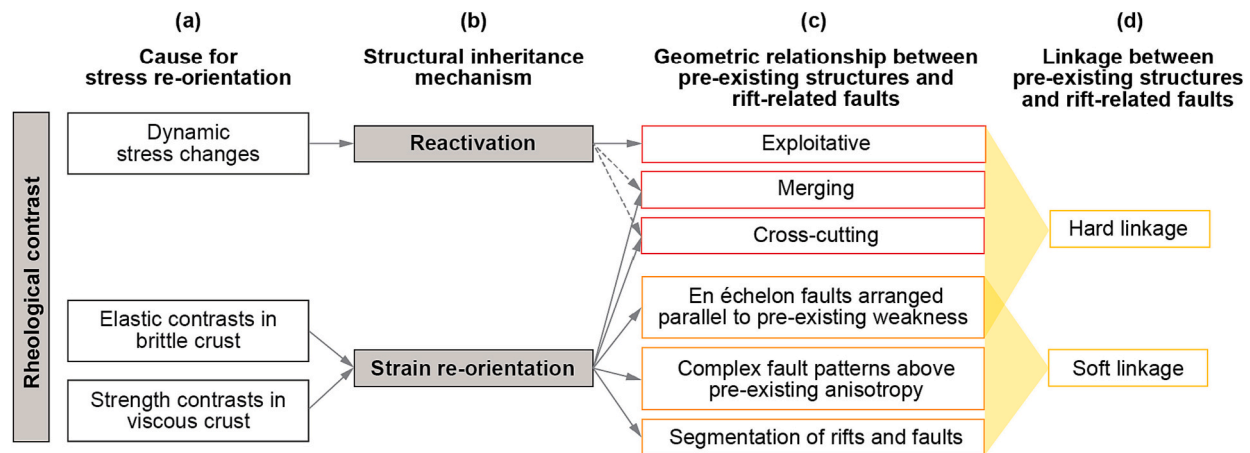


Fig. 19. Classification of the drivers (a), mechanisms (b), and expressions of structural inheritance (c and d) in rift-related faulting. of structural inheritance. Rheological contrast is a pre-requisite for both mechanisms of structural inheritance (i.e., reactivation and strain re-orientation), with which local perturbations of the far-field stress are associated. Such stress perturbations can be driven by dynamic stress changes due to movement along a pre-existing weakness or by elastic and strength contrasts in the brittle and viscously deforming crust, respectively. The two inheritance mechanisms can be inferred based on the 2D and 3D geometric relationships between pre-existing structures and rift-related faults. These geometric relationships which have been further classified into hard and soft linkage (referred to as hard-linked and soft-linked inheritance, respectively, in the text).

coaxial deformation patterns, which result from partitioning of the far-field extensional strain at the interface between two mechanically distinct rock units (e.g., adjacent blocks of metamorphic or igneous basement domains). For example, bulk stretching of anisotropic block – where the anisotropy is oblique to the far-field extension direction – is accommodated by different rates of extension in the strong and weak rocks, resulting in shearing along the strong-weak boundary (e.g., Samsu et al., 2021). Strain re-orientation can also occur in conjunction with movement along a pre-existing structure (i.e., reactivation) (Phillips et al., 2016).

Both reactivation and strain re-orientation may be associated with local perturbations of the far-field stress around a pre-existing structure (i.e., local stress re-orientation) (Section 3.1.3). Stress re-orientation has been observed and modelled in three scenarios: (i) dynamic stress changes due to movement along a fault or shear zone (Barton and Zoback, 1994); (ii) deflection of stress trajectories due to elastic contrasts in the brittle crust (Fig. 11a and b) between a pre-existing structure and its host rock or between two adjacent basement domains (Bell, 1996; de Jossineau et al., 2003; Morley, 2010); and (iii) strength contrasts in the viscous crust that results in strain re-orientations (Samsu et al., 2021) which alters the stress field in an overlying mechanically coupled brittle crust. We therefore suggest that rheological contrast is a prerequisite for inheritance, which must be present for reactivation and/or strain re-orientation to occur. In sedimentary basins, a locally rotated stress field within the basement can be transferred to the overlying basin fill when the two units are mechanically coupled. If, however, an intervening weak layer separates basement and cover, then stress coupling between the basement and cover rocks is limited (Fig. 11c). This variable decoupling by an intervening weak layer (Phillips et al., 2022) has implications for hard and soft-linkage between pre-existing basement structures and rift-related faults in the overlying cover (see Section 4.2).

Reactivation and strain re-orientation can occur concurrently during a single rift episode but result in different spatial and geometric relationships between the pre-existing basement structures and rift-related faults (Fig. 19). Applied to the offshore southern Norway study area of Phillips et al. (2016), the distinction between these mechanisms and the extent of their influence may explain why rift-related faults exploit, merge with, or cross-cut different basement shear zones within the same basin (Section 3.1.2). Strain re-orientation can also explain the occurrence of rift-related faults that form above – but do not exhibit geometric similarity with – a pre-existing basement weakness or anisotropy. The

range of geometric relationships associated with strain re-orientation emphasises that reactivation is not synonymous with structural inheritance, of which strain re-orientation is a common and important mechanism.

Whether reactivation or strain re-orientation occurs may depend on whether a pre-existing structure behaves in a frictional or viscous manner. Discrete, pre-existing weaknesses in the brittle upper crust undergo frictional reactivation when they are appropriately oriented relative to the far-field stress (Section 3.4). On the other hand, weak zones with relatively low viscosity in the viscous lower crust or lithospheric mantle influence deformation by localising and/or re-orienting strain, as demonstrated by brittle-ductile analogue models (Section 3.2). In natural rifts, this distinction may be used to determine whether the inherited weakness lies in the frictional or viscous crustal regimes (cf. Holdsworth et al., 2001a; Fig. 1).

4.2. Hard and soft-linkage classification

The natural examples presented in Section 3.1 demonstrate an array of geometric relationships between pre-existing structures and younger rift-related faults (Fig. 6). We suggest that these relationships can be classified into hard- and soft-linked inheritance, to denote whether a rift-related fault is physically connected to a deeper pre-existing structure (Fig. 19c and d): **Hard-linked inheritance** is characterised by a physical link between a deeper pre-existing structure and a younger, rift-related fault in the overlying sedimentary cover. **Soft-linked inheritance** is defined as the apparent influence of a deeper pre-existing structure on a rift-related fault, where a physical link between the two is not observed. We note that this classification does not describe the genetic relationship between the pre-existing and rift-related structures or the inheritance mechanism (Fig. 19a and b).

4.2.1. Hard-linked inheritance

A shallow, rift-related fault and a deeper, pre-existing structure are classified as hard-linked if they have identical strike and dip direction and an exploitative, merging, or cross-cutting relationship (*sensu* Phillips et al., 2016; Section 3.1.2) (Fig. 19). We established that an exploitative relationship between a rift-related fault and pre-existing weakness (Fig. 6a) relies on reactivation of the pre-existing weakness. The relative contributions of strain re-orientation and reactivation mechanisms to the merging and cross-cutting relationships are exemplified by rift-related normal faults that inherit the strike of a nearby, pre-existing

shear zone with a gentler dip than the rift-related normal faults (e.g., Fazzlikhani et al., 2017; Rotevatn et al., 2018; Osagiede et al., 2020). Geometric similarity between the rift-related faults and the pre-existing shear zone may be initiated by strain re-orientation, for example caused by a pervasive grain-scale fabric that formed in the same deformation event as the shear zone (Kirkpatrick et al., 2013). In this case, movement along the weak layers within the fabric enables strain re-orientation. Evidence from in-situ stress measurements and earthquake focal mechanisms suggest that such strain re-orientation is associated with local re-orientation of the far-field maximum (and minimum) horizontal stress trajectories by the mechanically weak zones (Bell, 1996; Morley, 2010).

The combination of geometric similarity with hard-linked inheritance may be limited to deeper rift-related faults which are closer to the pre-existing structure in terms of vertical distance (Section 3.2.3). This depth dependence is demonstrated by rift-related faults that are segmented and oblique to a pre-existing structure in the upper part of the cover but appear to merge into a continuous structure striking parallel to the pre-existing structure at depth, where the weak (relative to the surrounding rock) pre-existing structure has re-oriented the local stress field (Tingay et al., 2010b; Deng et al., 2017b; Collanega et al., 2019). The influence of this pre-existing weakness decreases with increasing vertical distance from the basement structure. Near the surface, the far-field stresses have a greater influence on fault orientation (Yale, 2003), so that the shallow faults exhibit an *en échelon* arrangement that strikes parallel to the basement structure and perpendicular to the far-field extension direction (i.e., the minimum horizontal far-field stress) (Fig. 3).

4.2.2. Soft-linked inheritance

The soft-linked inheritance classification applies when rift-related faults are spatially co-located with a deep pre-existing structure, but the fault strikes are oblique to both the pre-existing structure and inferred regional extension direction (e.g., Samsu et al., 2019) and/or we cannot observe hard linkage between the pre-existing structure and rift-related fault in cross section (e.g., Phillips et al., 2022). Analogue experiments suggest that such “misoriented” faults form when the pre-existing structures behave in a viscous as opposed to frictional manner during rifting, regardless of whether they are discrete or pervasive (Section 3.2). Models with a discrete weakness in the ductile lower crust, which strikes $\leq 45^\circ$ relative to the extension direction, demonstrate the formation of extension-oblique faults in the overlying crust (Agostini et al., 2009; Corti et al., 2013b) (Fig. 14). Dip-slip kinematics and slip re-orientation along the extension-oblique faults (Philippon et al., 2015) reflect strain re-orientation near the boundary between the weaker and stronger lower crust domains and in the overlying upper crust. Strain re-orientation can also occur across a wider area when the ductile layer is mechanically anisotropic, with pervasive, closely spaced weaknesses that are oblique to the far-field extension direction (Samsu et al., 2021). The anisotropy gives rise to transtensional strain, even under boundary conditions that simulate orthogonal rifting, resulting in sets of non-Andersonian faults with strikes that are oblique to the anisotropy in map view (cf. Fig. 16).

The presence of a relatively weak, ductile layer (e.g., clay, salt) can decouple the basement from cover units, as observed in seismic reflection data and through in-situ stress measurements (Bell, 1996) (Fig. 11, Fig. 10). Where an intervening weak layer is present between two cover units, this decoupling effect can result in a combination of soft-linked and hard-linked inheritance. In this case, the pre-existing basement weakness is geometrically similar to rift-related faults below the mechanically weak layer but geometrically dissimilar to an *en échelon* fault array above the weak layer (e.g., Jackson and Rotevatn, 2013; Roche et al., 2020; Phillips et al., 2022).

The spatial co-location of inferred, deep-seated basement structures with transfer zones (also known as accommodation zones) that separate distinct rift segments and basins (e.g., Rowland and Sibson, 2004; Fossen et al., 2016) can also be described as soft-linked inheritance. The

absence of cover faults parallel to the inferred pre-existing structures imply that the pre-existing structures were not directly reactivated and are not hard-linked to any of the rift-related faults. Therefore, we can infer that the pre-existing structure, which strikes at a high angle to the main rift trend, is not favourably oriented for reactivation but locally re-orientates the far-field extension direction. While it is widely acknowledged that such pre-existing structures contribute to continental-scale rift segmentation, there is scope for further exploring the relationship between soft-linked inheritance and the formation of sub-basin-scale relay structures (cf. Fossen and Rotevatn, 2016).

4.3. Applying the structural inheritance framework to the East African Rift System

In the following section, we use the East African Rift System (EARS) to consider how the structural inheritance framework presented above (Sections 4.1 and 4.2) can be applied to a continental rift. We have chosen an active rift as multi-disciplinary and multi-scale datasets are readily available to constrain rift extension directions (e.g., geodesy, earthquake focal mechanisms, fault slickensides) and hence to investigate the occurrence of reactivation and strain re-orientation inheritance mechanisms. Furthermore, as the pre-eminent example of an active continental rift, the EARS allows us to investigate inheritance at all stages of continental rift evolution from nascent seafloor spreading in Afar to incipient faulting in the Okavango Rift of Botswana (Fig. 2; McConnell, 1972; Chorowicz, 2005; Ebinger, 2005; Macgregor, 2015; Daly et al., 2020).

Hard- and soft-linked structural inheritance has influenced the evolution of the EARS at many spatial scales (and also magma emplacement mechanisms and volcanic activity; see Corti et al., 2022 for examples from the Main Ethiopian Rift). A famous example of plate-scale inheritance is present south of the Main Ethiopian Rift, where the Eastern and Western Branches of the EARS wrap around the relatively rigid Archean Tanzanian craton and spatially co-locate with orogenic belts that formed during the progressive Proterozoic amalgamation of the African Continent (Fig. 2; Daly et al., 1989; Versfelt and Rosendahl, 1989; Nyblade and Brazier, 2002; Corti et al., 2007). New geodetic and geologic evidence indicates that this is just one of several cases of plate-scale structural inheritance where the EARS bifurcates to co-locate with pre-existing weak zones around Archean cratons; in this context, the initiation and propagation of EARS rifting appears to be facilitated by relatively weak, previously deformed Proterozoic lithosphere that bound more rigid blocks (Fig. 2; Daly et al., 2020; Stamps et al., 2021; Wedmore et al., 2021). However, these pre-existing structures alone may not be sufficient for the extension of thick, cold, continental lithosphere in the magma-poor western branch of the EARS to proceed to full continental break-up (Muirhead et al., 2019; Brune et al., 2023).

At the ~ 10 – 100 km scale, the EARS can be divided along strike into distinct half-graben or graben basins (e.g. Ebinger et al., 1987; Laó-Dávila et al., 2015). It is debated whether the along-strike extent of these basins is guided by the intrinsic strength of the lithosphere or pre-existing rift-perpendicular structures (e.g., Fig. 12 and Fig. 20) (Ebinger et al., 1987; Ebinger, 1989; Upcott et al., 1996; Katumwehe et al., 2015; Laó-Dávila et al., 2015; Heilman et al., 2019; Scholz et al., 2020; Corti et al., 2022; Kolawole et al., 2022); nevertheless, in either case the patterns of faulting within these basins can be linked to structural inheritance. The most commonly described examples are fault traces that are subparallel to surface foliations (i.e., “geometric similarity”) imparted by Proterozoic orogenic events in East Africa, as observed, for example, in the Malawi (Fig. 21) (Ring, 1994; Laó-Dávila et al., 2015; Dawson et al., 2018; Hodge et al., 2018; Kolawole et al., 2018; Williams et al., 2019; Scholz et al., 2020; Shillington et al., 2020; Wedmore et al., 2020b), Albertine (Fig. 12) (Katumwehe et al., 2015; Kolawole et al., 2021a), Kivu (Smets et al., 2016; Delvaux et al., 2017), Kenya (Smith and Mosley, 1993; Robertson et al., 2016; Muirhead and Kattenhorn, 2018; Ragon et al., 2019), Turkana (Fig. 20; Vétel et al.,

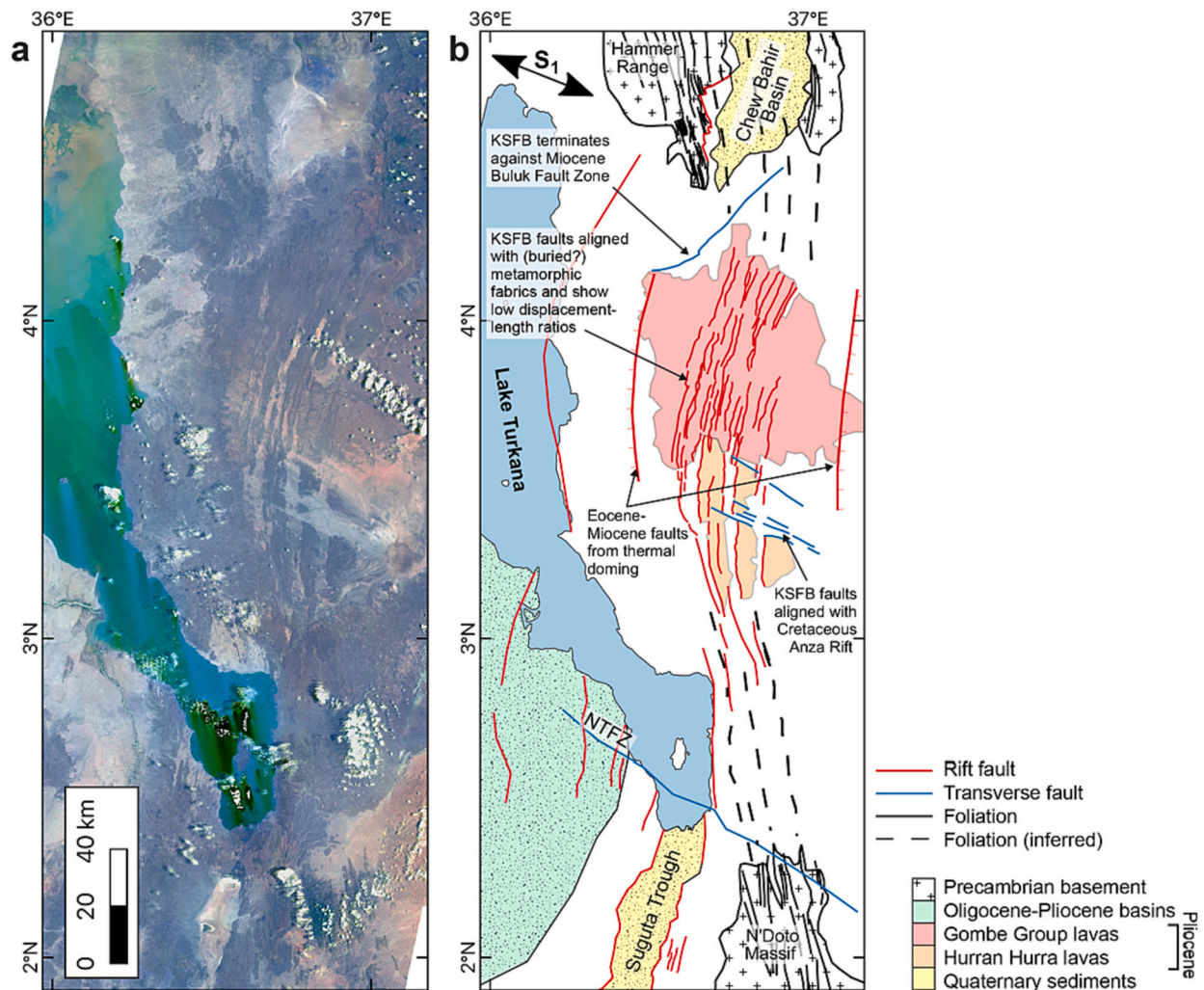


Fig. 20. Basin-scale structural inheritance in the Turkana Rift. (a) Landsat 8 natural colour image and (b) simplified geological map (after Vétel et al., 2005, and references therein). We highlight in (b) the influence of structural inheritance on the post-Pliocene Kino Sogo Fault Belt (KSFB) from: (1) an arcuate belt of Proterozoic metamorphic fabrics that are inferred to occur from the Hammer Range in the north, below faulted Pliocene-age lavas within the KSFB, to the N'Doto massif in the south; (2) NW-SE striking structures from Cretaceous-Paleogene Anza Rift; and (3) Eocene-Miocene faults that formed in response to magmatism and thermal doming, and that uplifted and tilted the KSFB block (Vétel et al., 2005). Landsat 8 image provided from USGS Earth Explorer. NTFZ = N'Doto Transverse Fault Zone; S_1 = extension direction.

2005; Nutz et al., 2022), the Main Ethiopian (Corti et al., 2022), Okavango (Kinabo et al., 2007), Tanganyika (Daly et al., 1989; Muirhead et al., 2019; Shaban et al., 2023), and Rukwa Rifts (Morley, 2010; Delvaux et al., 2012; Heilman et al., 2019; Kolawole et al., 2021b). East Africa also experienced a Mesozoic (or “Karoo”) phase of rifting related to Gondwana fragmentation. The segmentation and orientation of Karoo structures was also affected by Proterozoic structures and fabrics (Ring, 1994; Delvaux, 2001; Paton, 2006; Bingen et al., 2009; Kolawole et al., 2022). In turn, Karoo structures have been reactivated during East African rifting (Castaing, 1991; Macgregor, 2015; Daly et al., 2020; Wedmore et al., 2020b, 2022) or have influenced rift segmentation (Accardo et al., 2018), depending on their orientation relative to the regional stresses. Strain localisation during multiphase rifting is also controlled by changes in rheology. For example, the Turkana Depression, a WNW-ESE trending failed Mesozoic rift zone, comprised thinned and weak lithosphere that may have localised strain during the initial East African rift phase (Morley et al., 1992). However, subsequent Paleogene and Miocene rift phases are interpreted to have strengthened the lithosphere (due to crustal thinning and thermal re-equilibration of the lithosphere; Brune et al., 2017; Ogden et al., 2023), causing fault activity in the Turkana Depression to migrate eastwards away from the

initial locus of rifting (Ebinger et al., 2000).

The 3D geometric relationship between faults and fabrics in the EARS at depth is uncertain. However, it is likely that where fabrics are moderately dipping (e.g., southern Malawi Rift, Fig. 21a; Wedmore et al., 2020b), relationships are exploitative (*sensu* Phillips et al., 2016). Merging or cross-cutting relationships are present in regions where the fabrics are subvertical (e.g., northern Malawi Rift; Dawson et al., 2018; Kolawole et al., 2018). Geometric similarity is not ubiquitous within the EARS. For example, some faults in the Tanganyika Rift and central Malawi Rift are not parallel to surrounding crustal fabrics (Muirhead et al., 2019; Scholz et al., 2020), and the degree to which metamorphic fabrics influence fault orientations can change as rift extension progresses (Muirhead and Kattenhorn, 2018; Nutz et al., 2022). Furthermore, local variations in fabric orientation may disrupt geometric similarity at the scale of an individual fault, resulting in faults that locally cross-cut fabrics, along-strike fault segmentation, and/or faults that are Z-shaped in plan-view due to scarps that are continuous across perpendicular bends (Fig. 21b; Hodge et al., 2018; Corti et al., 2022).

When invoking a mechanism for the geometric similarity in the EARS it is not always clear if: (1) fabrics are non-optimally oriented to the regional extensional direction, but reactivate because they are

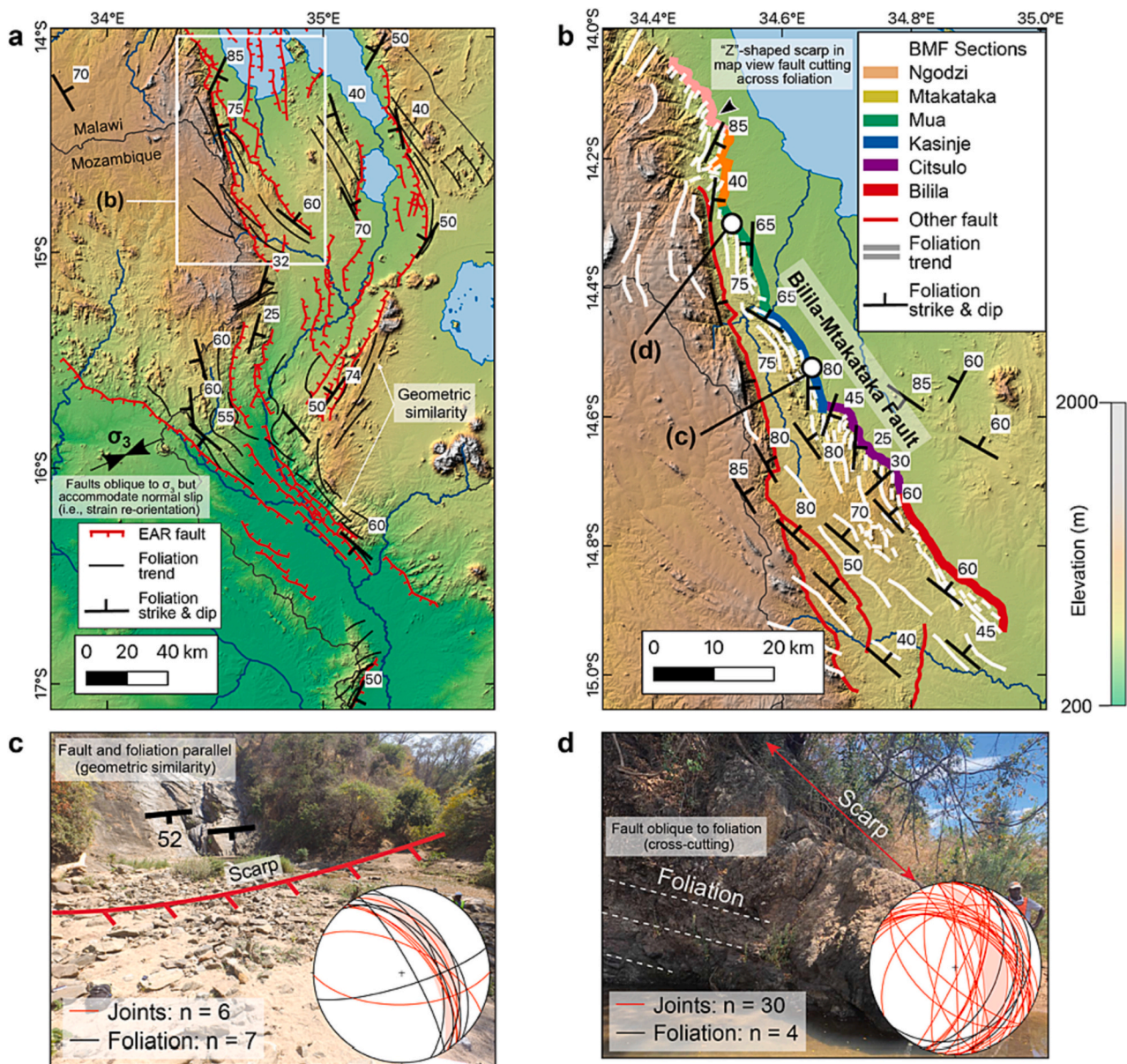


Fig. 21. (a) Basin and (b-d) fault-scale structural inheritance in the EARS using the example of southern Malawi Rift and the Bilila-Mtakataka Fault (BMF) (Jackson and Blenkinsop, 1997; Hodge et al., 2018). (a) Surface traces of faults and foliation in southern Malawi (Williams et al., 2019, 2021; Kolawole et al., 2021a). Trend of the minimum principal compressive stress (σ_3), foliation trend lines and strike and dip measurements from (Williams et al., 2019 and references therein). (b) Map of the BMF and surrounding surface foliation orientations (Hodge et al., 2018 and references therein). The relative orientation of the fault, surrounding foliation, and along strike minima in fault scarp height have been used to divide it into the sections illustrated by thick, coloured lines (Hodge et al., 2018). Field examples of where the BMF is (c) parallel and (d) oblique to the surrounding foliation (Williams et al., 2022). Equal area, lower hemisphere stereonet projections indicate relative orientations of foliation planes and joints in damage zones surrounding faults, shaded great circle region indicates local trend of BMF scarp and a range of plausible fault dips (40–65°; Hodge et al., 2018; Stevens et al., 2021; Williams et al., 2022). Maps in (a) & (b) are underlain by SRTM 30 m DEM and TanDEM-X 12 m DEM respectively.

frictionally weak and/or incohesive (i.e., hard-linked exploitative reactivation, Fig. 6a; Dawson et al., 2018; Wedmore et al., 2020b), (2) fabrics are optimally oriented to the regional extension direction and so geometric similarity is a coincidence (Baker et al., 1972; Smith and Mosley, 1993), or (3) non-optimally oriented fabrics are actively rotating the local (i.e., at the scale of the fault; Twiss and Unruh, 1998) extension direction, so that foliation-parallel faults exhibit dip-slip displacement despite striking oblique to the regional extension direction (Fig. 21b) (Tingay et al., 2010b; Corti et al., 2013b, 2022; Muirhead and Kattenhorn, 2018; Williams et al., 2019). Analogue models imply that the latter is an example of soft-linked structural inheritance, as these local extension directions reflect deep-seated (not surface or

shallow) weaknesses in the crust (Corti et al., 2013b; Philippon et al., 2015). Therefore, mechanisms (1) and (3) could apply at different depths to the same fault (Hodge et al., 2018; Wedmore et al., 2020b).

Structural inheritance in the EARS is not limited to geometric similarity. For example, as rift extension proceeds in the EARS, it is typically observed that strain migrates from large basin-bounding faults to a network of smaller intrabasin faults in the rift valley (Ebinger, 2005). Early localisation of rift-related strain onto a border fault may be facilitated by the exploitation of a discrete pre-existing weakness (e.g., a terrane boundary or viscous shear zone; Wheeler and Karson, 1989; Katumwehe et al., 2015; Scholz et al., 2020; Wedmore et al., 2020b; Kolawole et al., 2021b). Alternatively, pervasive lateral heterogeneities

in the crust (e.g., a wide anastomosing shear zone) can promote distributed deformation involving migration of extensional strain from the basin boundary to intrabasin faults (Kolawole et al., 2018, 2021b; Wedmore et al., 2020a). Normal fault lengthening by exploitation of pre-existing fabrics (Section 3.1.5; Walsh et al., 2002) may account for why faults in the EARS achieved their full length at an early stage of their displacement accumulation (Fig. 20) (Vétel et al., 2005; Accardo et al., 2018; Corti et al., 2019; Ojo et al., 2022) and exhibit narrow fault damage zones (Fig. 21c) (Hodge et al., 2020; Carpenter et al., 2022; Williams et al., 2022). Therefore, an important observation at the <100 km scale is that although the EARS is a classic example of plate-scale structural inheritance and co-location with relatively weak lithosphere (e.g., Versfelt and Rosendahl, 1989), this inheritance is not synonymous with reactivation. Instead, reactivation is limited to where discrete, relatively weak structures are available in an orientation that is favourable for reactivation as the dominant (frictional or viscous) deformation mechanism (Wheeler and Karson, 1989; Kolawole et al., 2018; Heilman et al., 2019). However, at depths or locations where such structures are not available, the orientations and dimensions of new structures are locally variable and likely related to underlying basement anisotropy (Hodge et al., 2018; Williams et al., 2019; Wedmore et al., 2020b; Carpenter et al., 2022).

4.4. Implications of structural inheritance for natural hazards and resources

Conceptual understanding of tectonic inheritance and fault/fabric reactivation has been integrated into previous studies on rift evolution and basin formation in the context of paleotectonic reconstructions (e.g., Gouiza and Paton, 2019; Heron et al., 2019) and hydrocarbon exploration (e.g., Morley, 1995; Lyon et al., 2007; Whipp et al., 2014; Wang et al., 2021b). However, there is still scope for investigating the wide-ranging implications of structural inheritance from a hazards and risk, geo-energy, and minerals exploration perspective.

Seismic hazard investigation is a practical application for the study of structural inheritance in rift basins. For example, since there is spatial co-location between rift basins and Proterozoic orogenic belts in the EARS (Section 4.3), historical seismicity in East Africa is broadly co-located with these pre-existing structures (Fairhead and Henderson, 1977; Sykes, 1978; Craig et al., 2011). Indeed, it has been demonstrated that individual earthquakes in the EARS can have slip surfaces subparallel to pre-existing metamorphic fabrics (Kolawole et al., 2018). Further, the influence of structural inheritance on the distribution of extensional strain between border and intra-rift faults will dictate whether regions of high seismic hazard are in the basin interior or along the margin(s) (Dawson et al., 2018; Wedmore et al., 2020a; Williams et al., 2021). Pre-existing crustal fabrics also modulate the along-strike segmentation of faults, and this can affect whether faults rupture in relatively frequent, moderate-magnitude segmented fault ruptures, or more uncommon whole-fault, large magnitude ruptures (Biasi and Wesnousky, 2016; Hodge et al., 2015, 2018; Wedmore et al., 2020b). There is also increasing evidence that the dynamics of individual earthquake ruptures (e.g., stress drop, fracture energy, ground motions, slip distributions) will be influenced by pre-existing structures (Heermann, 2003; Williams et al., 2022; Nevitt et al., 2023; Mo and Attanayake, 2023). These implications of structural inheritance for earthquake modelling and hazards assessment are worthy of further study, including in “stable” continental regions, where earthquakes are often observed to follow pre-existing structures (e.g., Calais et al., 2016; Yang et al., 2021; Rimando and Peace, 2021; Muir et al., 2023).

From a geo-energy perspective, inherited structures can impact the architecture of fluid flow pathways, including connectivity between deep and shallow units. The extraction of geothermal energy and the formation of hydrothermal mineral systems rely on hydrothermal fluid circulation, which is affected by the spatiotemporal pattern of deformation. For example, heat and mass transfer from deep sources to

shallower depths are facilitated by convection through networks of open fractures (e.g., Rowland and Simmons, 2012). These fractures are especially important in rocks with low primary porosity and permeability, such as crystalline basement. At the plate scale, tectonic inheritance controls the location and lithology of sedimentary basins as well as the preservation of fluid pathways between deep heat and metal sources and shallow reservoirs (e.g., Hoggard et al., 2020). At the basin scale, rifting can bring about favourable stress conditions for reactivating pre-existing faults as permeable fractures.

The Upper Rhine Graben is an example of a deep geothermal system where the most permeable reservoir is located at the top of the granitic basement (e.g., Vidal and Genter, 2018; Glaas et al., 2021). NNW-SSE to N-E striking Variscan faults and fabrics in the basement may have been reactivated in a normal sense during the basin’s multiphase history of Cenozoic regional shortening and extension (e.g., Schumacher, 2002), contributing to thick (i.e., wide-aperture) fractures with enhanced permeability (Glaas et al., 2021). Bertrand et al. (2018) show that pre-existing faults, fabrics, and lithologies in the Upper Rhine Graben can impact fracture patterns at some scales but not others, demonstrating that the impact of inheritance on flow modelling is scale dependent. Structural mapping, with an aim to understand the multi-scale controls of inheritance on fractures, has been applied to other geothermal systems, including in France (Dezayes et al., 2010), Mexico (Norini et al., 2019), and the UK (Yeomans et al., 2020).

In the Taupō Volcanic Zone (New Zealand), structural inheritance appears to control shallow geothermal systems and the formation of hydrothermal gold and silver deposits at <2000 m depths (i.e., epithermal ore deposits). Upwelling of hot water plumes is enhanced at the intersections of mapped or inferred structures, including faults, basement-controlled transfer zones, and caldera boundaries (Rowland and Sibson, 2004; Rowland and Simmons, 2012; Villamor et al., 2017; Milicich et al., 2021). Rowland and Sibson (2004) associated the segmentation of the NNE-SSW trending rift system, via so-called accommodation zones, with WNW-ESE trending basement structures interpreted from geophysics. The same geometric relationship has also been inferred for the similarly NNE-SSW trending Coromandel Volcanic Zone farther north (Bahiru et al., 2019). Rowland and Simmons (2012) suggested that such basement structures may be physically linked with potentially permeable shear zones in the lower crust, enabling fluid transport across the frictional-viscous transition zone (Cox et al., 2001), though at present there is no evidence of hard linkage between the basement structures and shallower rift-related structures.

Inheritance of lithospheric boundaries and crustal-scale weaknesses during rifting contributes to the formation of world-class sediment-hosted base metal deposits (i.e., copper, lead, zinc, and nickel) near craton edges (e.g., Mount Isa, Australia; Gibson et al., 2016; Hoggard et al., 2020). Here, the long-lived nature of the craton edge is attributed to focusing of deformation over multiple extensional and contractional events. Rifting of thick cratonic lithosphere facilitates the formation of deep, widely spaced faults that remain active (through reactivation) for up to 100 Ma, extending the time window for mineralisation (Allen and Armitage, 2012) and the distribution of basin fill lithologies that are conducive to mineralisation (Hoggard et al., 2020 and references therein). In addition, reactivation of crustal structures maintains focused fluid flow between the deep and shallow levels of basins (Gibson et al., 2016).

The examples we discuss here suggest that there is scope for applying our knowledge of lithospheric and crustal-scale controls of inheritance to geothermal and mineral systems, which can contribute to successful exploration and development of geothermal energy, base metals, and critical metals. Characterising pre-existing structures in detail and quantifying their reactivation potential under in-situ stresses are essential for geothermal drilling projects (Deichmann and Giardini, 2009; Diehl et al., 2017), in addition to exploring the feasibility of geological storage of both CO₂ (e.g., Andrés et al., 2016) and disposal of spent nuclear fuel (e.g., Barton and Zoback, 1994) to support the current energy transition.

5. Concluding remarks

Compositional heterogeneities and mechanical discontinuities in pre-deformed lithosphere can locally alter the local stress and/or strain field. This structural inheritance, which has been observed from the plate scale down to the outcrop scale, is probably the norm rather than exception, and it influences the location and geometry of entire rift systems, basins, and faults during rifting. Lithospheric and crustal-scale zones of weakness facilitate localised thinning, that contributes to the formation and propagation of rifts along inherited higher strain belts, and guides potential magmatism. At the same scale, accommodation zones are spatially co-located with inferred deep-seated structures that strike at high angles to the main rift. The boundaries and evolution of rift basins are controlled by boundary faults that, if inconsistent with the far-field strain, may indicate exploitation of a reactivated basement weakness and/or reflect a locally re-oriented strain field above a deep, potentially viscously deforming structure. Individual faults at the sub-basin scale may also exploit weak surfaces in the basement or a pre-existing rift fabric. Some faults may appear to be unaffected by inheritance and reflect the far-field regional extension, suggesting that the vertical and lateral extents of stress and strain re-orientation are limited by the depth, size, orientation, and relative strength of the pre-existing structure. Additionally, the influence of the pre-existing structure over time is modulated by weakening or strengthening (e.g., healing), as well as the evolving thermal and rheological structure of the lithosphere during rifting (e.g., Bell et al., 2014; Claringbould et al., 2017).

We have distilled observations of structural inheritance into two key mechanisms: reactivation and strain re-orientation. One or both of these mechanisms are activated when extension affects two mechanically distinct terranes or occurs in the presence of a pre-existing, anomalously weak (or strong) structure within relatively homogeneous-strength rock. Reactivation is generally associated with geometric similarity and hard linkage between a pre-existing structure and younger, rift-related faults. These observations are consistent with many of the expressions of inheritance found around the world, most notably around the Atlantic passive margins and in the East African Rift System (Table 1). However, strain re-orientation is invoked for observations of soft linkage, particularly where a rift-related fault is oblique to both the far-field extension direction and pre-existing structures (e.g., Tingay et al., 2010b; Giba et al., 2012; Collanega et al., 2019; Phillips et al., 2022). While strain re-orientation is not as readily recognisable as reactivation, further understanding of the conditions under which strain re-orientation applies can help us explain the presence of complex fault patterns in rift basins, better constrain the far-field paleostress in ancient rifts, and more confidently map basement structures under cover. The conclusion that structural inheritance in rift settings is the norm, not the exception, implies that inheritance mechanisms are also important in other tectonic settings (e.g., strike-slip and orogenic systems); examining whether or not this is true could be a fruitful avenue for future research.

In this review, we offer ideas on how our collective knowledge of structural inheritance in rift basins (summarised in Section 3) can be organised into a loose framework for: (i) identifying natural examples of structural inheritance, (ii) considering possible mechanisms for this inheritance and the conditions that promote them, and (iii) evaluating how structural inheritance can impact projects related to geological hazards and natural resources. We acknowledge fully that the framework presented here can be expanded upon as new insights emerge. Recognising the various expressions and drivers of structural inheritance is a necessary step in broadening and deepening our understanding of this phenomenon.

Declaration of Competing Interest

The authors declare that they have no known competing financial interests or personal relationships that could have appeared to influence the work reported in this paper.

Data availability

No data was used for the research described in the article.

Acknowledgements

A. Samsu was supported by a Monash University Faculty of Science Dean's International Postgraduate Research Scholarship. The work was also made possible by the Australian Research Council Linkage grant LP190100146 and MRIWA project no. M554. We thank Gillian R. Foulger for editorial handling of this contribution and three anonymous reviewers, whose thorough and constructive comments have significantly improved the manuscript.

References

- Accardo, N.J., Shillington, D.J., Gaherty, J.B., Scholz, C.A., Nyblade, A.A., Chindandali, P.R.N., Kamihanda, G., McCartney, T., Wood, D., Wambura Ferdinand, R., 2018. Constraints on Rift Basin Structure and Border Fault Growth in the Northern Malawi Rift From 3-D Seismic Refraction Imaging. *J. Geophys. Res. Solid Earth* 123. <https://doi.org/10.1029/2018JB016504>, 3–10,10,25.
- Acocella, V., Faccenna, C., Funicello, R., Rossetti, F., 1999. Sand-box modelling of basement-controlled transfer zones in extensional domains. *Terra Nova* 11, 149–156. <https://doi.org/10.1046/j.1365-3121.1999.00238.x>.
- Agostini, A., Corti, G., Zeoli, A., Mulugeta, G., 2009. Evolution, pattern, and partitioning of deformation during oblique continental rifting: Inferences from lithospheric-scale centrifuge models. *Geochem. Geophys. Geosyst.* 10 <https://doi.org/10.1029/2009GC002676>.
- Allemand, P., Brun, J.-P., 1991. Width of continental rifts and rheological layering of the lithosphere. *Tectonophysics* 188, 63–69. [https://doi.org/10.1016/0040-1951\(91\)90314-1](https://doi.org/10.1016/0040-1951(91)90314-1).
- Allen, P.A., Armitage, J.J., 2012. Cratonic basins. In: Busby, C., Azor, A. (Eds.), *Tectonics of Sedimentary Basins: Recent Advances*. Blackwell Publishing, pp. 602–620.
- Amigo Marx, B., Fernandez, O., Olaiz, A., Poblet, J., Zamora, G., 2022. On the influence of Variscan inheritance on rifting of the Western Iberian margin. *Terra Nova* 34, 424–432. <https://doi.org/10.1111/ter.12595>.
- Anderson, E.M., 1905. The dynamics of faulting. *Trans. Edinb. Geol. Soc.* 8, 387–402. <https://doi.org/10.1144/transed.17.3.217>.
- Andrés, J., Alcalde, J., Ayarza, P., Saura, E., Marzán, I., Martí, D., Catalán, J.R.M., Carbonell, R., Pérez-Estaún, A., Gariña-Lobón, J.L., Rubio, F.M., 2016. Basement structure of the Hontomín CO₂ storage site (Spain) determined by integration of microgravity and 3-D seismic data. *Solid Earth* 7, 827–841. <https://doi.org/10.5194/se-7-827-2016>.
- Ashby, D.E., 2013. *Influences on Continental Margin Development: A Case Study from the Santos Basin, south-eastern Brazil*. Durham University. PhD Thesis.
- Audet, P., Bürgmann, R., 2011. Dominant role of tectonic inheritance in supercontinent cycles. *Nat. Geosci.* 4, 184–187. <https://doi.org/10.1038/ngeo1080>.
- Autin, J., Bellahsen, N., Husson, L., Beslier, M.O., Leroy, S., D'Acremont, E., 2010. Analog models of oblique rifting in a cold lithosphere. *Tectonics* 29, 1–23. <https://doi.org/10.1029/2010TC002671>.
- Autin, J., Bellahsen, N., Leroy, S., Husson, L., Beslier, M.O., D'Acremont, E., 2013. The role of structural inheritance in oblique rifting: Insights from analogue models and application to the Gulf of Aden. *Tectonophysics* 607, 51–64. <https://doi.org/10.1016/j.tecto.2013.05.041>.
- Bahiru, E.A., Rowland, J.V., Eccles, J.D., Kellett, R.L., 2019. Regional crustal-scale structural control on epithermal deposits within the Hauraki Goldfield, Coromandel Volcanic Zone, New Zealand: insight from integrated geological and aeromagnetic structural patterns. *N. Z. J. Geol. Geophys.* 62, 461–482. <https://doi.org/10.1080/00288306.2019.1574268>.
- Bailey, W.R., Walsh, J.J., Manzocchi, T., 2005. Fault populations, strain distribution and basement fault reactivation in the East Pennines Coalfield, UK. *J. Struct. Geol.* 27, 913–928. <https://doi.org/10.1016/j.jsg.2004.10.014>.
- Baker, B.H., Mohr, P.A., Williams, L.A.J., 1972. Geology of the Eastern Rift System of Africa. *GSA Special Papers*, pp. 1–68. <https://doi.org/10.1130/SPE136-p1>.
- Barton, C.A., Zoback, M.D., 1994. Stress perturbations associated with active faults penetrated by boreholes: possible evidence for near-complete stress drop and a new technique for stress magnitude measurement. *J. Geophys. Res. Solid Earth* 99, 9373–9390. <https://doi.org/10.1029/93JB03359>.
- Bell, J.S., 1993. Attached and detached in-situ stress regimes in sedimentary basins. 5th Conference & Technical Exhibition. Euro-pean Association of Petroleum Geoscientists & Engineers, Stavanger, Norway, 7–11 June 1993, F046. <https://doi.org/10.3997/2214-4609.201411772>.
- Bell, J.S., 1996. Petro geoscience 2. In situ stresses in sedimentary rocks (part 2): Applications of stress measurements. *Geosci. Can.* 23, 135–153.
- Bell, R.E., Jackson, C.A.L., Whipp, P.S., Clements, B., 2014. Strain migration during multiphase extension: observations from the northern North Sea. *Tectonics* 33, 1936–1963. <https://doi.org/10.1002/2014TC003551>.
- Bellahsen, N., Daniel, J.M., 2005. Fault reactivation control on normal fault growth: an experimental study. *J. Struct. Geol.* 27, 769–780. <https://doi.org/10.1016/j.jsg.2004.12.003>.

- Beniest, A., Willingshofer, E., Sokoutis, D., Sassi, W., 2018. Extending continental lithosphere with lateral strength variations: effects on deformation localization and margin geometries. *Front. Earth Sci.* 6, 1–11. <https://doi.org/10.3389/feart.2018.00148>.
- Bertrand, L., Jusseume, J., Gérard, Y., Diraison, M., Damy, P.-C., Navelot, V., Haffen, S., 2018. Structural heritage, reactivation and distribution of fault and fracture network in a rifting context: case study of the western shoulder of the Upper Rhine Graben. *J. Struct. Geol.* 108, 243–255. <https://doi.org/10.1016/j.jsg.2017.09.006>.
- Biasi, G.P., Wesnousky, S.G., 2016. Steps and gaps in ground ruptures: empirical bounds on rupture propagation. *Bull. Seismol. Soc. Am.* 106, 1110–1124. <https://doi.org/10.1785/B0120150175>.
- Bingen, B., Jacobs, J., Viola, G., Henderson, I.H.C., Skår, Boyd, Thomas, R.J., Solli, A., Key, R.M., Daudi, E.X.F., 2009. Geochronology of the Precambrian crust in the Mozambique belt in NE Mozambique, and implications for Gondwana assembly. *Precambrian Res.* 170, 231–255. <https://doi.org/10.1016/j.precamres.2009.01.005>.
- Bird, P.C., Cartwright, J.A., Davies, T.L., 2014. Basement reactivation in the development of rift basins: an example of reactivated Caledonide structures in the West Orkney Basin. *J. Geol. Soc.* 172, 77–85. <https://doi.org/10.1144/jgs2013-098>.
- Bladon, A.J., Clarke, S.M., Burley, S.D., 2015. Complex rift geometries resulting from inheritance of pre-existing structures: insights and regional implications from the Barmer Basin rift. *J. Struct. Geol.* 71, 136–154. <https://doi.org/10.1016/j.jsg.2014.09.017>.
- Bosworth, W., Tari, G., 2021. Hydrocarbon accumulation in basins with multiple phases of extension and inversion: examples from the Western Desert (Egypt) and the western Black Sea. *Solid Earth* 12, 59–77. <https://doi.org/10.5194/se-12-59-2021>.
- Brun, J.P., 1999. Narrow rifts versus wide rifts: Inferences for the mechanics of rifting from laboratory experiments. *Philos. Trans. R. Soc. A Math. Phys. Eng. Sci.* 357, 695–712. <https://doi.org/10.1098/rsta.1999.0349>.
- Brun, J.P., Tron, V., 1993. Development of the North Viking Graben: inferences from laboratory modelling. *Sediment. Geol.* 86, 31–51. [https://doi.org/10.1016/0037-0738\(93\)90132-0](https://doi.org/10.1016/0037-0738(93)90132-0).
- Brune, S., Corti, G., Ranalli, G., 2017. Controls of inherited lithospheric heterogeneity on rift linkage: Numerical and analogue models of interaction between the Kenyan and Ethiopian rifts across the Turkana depression. *Tectonics* 1–20. <https://doi.org/10.1002/2017TC004739>.
- Brune, S., Kolawole, F., Olive, J.-A., Stamps, D.S., Buck, W.R., Buitter, S.J.H., Furman, T., Shillington, D.J., 2023. Geodynamics of continental rift initiation and evolution. *Nat. Rev. Earth Environ.* 4, 235–253. <https://doi.org/10.1038/s43017-023-00391-3>.
- Buitter, S.J.H., Torsvik, T.H., 2014. A review of Wilson Cycle plate margins: a role for mantle plumes in continental break-up along sutures? *Gondwana Res.* 26, 627–653. <https://doi.org/10.1016/j.jgr.2014.02.007>.
- Butler, R.W.H., Holdsworth, R.E., Lloyd, G.E., 1997. The role of basement reactivation in continental deformation. *J. Geol. Soc.* 154, 69–71. <https://doi.org/10.1144/gsjgs.154.1.0069>.
- Byerlee, J., 1978. Friction of rocks. *Pure Appl. Geophys.* 116, 615–626. <https://doi.org/10.1007/BF00876528>.
- Calais, E., Camelbeeck, T., Stein, S., Liu, M., Craig, T.J., 2016. A new paradigm for large earthquakes in stable continental plate interiors. *Geophys. Res. Lett.* 43 <https://doi.org/10.1002/2016GL070815>.
- Carpenter, M., Williams, J.N., Fagereng, Å., Wedmore, L.N.J., Biggs, J., Mpheto, F., Mdala, H., Dulanya, Z., Manda, B., 2022. Comparing intrarift and border fault structure in the Malawi Rift: implications for normal fault growth. *J. Struct. Geol.* 165, 104761. <https://doi.org/10.1016/j.jsg.2022.104761>.
- Castaing, C., 1991. Post-Pan-African tectonic evolution of South Malawi in relation to the Karroo and recent East African rift systems. *Tectonophysics* 191, 55–73. [https://doi.org/10.1016/0040-1951\(91\)90232-H](https://doi.org/10.1016/0040-1951(91)90232-H).
- Cayley, R.A., Taylor, D.H., VandenBerg, A.H.M., Moore, D.H., 2002. Proterozoic - Early Palaeozoic rocks and the Tyennan Orogeny in central Victoria: The Selwyn Block and its tectonic implications. *Australian Journal of Earth Sciences* 49, 225–254. <https://doi.org/10.1046/j.1440-0952.2002.00921.x>.
- Chattopadhyay, A., Chakra, M., 2013. Influence of pre-existing pervasive fabrics on fault patterns during orthogonal and oblique rifting: an experimental approach. *Mar. Pet. Geol.* 39, 74–91. <https://doi.org/10.1016/j.marpetgeo.2012.09.009>.
- Chenin, P., Beaumont, C., 2013. Influence of offset weak zones on the development of rift basins: Activation and abandonment during continental extension and breakup. *J. Geophys. Res.* Solid Earth 118, 1698–1720. <https://doi.org/10.1002/jgrb.50138>.
- Childs, C., Manzocchi, T., Walsh, J.J., Bonson, C.G., Nicol, A., Schöpfer, M.P.J., 2009. A geometric model of fault zone and fault rock thickness variations. *J. Struct. Geol.* 31, 117–127. <https://doi.org/10.1016/j.jsg.2008.08.009>.
- Chorowicz, J., 2005. The East African rift system. *J. Afr. Earth Sci.* 43, 379–410. <https://doi.org/10.1016/j.jafrearsci.2005.07.019>.
- Claringbould, J.S., Bell, R.E., Jackson, C.A.L., Gawthorpe, R.L., Odinsen, T., 2017. Pre-existing normal faults have limited control on the rift geometry of the northern North Sea. *Earth Planet. Sci. Lett.* 475, 190–206. <https://doi.org/10.1016/j.epsl.2017.07.014>.
- Collanega, L., Siuda, K., Jackson, A.-L., Bell, R.E., Coleman, A.J., Lenhart, A., Magee, C., Breda, A., 2019. Normal fault growth influenced by basement fabrics: The importance of preferential nucleation from pre-existing structures. *Basin Res.* 31, 659–687. <https://doi.org/10.1111/bre.12327>.
- Collettini, C., Sibson, R.H., 2001. Normal faults, normal friction? *Geology* 29, 927–930. [https://doi.org/10.1130/0091-7613\(2001\)029<0927:NFNF>2.0.CO;2](https://doi.org/10.1130/0091-7613(2001)029<0927:NFNF>2.0.CO;2).
- Collettini, C., Niemeijer, A., Viti, C., Marone, C., 2009a. Fault zone fabric and fault weakness. *Nature* 462, 907–910. <https://doi.org/10.1038/nature08585>.
- Collettini, C., Viti, C., Smith, S.A.F., Holdsworth, R.E., 2009b. Development of interconnected talc networks and weakening of continental low-angle normal faults. *Geology* 37, 567–570. <https://doi.org/10.1130/G25645A.1>.
- Collettini, C., Tesi, T., Scuderi, M.M., Carpenter, B.M., Viti, C., 2019. Beyond Byerlee friction, weak faults and implications for slip behavior. *Earth Planet. Sci. Lett.* 519, 245–263. <https://doi.org/10.1016/j.epsl.2019.05.011>.
- Corti, G., 2004. Centrifuge modelling of the influence of crustal fabrics on the development of transfer zones: insights into the mechanics of continental rifting architecture. *Tectonophysics* 384, 191–208. <https://doi.org/10.1016/j.tecto.2004.03.014>.
- Corti, G., 2008. Control of rift obliquity on the evolution and segmentation of the main Ethiopian rift. *Nat. Geosci.* 1, 258–262. <https://doi.org/10.1038/ngeo160>.
- Corti, G., 2009. Continental rift evolution: From rift initiation to incipient break-up in the Main Ethiopian Rift, East Africa. *Earth Sci. Rev.* 96, 1–53. <https://doi.org/10.1016/j.earscirev.2009.06.005>.
- Corti, G., 2012. Evolution and characteristics of continental rifting: Analog modeling-inspired view and comparison with examples from the East African Rift System. *Tectonophysics* 522–523, 1–33. <https://doi.org/10.1016/j.tecto.2011.06.010>.
- Corti, G., van Wijk, J., Cloetingh, S., Morley, C.K., 2007. Tectonic inheritance and continental rift architecture: Numerical and analogue models of the East African Rift system. *Tectonics* 26, 1–13. <https://doi.org/10.1029/2006TC002086>.
- Corti, G., Iandelli, I., Cerca, M., 2013a. Experimental modeling of rifting at craton margins. *Geosphere* 9, 138–154. <https://doi.org/10.1130/GES00863.1>.
- Corti, G., Philippon, M., Sani, F., Keir, D., Kidane, T., 2013b. Re-orientation of the extension direction and pure extensional faulting at oblique rift margins: comparison between the Main Ethiopian Rift and laboratory experiments. *Terra Nova* 25, 396–404. <https://doi.org/10.1111/ter.12049>.
- Corti, G., Cioni, R., Franceschini, Z., Sani, F., Scaillet, S., Molin, P., Isola, I., Mazzarini, F., Brune, S., Keir, D., Erbello, A., Muluneh, A., Illsley-Kemp, F., Glerum, A., 2019. Aborted propagation of the Ethiopian rift caused by linkage with the Kenyan rift. *Nat. Commun.* 10, 1309. <https://doi.org/10.1038/s41467-019-09335-2>.
- Corti, G., Maestrelli, D., Sani, F., 2022. Large-to Local-Scale Control of Pre-Existing Structures on Continental Rifting: Examples from the Main Ethiopian Rift, East Africa, 10, pp. 1–18. <https://doi.org/10.3389/feart.2022.808503>.
- Courtillot, V., Jaupart, C., Manighetti, I., Taponnier, P., Besse, J., 1999. On causal links between flood basalts and continental breakup. *Earth Planet. Sci. Lett.* 166, 177–195. [https://doi.org/10.1016/S0012-821X\(98\)00282-9](https://doi.org/10.1016/S0012-821X(98)00282-9).
- Cowie, P.A., Underhill, J.R., Behn, M.D., Lin, J., Gill, C.E., 2005. Spatio-temporal evolution of strain accumulation derived from multi-scale observations of Late Jurassic rifting in the northern North Sea: a critical test of models for lithospheric extension. *Earth Planet. Sci. Lett.* 234, 401–419. <https://doi.org/10.1016/j.epsl.2005.01.039>.
- Cox, S.F., 2010. The application of failure mode diagrams for exploring the roles of fluid pressure and stress states in controlling styles of fracture-controlled permeability enhancement in faults and shear zones. *Geofluids* 10, 217–233. <https://doi.org/10.1111/j.1468-8123.2010.00281.x>.
- Cox, S.F., Knackstedt, M.A., Braun, J., 2001. Principles of structural control on permeability and fluid flow in hydrothermal systems. In: Richards, J.P., Tosdal, R.M. (Eds.), *Structural Controls on Ore Genesis*. Society of Economic Geologists, pp. 1–24.
- Craig, T.J., Jackson, J.A., Priestley, K., McKenzie, D., 2011. Earthquake distribution patterns in Africa: their relationship to variations in lithospheric and geological structure, and their rheological implications. *Geophys. J. Int.* 185, 403–434. <https://doi.org/10.1111/j.1365-246X.2011.04950.x>.
- Cruikshank, K.M., Aydin, A., 1995. Unweaving the joints in Entrada Sandstone, Arches National Park, Utah, U.S.A. *J. Struct. Geol.* 17, 409–421. [https://doi.org/10.1016/0191-8141\(94\)00061-4](https://doi.org/10.1016/0191-8141(94)00061-4).
- Daly, M.C., Chorowicz, J., Fairhead, J.D., 1989. Rift basin evolution in Africa: the influence of reactivated steep basement shear zones. *Geol. Soc. Lond., Spec. Publ.* 44, 309–334. <https://doi.org/10.1144/GSL.SP.1989.044.01.17>.
- Daly, M.C., Green, P., Watts, A.B., Davies, O., Chibesakunda, F., Walker, R., 2020. Tectonics and Landscape of the Central African Plateau and their Implications for a Propagating Southwestern Rift in Africa. *Geochem. Geophys. Geosyst.* 21 <https://doi.org/10.1029/2019GC008746>.
- Dávalos-Elizondo, E., Laó-Dávila, D.A., 2023. Structural analysis of fracture networks controlling geothermal activity in the northern part of the Malawi Rifted Zone from aeromagnetic and remote sensing data. *J. Volcanol. Geotherm. Res.* 433 <https://doi.org/10.1016/j.jvolgeores.2022.107713>.
- Dawson, S.M., Laó-Dávila, D.A., Atekwana, E.A., Abdelsalam, M.G., 2018. The influence of the Precambrian Mughese Shear Zone structures on strain accommodation in the northern Malawi Rift. *Tectonophysics* 722, 53–68. <https://doi.org/10.1016/j.tecto.2017.10.010>.
- de Jossineau, G., Petit, J.P., Gauthier, B.D.M., 2003. Photoelastic and numerical investigation of stress distributions around fault models under biaxial compressive loading conditions. *Tectonophysics* 363, 19–43. [https://doi.org/10.1016/S0040-1951\(02\)00648-0](https://doi.org/10.1016/S0040-1951(02)00648-0).
- De Paola, N., Holdsworth, R.E., McCaffrey, K.J.W., 2005. The influence of lithology and pre-existing structures on reservoir-scale faulting patterns in transensional rift zones. *J. Geol. Soc.* 162, 471–480. <https://doi.org/10.1144/0016-764904-043>.
- Deichmann, N., Giardini, D., 2009. Earthquakes induced by the stimulation of an enhanced geothermal system below Basel (Switzerland). *Seismol. Res. Lett.* 80, 784–798. <https://doi.org/10.1785/gssrl.80.5.784>.
- Delvaux, D., 2001. Tectonic and palaeostress evolution of the Tanganyika-Rukwa-Malawi rift segment, East African Rift System. In: Ziegler, P.A., Cavazza, W., Robertson, A.H.F., Crasquin-Soleau, S. (Eds.), *Peri-Tethys Memoir 6: Peri-Tethyan Rift/Wrench Basins and Passive Margins*, pp. 545–567.
- Delvaux, D., Barth, A., 2010. African stress pattern from formal inversion of focal mechanism data. *Tectonophysics* 482, 105–128. <https://doi.org/10.1016/j.tecto.2009.05.009>.

- Delvaux, D., Kervyn, F., Macheyski, A.S., Temu, E.B., 2012. Geodynamic significance of the TRM segment in the East African Rift (W-Tanzania): active tectonics and paleostress in the Ufipa plateau and Rukwa basin. *J. Struct. Geol.* 37, 161–180. <https://doi.org/10.1016/j.jsg.2012.01.008>.
- Delvaux, D., Mulumba, J.-L., Sebagenzi, M.N.S., Bondo, S.F., Kervyn, F., Havenith, H.-B., 2017. Seismic hazard assessment of the Kivu rift segment based on a new seismotectonic zonation model (western branch, East African Rift system). *J. Afr. Earth Sci.* 134, 831–855. <https://doi.org/10.1016/j.jafrearsci.2016.10.004>.
- Demurtas, M., Fondriest, M., Balsamo, F., Clemenzi, L., Storti, F., Bistacchi, A., Di Toro, G., 2016. Structure of a normal seismogenic fault zone in carbonates: the Vado di Corno Fault, Campo Imperatore, Central Apennines (Italy). *J. Struct. Geol.* 90, 185–206. <https://doi.org/10.1016/j.jsg.2016.08.004>.
- Deng, H., McClay, K., 2021. Three-dimensional geometry and growth of a basement-involved fault network developed during multiphase extension, Enderby Terrace, North West Shelf of Australia. *Bull. Geol. Soc. Am.* 133, 2051–2078. <https://doi.org/10.1130/B35779.1>.
- Deng, C., Fossen, H., Gawthorpe, R.L., Rotevatn, A., Jackson, C.A.L., Fazlikhani, H., 2017a. Influence of fault reactivation during multiphase rifting: the Oseberg area, northern North Sea rift. *Mar. Pet. Geol.* 86, 1252–1272. <https://doi.org/10.1016/j.marpetgeo.2017.07.025>.
- Deng, C., Gawthorpe, R.L., Finch, E., Fossen, H., 2017b. Influence of a pre-existing basement weakness on normal fault growth during oblique extension: Insights from discrete element modeling. *J. Struct. Geol.* 105, 44–61. <https://doi.org/10.1016/j.jsg.2017.11.005>.
- Deng, C., Gawthorpe, R.L., Fossen, H., Finch, E., 2018. How does the orientation of a preexisting basement weakness influence fault development during renewed rifting? Insights from three-dimensional discrete element modeling. *Tectonics* 37, 2221–2242. <https://doi.org/10.1029/2017TC004776>.
- Deng, H., McClay, K., Bilal, A., 2020. 3D structure and evolution of an extensional fault network of the eastern Dampier Sub-basin, North West Shelf of Australia. *J. Struct. Geol.* 132, 103972. <https://doi.org/10.1016/j.jsg.2019.103972>.
- Dezayes, C., Genter, A., Valley, B., 2010. Overview of the Fracture Network at Different Scales Within the Granite Reservoir of the EGS Soultz Site (Alsace, France). *Proceedings World Geothermal Congress 2010*, Bali, Indonesia, p. 13.
- Diehl, T., Kraft, T., Kissling, E., Wiemer, S., 2017. The induced earthquake sequence related to the St. Gallen deep geothermal project (Switzerland): fault reactivation and fluid interactions imaged by microseismicity. *J. Geophys. Res. Solid Earth* 122, 7272–7290. <https://doi.org/10.1002/2017JB014473>.
- Doré, A.G., Lundin, E.R., Fichler, C., Olesen, O., 1997. Patterns of basement structure and reactivation along the NE Atlantic margin. *J. Geol. Soc.* 154, 85–92.
- Duffy, O.B., Bell, R.E., Jackson, C.A.L., Gawthorpe, R.L., Whipp, P.S., 2015. Fault growth and interactions in a multiphase rift fault network: Horda Platform, Norwegian North Sea. *J. Struct. Geol.* 80, 99–119. <https://doi.org/10.1016/j.jsg.2015.08.015>.
- Dunbar, J.A., Sawyer, D.S., 1989. How preexisting weaknesses control the style of continental breakup. *J. Geophys. Res.* 94, 7278–7292. <https://doi.org/10.1029/JB094iB06p07278>.
- Ebinger, C.J., 1989. Tectonic development of the western branch of the East African rift system. *Geol. Soc. Am. Bull.* [https://doi.org/10.1130/0016-7606\(1989\)101<0885:TDOTWB>2.3.CO;2](https://doi.org/10.1130/0016-7606(1989)101<0885:TDOTWB>2.3.CO;2).
- Ebinger, C., 2005. Continental break-up: the East African perspective. *Astron. Geophys.* 46, 2.16–2.21. <https://doi.org/10.1111/j.1468-4004.2005.46216.x>.
- Ebinger, C.J., Rosendahl, B.R., Reynolds, D.J., 1987. Tectonic model of the Malawi rift, Africa. *Tectonophysics* 141, 215–235. [https://doi.org/10.1016/0040-1951\(87\)90187-9](https://doi.org/10.1016/0040-1951(87)90187-9).
- Ebinger, C.J., Yemane, T., Harding, D.J., Tesfaye, S., Kelley, S., Rex, D.C., 2000. Rift deflection, migration, and propagation: linkage of the Ethiopian and Eastern rifts, Africa. *GSA Bull.* 112, 163–176. [https://doi.org/10.1130/0016-7606\(2000\)112<163:RDMAPL>2.0.CO;2](https://doi.org/10.1130/0016-7606(2000)112<163:RDMAPL>2.0.CO;2).
- Etheridge, M.A., 1986. On the reactivation of extensional fault systems. *Philos. Trans. Roy. Soc. Lond. Ser. A* 317, 179–194. <https://doi.org/10.1098/rsta.1986.0031>.
- Færseth, R.B., Gabrielsen, R.H., Hurich, C.A., 1995. Influence of basement in structuring of the North Sea Basin, offshore southwest Norway. *Nor. Geol. Tidsskr.* 75, 105–119.
- Fairhead, J.D., Henderson, N.B., 1977. The seismicity of southern Africa and incipient rifting. *Tectonophysics* 41, T19–T26. [https://doi.org/10.1016/0040-1951\(77\)90133-0](https://doi.org/10.1016/0040-1951(77)90133-0).
- Fazlikhani, H., Fossen, H., Gawthorpe, R.L., Faleide, J.I., Bell, R.E., 2017. Basement structure and its influence on the structural configuration of the northern North Sea rift. *Tectonics* 36, 1151–1177. <https://doi.org/10.1002/2017TC004514>.
- Fazlikhani, H., Aagotnes, S.S., Refvem, M.A., Hamilton-Wright, J., Bell, R.E., Fossen, H., Gawthorpe, R.L., Jackson, C.A.L., Rotevatn, A., 2021. Strain migration during multiphase extension, Stord Basin, northern North Sea rift. *Basin Res.* 33, 1474–1496. <https://doi.org/10.1111/bre.12522>.
- Fonseca, J., 1988. The Sou Hills: a barrier to faulting in the central Nevada Seismic Belt. *J. Geophys. Res. Solid Earth* 93, 475–489. <https://doi.org/10.1029/JB093iB01p00475>.
- Fossen, H., Hurich, C.A., 2005. The Hardangerfjord Shear Zone in SW Norway and the North Sea: a large-scale low-angle shear zone in the Caledonian crust. *J. Geol. Soc.* 162, 675–687. <https://doi.org/10.1144/0016-764904-136>.
- Fossen, H., Rotevatn, A., 2016. Fault linkage and relay structures in extensional settings—a review. *Earth Sci. Rev.* 154, 14–28. <https://doi.org/10.1016/j.earscirev.2015.11.014>.
- Fossen, H., Gabrielsen, R.H., Faleide, J.I., Hurich, C.A., 2014. Crustal stretching in the Scandinavian Caledonides as revealed by deep seismic data. *Geology* 42, 791–794. <https://doi.org/10.1130/G35842.1>.
- Fossen, H., Khani, H.F., Faleide, J.I., Ksienzyk, A.K., Dunlap, W.J., 2016. Post-Caledonian extension in the West Norway-northern North Sea region: the role of structural inheritance. *Geol. Soc. Lond., Spec. Publ.* <https://doi.org/10.1144/SP439.6>.
- Franceschini, Z., Cioni, R., Scaillet, S., Corti, G., Sani, F., Isola, I., Mazzarini, F., Duval, F., Erbello, A., Muluneh, A., Brune, S., 2020. Recent volcano-tectonic activity of the Ririba rift and the evolution of rifting in South Ethiopia. *J. Volcanol. Geotherm. Res.* 403, 106989. <https://doi.org/10.1016/j.jvolgeores.2020.106989>.
- Ghosh, N., Hatui, K., Chattopadhyay, A., 2020. Evolution of fault patterns within a zone of pre-existing pervasive anisotropy during two successive phases of extensions: an experimental study. *Geo-Mar. Lett.* 40, 53–74. <https://doi.org/10.1007/s00367-019-00627-6>.
- Giba, M., Walsh, J.J., Nicol, A., 2012. Segmentation and growth of an obliquely reactivated normal fault. *J. Struct. Geol.* 39, 253–267. <https://doi.org/10.1016/j.jsg.2012.01.004>.
- Gibson, G.M., Totterdell, J.M., White, L.T., Mitchell, C.H., Stacey, A.R., Morse, M.P., Whitaker, A., 2013. Pre-existing basement structure and its influence on continental rifting and fracture zone development along Australia's southern rifted margin. *J. Geol. Soc.* 170, 365–377. <https://doi.org/10.1144/jgs2012-040>.
- Gibson, G.M., Meixner, A.J., Withnall, I.W., Korsch, R.J., Hutton, L.J., Jones, L.E.A., Holzschuh, J., Costelloe, R.D., Henson, P.A., Saygin, E., 2016. Basin architecture and evolution in the Mount Isa mineral province, northern Australia: constraints from deep seismic reflection profiling and implications for ore genesis. *Ore Geol. Rev.* 76, 414–441. <https://doi.org/10.1016/j.oregeorev.2015.07.013>.
- Glaas, C., Vidal, J., Genter, A., 2021. Structural characterization of naturally fractured geothermal reservoirs in the central Upper Rhine Graben. *J. Struct. Geol.* 148, 104370. <https://doi.org/10.1016/j.jsg.2021.104370>.
- Gleeson, S.A., Dyardley, B.W., Munz, I.A., Boyce, A.J., 2003. Infiltration of basinal fluids into high-grade basement, South Norway: sources and behaviour of waters and brines. *Geofluids* 3, 33–48. <https://doi.org/10.1046/j.1468-8123.2003.00047.x>.
- Global Volcanism Project, 2013. *Volcanoes of the World*, v. 4.10.3 (15 Oct 2021). <https://doi.org/10.5479/si.GVP.VOTW4-2013>.
- Gouiza, M., Naliboff, J., 2021. Rheological inheritance controls the formation of segmented rifted margins in cratonic lithosphere. *Nat. Commun.* 12, 1–9. <https://doi.org/10.1038/s41467-021-24945-5>.
- Gouiza, M., Paton, D.A., 2019. The role of inherited lithospheric heterogeneities in defining the crustal architecture of rifted margins and the magmatic budget during continental breakup. *Geochem. Geophys. Geosyst.* 20, 1836–1853. <https://doi.org/10.1029/2018GC007808>.
- Haimson, B., 2006. True triaxial stresses and the brittle fracture of rock. In: Dresen, G., Zang, A., Stephansson, O. (Eds.), *Rock Damage and Fluid Transport*, Part I. Birkhäuser Basel, Basel, pp. 1101–1130. https://doi.org/10.1007/3-7643-7712-7_12.
- Handy, M.R., Hirth, G., Bürgmann, R., 2007. Continental fault structure and rheology from the frictional-to-viscous transition downward. In: Handy, M.R., Hirth, G., Hovius, N. (Eds.), *Tectonic Faults: Agents of Change on a Dynamic Earth*. The MIT Press. <https://doi.org/10.7551/mitpress/6703.003.0008>.
- Hansen, J.A., Bergh, S.G., Henningsen, T., 2011. Mesozoic rifting and basin evolution on the Lofoten and Vesterålen Margin, North-Norway; time constraints and regional implications. *Nor. Geol. Tidsskr.* 91, 203–228.
- Healy, D., 2009. Anisotropy, pore fluid pressure and low angle normal faults. *J. Struct. Geol.* 31, 561–574. <https://doi.org/10.1016/j.jsg.2009.03.001>.
- Hecker, S., DeLong, S.B., Schwartz, D.P., 2021. Rapid strain release on the Bear River fault zone, Utah–Wyoming—the impact of preexisting structure on the rupture behavior of a new normal fault. *Tectonophysics* 808, 228819. <https://doi.org/10.1016/j.tecto.2021.228819>.
- Heermance, R., 2003. Fault Structure Control on Fault Slip and Ground Motion during the 1999 Rupture of the Chelungpu Fault, Taiwan. *Bull. Seismol. Soc. Am.* 93, 1034–1050. <https://doi.org/10.1785/0120010230>.
- Heilman, E., Kolawole, F., Atekwana, E.A., Mayle, M., 2019. Controls of basement fabric on the linkage of rift segments. *Tectonics* 38, 1337–1366. <https://doi.org/10.1029/2018TC005362>.
- Henstra, G.A., Berg Kristensen, T., Rotevatn, A., Gawthorpe, R.L., 2019. How do pre-existing normal faults influence rift geometry? A comparison of adjacent basins with contrasting underlying structure on the Lofoten Margin, Norway. *Basin Res.* 31, 1083–1097. <https://doi.org/10.1111/bre.12358>.
- Henza, A.A., Withjack, M.O., Schlische, R.W., 2010. Normal-fault development during two phases of non-coaxial extension: An experimental study. *J. Struct. Geol.* 32, 1656–1667. <https://doi.org/10.1016/j.jsg.2009.07.007>.
- Henza, A.A., Withjack, M.O., Schlische, R.W., 2011. How do the properties of a pre-existing normal-fault population influence fault development during a subsequent phase of extension? *J. Struct. Geol.* 33, 1312–1324. <https://doi.org/10.1016/j.jsg.2011.06.010>.
- Heron, P.J., Peace, A.L., McCaffrey, K., Welford, J.K., Wilson, R., Hunen, J., Pysklywec, R.N., 2019. Segmentation of rifts through structural inheritance: creation of the Davis Strait. *Tectonics*. <https://doi.org/10.1029/2019TC005578>, 2019TC005578.
- Hodge, M., Biggs, J., Goda, K., Aspinall, W., 2015. Assessing infrequent large earthquakes using geomorphology and geodesy: the Malawi Rift. *Nat. Hazards* 76, 1781–1806. <https://doi.org/10.1007/s11069-014-1572-y>.
- Hodge, M., Fagereng, Å., Biggs, J., Mdala, H., 2018. Controls on Early-Rift Geometry: new perspectives from the Bilila-Mtakataka Fault, Malawi. *Geophys. Res. Lett.* 45, 3896–3905. <https://doi.org/10.1029/2018GL077343>.
- Hodge, M., Biggs, J., Fagereng, Å., Mdala, H., Wedmore, L.N.J., Williams, J.N., 2020. Evidence from high-resolution topography for multiple earthquakes on high slip-to-length fault scarps: the Bilila-Mtakataka Fault, Malawi. *Tectonics* 39, 1–24. <https://doi.org/10.1029/2019TC005933>.

- Hoggard, M.J., Czarnota, K., Richards, F.D., Huston, D.L., Jaques, A.L., Ghelichkhan, S., 2020. Global distribution of sediment-hosted metals controlled by craton edge stability. *Nat. Geosci.* 13, 504–510. <https://doi.org/10.1038/s41561-020-0593-2>.
- Holdsworth, R.E., 2004. Weak Faults–Rotten Cores. *Science* 303, 181–182. <https://doi.org/10.1126/science.1092491>.
- Holdsworth, R.E., Butler, C.A., Roberts, A.M., 1997. The recognition of reactivation during continental deformation. *J. Geol. Soc.* 154, 73–78. <https://doi.org/10.1144/gsjgs.154.1.0073>.
- Holdsworth, R.E., Handa, M., Miller, J.A., Buick, I.S., 2001a. Continental reactivation and reworking: an introduction. *Geol. Soc. Lond., Spec. Publ.* 184, 1–12. <https://doi.org/10.1144/GSL.SP.2001.184.01.01>.
- Holdsworth, R.E., Stewart, M., Imber, J., Strachan, R.A., 2001b. The structure and rheological evolution of reactivated continental fault zones: a review and case study. *Geol. Soc. Lond., Spec. Publ.* 184, 115–137. <https://doi.org/10.1144/GSL.SP.2001.184.01.07>.
- Holdsworth, R.E., Selby, D., Dempsey, E., Scott, L., Hardman, K., Fallick, A.E., Bullock, R., 2020. The nature and age of Mesoproterozoic strike-slip faulting based on Re–Os geochronology of syntectonic copper mineralization, Assynt Terrane, NW Scotland. *J. Geol. Soc.* 177, 686–699. <https://doi.org/10.1144/jgs2020-011>.
- Hopper, E., Gaherty, J.B., Shillington, D.J., Accardo, N.J., Nyblade, A.A., Holtzman, B.K., Havlin, C., Scholz, C.A., Chindandali, P.R.N., Ferdinand, R.W., Mulibo, G.D., Mbogoni, G., 2020. Preferential localized thinning of lithospheric mantle in the melt-poor Malawi Rift. *Nat. Geosci.* 13, 584–589. <https://doi.org/10.1038/s41561-020-0609-y>.
- Jackson, J., Blenkinsop, T., 1997. The Bilila-Mtakataka fault in Malawi: an active, 100-km long, normal fault segment in thick seismogenic crust. *Tectonics* 16, 137–150. <https://doi.org/10.1029/96TC02494>.
- Jackson, C.A.L., Rotevatn, A., 2013. 3D seismic analysis of the structure and evolution of a salt-influenced normal fault zone: a test of competing fault growth models. *J. Struct. Geol.* 54, 215–234. <https://doi.org/10.1016/j.jsg.2013.06.012>.
- Jaeger, J.C., Cook, N.G.W., 1979. *Fundamentals of Rock Mechanics*, 3rd ed. Chapman and Hall, London.
- Jaeger, J.C., Cook, N.G.W., Zimmerman, R., 2007. *Fundamentals of Rock Mechanics*, 4th ed. Wiley-Blackwell.
- Karp, T., Scholz, C.A., McGlue, M.M., 2012. Structure and Stratigraphy of the Lake Albert Rift, East Africa: Observations from Seismic Reflection and Gravity Data. In: Baganz, O.W., Bartov, Y., Bohacs, K.M., Nummedal, D. (Eds.), *Lacustrine Sandstone Reservoirs and Hydrocarbon Systems*, AAPG Memoir 95. American Association of Petroleum Geologists, pp. 299–318. <https://doi.org/10.1306/13291394M952903>.
- Katumwehe, A.B., Abdelsalam, M.G., Atekwana, E.A., 2015. The role of pre-existing Precambrian structures in rift evolution: the Albertine and Rhino grabens, Uganda. *Tectonophysics* 646, 117–129. <https://doi.org/10.1016/j.tecto.2015.01.022>.
- Keep, M., McClay, K.R., 1997. Analogue modelling of multiphase rift systems. *Tectonophysics* 273, 239–270. [https://doi.org/10.1016/S0040-1951\(96\)00272-7](https://doi.org/10.1016/S0040-1951(96)00272-7).
- Kinabo, B.D., Atekwana, E.A., Hogan, J.P., Modisi, M.P., Wheaton, D.D., Kampunzu, A.B., 2007. Early structural development of the Okavango rift zone, NW Botswana. *J. Afr. Earth Sci.* 48, 125–136. <https://doi.org/10.1016/j.jafrearsci.2007.02.005>.
- Kirkpatrick, J.D., Bezerra, F.H.R., Shipton, Z.K., Do Nascimento, A.F., Pytharoulis, S.I., Lunn, R.J., Soden, A.M., 2013. Scale-dependent influence of pre-existing basement shear zones on rift faulting: a case study from NE Brazil. *J. Geol. Soc.* 170, 237–247. <https://doi.org/10.1144/jgs2012-043>.
- Kolawole, F., Atekwana, E.A., Laó-Dávila, D.A., Abdelsalam, M.G., Chindandali, P.R., Salima, J., Kalindekaffe, L., 2018. Active deformation of Malawi Rift's North Basin Hinge zone modulated by reactivation of preexisting Precambrian Shear Zone fabric. *Tectonics* 37, 683–704. <https://doi.org/10.1002/2017TC004628>.
- Kolawole, F., Firkins, M.C., Al Wahaihi, T.S., Atekwana, E.A., Soreghan, M.J., 2021a. Rift interaction zones and the stages of rift linkage in active segmented continental rift systems. *Basin Res.* 33, 2984–3020. <https://doi.org/10.1111/bre.12592>.
- Kolawole, F., Phillips, T.B., Atekwana, E.A., Jackson, C.A.L., 2021b. Structural inheritance controls strain distribution during early continental rifting, Rukwa Rift. *Front. Earth Sci.* 9, 1–14. <https://doi.org/10.3389/feart.2021.707869>.
- Kolawole, F., Vick, T., Atekwana, E.A., Laó-Dávila, D.A., Costa, A.G., Carpenter, B.M., 2022. Strain localization and migration during the pulsed lateral propagation of the Shire Rift Zone, East Africa. *Tectonophysics* 839. <https://doi.org/10.1016/j.tecto.2022.229499>.
- Krabbendam, M., Barr, T.D., 2000. Proterozoic orogens and the break-up of Gondwana: why did some orogens not rift? *J. Afr. Earth Sci.* 31, 35–49. [https://doi.org/10.1016/S0899-5362\(00\)00071-3](https://doi.org/10.1016/S0899-5362(00)00071-3).
- Kusznir, N.J., Park, R.G., 1986. Continental lithosphere strength: the critical role of lower crustal deformation. *Geol. Soc. Spec. Publ.* 24, 79–93. <https://doi.org/10.1144/GSL.SP.1986.024.01.09>.
- Laó-Dávila, D.A., Al-Salmi, H.S., Abdelsalam, M.G., Atekwana, E.A., 2015. Hierarchical segmentation of the Malawi Rift: the influence of inherited lithospheric heterogeneity and kinematics in the evolution of continental rifts. *Tectonics* 34, 2399–2417. <https://doi.org/10.1002/2015TC003953>.
- Lathrop, B.A., Jackson, C.A.L., Bell, R.E., Rotevatn, A., 2021. Normal fault kinematics and the role of lateral tip retreat: an example from Offshore NW Australia. *Tectonics* 40. <https://doi.org/10.1029/2020TC006631>.
- Lathrop, B.A., Jackson, C.A.L., Bell, R.E., Rotevatn, A., 2022. Displacement/length scaling relationships for normal faults; a review, critique, and revised compilation. *Front. Earth Sci.* 10, 1–23. <https://doi.org/10.3389/feart.2022.907543>.
- Leclère, H., Fabbri, O., 2013. A new three-dimensional method of fault reactivation analysis. *J. Struct. Geol.* 48, 153–161. <https://doi.org/10.1016/j.jsg.2012.11.004>.
- Lezzar, K.E., Tiercelin, J.-J., Le Turdu, C., Cohen, A.S., Reynolds, D.J., Le Gall, B., Scholz, C.A., 2002. Control of normal fault interaction on the distribution of major Neogene sedimentary depocenters, Lake Tanganyika, East African rift. *AAPG Bull.* 86, 1027–1059.
- Lisle, R.J., Srivastava, D.C., 2004. Test of the frictional reactivation theory for faults and validity of fault-slip analysis. *Geology* 32, 569–572. <https://doi.org/10.1130/G20408.1>.
- Lloyd, R., Biggs, J., Wilks, M., Nowacki, A., Kendall, J.M., Ayele, A., Lewi, E., Eysteinnsson, H., 2018. Evidence for cross rift structural controls on deformation and seismicity at a continental rift caldera. *Earth Planet. Sci. Lett.* 487, 190–200. <https://doi.org/10.1016/j.epsl.2018.01.037>.
- Lovecchio, J.P., Rohais, S., Joseph, P., Bolatti, N.D., Kress, P.R., Gerster, R., Ramos, V.A., 2018. Multistage rifting evolution of the Colorado basin (offshore Argentina): evidence for extensional settings prior to the South Atlantic opening. *Terra Nova* 30, 359–368. <https://doi.org/10.1111/ter.12351>.
- Lyon, P.J., Boul, P.J., Hillis, R.R., Bierbrauer, K., 2007. Basement controls on fault development in the Penola Trough, Otway Basin, and implications for fault-bounded hydrocarbon traps. *Aust. J. Earth Sci.* 54, 675–689. <https://doi.org/10.1080/08120090701305228>.
- Macgregor, D., 2015. History of the development of the East African Rift System: a series of interpreted maps through time. *J. Afr. Earth Sci.* 101, 232–252. <https://doi.org/10.1016/j.jafrearsci.2014.09.016>.
- Maerten, L., Gillespie, P., Pollard, D., 2002. Effects of local stress perturbation on secondary fault development. *J. Struct. Geol.* 24, 145–153. [https://doi.org/10.1016/S0191-8141\(01\)00054-2](https://doi.org/10.1016/S0191-8141(01)00054-2).
- Maestrelli, D., Montanari, D., Corti, G., Del Ventisette, C., Moratti, G., Bonini, M., 2020. Exploring the interactions between rift propagation and inherited crustal fabrics through experimental modeling. *Tectonics* 39, 1–24. <https://doi.org/10.1029/2020TC006211>.
- Maestrelli, D., Brune, S., Corti, G., Keir, D., Muluneh, A.A., Sani, F., 2022. Analog and numerical modeling of rift-rift-rift triple junctions. *Tectonics* 41, 1–27. <https://doi.org/10.1029/2022TC007491>.
- Manatschal, G., Lavier, L., Chenin, P., 2015. The role of inheritance in structuring hyperextended rift systems: Some considerations based on observations and numerical modeling. *Gondwana Res.* 27, 140–164. <https://doi.org/10.1016/j.gr.2014.08.006>.
- Massironi, M., Bistacchi, A., Menegon, L., 2011. Misoriented faults in exhumed metamorphic complexes: rule or exception? *Earth Planet. Sci. Lett.* 307, 233–239. <https://doi.org/10.1016/j.epsl.2011.04.041>.
- McCaffrey, K.J.W., 1997. Controls on reactivation of a major fault zone: the Fair Head–Clew Bay line in Ireland. *J. Geol. Soc.* 154, 129–133. <https://doi.org/10.1144/gsjgs.154.1.0129>.
- McClay, K.R., White, M.J., 1995. Analogue modelling of orthogonal and oblique rifting. *Mar. Pet. Geol.* 12, 137–151. [https://doi.org/10.1016/0264-8172\(95\)92835-K](https://doi.org/10.1016/0264-8172(95)92835-K).
- McConnell, R.B., 1967. The East African Rift System. *Nature* 215, 578–581. <https://doi.org/10.1038/215578a0>.
- McConnell, R.B., 1972. Geological development of the rift system of Eastern Africa. *GSA Bull.* 2549–2572.
- McHarg, S., Elders, C., Cunneen, J., 2019. Normal fault linkage and reactivation, Dampier Sub-basin, Western Australia. *Aust. J. Earth Sci.* 66, 209–225. <https://doi.org/10.1080/08120099.2019.1519848>.
- McLean, M.A., Morand, V.J., Cayley, R.A., 2010. Gravity and magnetic modelling of crustal structure in central Victoria: what lies under the Melbourne Zone? *Australian Journal of Earth Sciences* 57, 153–173. <https://doi.org/10.1080/08120090903416245>.
- Michon, L., Merle, O., 2000. Crustal structures of the Rhinegraben and the Massif Central grabens: an experimental approach. *Tectonics* 19, 896–904. <https://doi.org/10.1029/2000TC900015>.
- Michon, L., Sokoutis, D., 2005. Interaction between structural inheritance and extension direction during graben and depocentre formation: an experimental approach. *Tectonophysics* 409, 125–146. <https://doi.org/10.1016/j.tecto.2005.08.020>.
- Milicich, S.D., Mortimer, N., Villamor, P., Wilson, C.J.N., Chambeform, I., Sagar, M.W., Ireland, T.R., 2021. The Mesozoic terrane boundary beneath the Taupo Volcanic Zone, New Zealand, and potential controls on geothermal system characteristics. *N. Z. J. Geol. Geophys.* 64, 518–529. <https://doi.org/10.1080/00288306.2020.1823434>.
- Miller, J.M.L., Norvick, M.S., Wilson, C.J.L., 2002. Basement controls on rifting and the associated formation of ocean transform faults – Cretaceous continental extension of the southern margin of Australia. *Tectonophysics* 359, 131–155. [https://doi.org/10.1016/S0040-1951\(02\)00508-5](https://doi.org/10.1016/S0040-1951(02)00508-5).
- Milnes, A.G., Wennberg, O.P., Skår, Ø., Koestler, A.G., 1997. Contraction, extension and timing in the South Norwegian Caledonides: the Sognefjord transect. *Geol. Soc. Lond. Spec. Publ.* 121, 123–148.
- Mo, T., Attanayake, J., 2023. Modulation of Seismic Radiation by Fault-Scale Geology of the 2016 Mw 6.0 Shallow Petermann Ranges Earthquake (PRE) in Central Australia. *Bull. Seismol. Soc. Am.* 113, 604–612. <https://doi.org/10.1785/0120220137>.
- Molnar, N.E., Cruden, A.R., Betts, P.G., 2017. Interactions between propagating rotational rifts and linear rheological heterogeneities: insights from three-dimensional laboratory experiments. *Tectonics* 36, 420–443. <https://doi.org/10.1002/2016TC004447>.
- Molnar, N.E., Cruden, A.R., Betts, P.G., 2018. Unzipping continents and the birth of microcontinents. *Geology* 46, 451–454. <https://doi.org/10.1130/G40021.1>.
- Molnar, N.E., Cruden, A.R., Betts, P.G., 2019. Interactions between propagating rifts and linear weaknesses in the lower crust. *Geosphere* 15, 1617–1640. <https://doi.org/10.1130/GES02119.1>.
- Molnar, N., Cruden, A., Betts, P., 2020. The role of inherited crustal and lithospheric architecture during the evolution of the Red Sea: insights from three dimensional

- analogue experiments. *Earth Planet. Sci. Lett.* 544, 116377. <https://doi.org/10.1016/j.epsl.2020.116377>.
- Moore, D.E., Lockner, D.A., 2004. Crystallographic controls on the frictional behavior of dry and water-saturated shear fracture minerals. *J. Geophys. Res.* 109, B03401 <https://doi.org/10.1029/2003JB002582>.
- Morgan, W.J., 1971. Convection plumes in the lower mantle. *Nature* 230, 42–43. <https://doi.org/10.1038/230042a0>.
- Morley, C.K., 1995. Developments in the structural geology of rifts over the last decade and their impact on hydrocarbon exploration. *Hydrocarbon Habitat in Rift Basins* 1–32.
- Morley, C.K., 2010. Stress re-orientation along zones of weak fabrics in rifts: an explanation for pure extension in “oblique” rift segments? *Earth Planet. Sci. Lett.* 297, 667–673. <https://doi.org/10.1016/j.epsl.2010.07.022>.
- Morley, C.K., Wescott, W.A., Stone, D.M., Harper, R.M., Wigger, S.T., Karanja, F.M., 1992. Tectonic evolution of the northern Kenyan Rift. *J. Geol. Soc.* 149, 333–348. <https://doi.org/10.1144/gsjgs.149.3.0333>.
- Morley, C.K., Haranya, C., Phoosongsee, W., Pongwapee, S., Kornawan, A., Wonganan, N., 2004. Activation of rift oblique and rift parallel pre-existing fabrics during extension and their effect on deformation style: examples from the rifts of Thailand. *J. Struct. Geol.* 26, 1803–1829. <https://doi.org/10.1016/j.jsg.2004.02.014>.
- Morris, A., Ferrill, D.A., Henderson, D.B., 1996. Slip-tendency analysis and fault reactivation. *Geology* 24, 275–278. [https://doi.org/10.1130/0091-7613\(1996\)024<0275:STAAFR>2.3.CO;2](https://doi.org/10.1130/0091-7613(1996)024<0275:STAAFR>2.3.CO;2).
- Mortimer, N., 2004. New Zealand’s geological foundations. *Gondwana Res.* 7, 261–272. [https://doi.org/10.1016/S1342-937X\(05\)70324-5](https://doi.org/10.1016/S1342-937X(05)70324-5).
- Mortimer, N., Davey, F.J., Melhuish, A., Yu, J., Godfrey, N.J., 2002. Geological interpretation of a deep seismic reflection profile across the Eastern Province and Median Batholith, New Zealand: crustal architecture of an extended Phanerozoic convergent orogen. *N. Z. J. Geol. Geophys.* 45, 349–363. <https://doi.org/10.1080/00288306.2002.9514978>.
- Muir, R.J., Bradshaw, J.D., Weaver, S.D., Laird, M.G., 2000. The influence of basement structure on the evolution of the Taranaki Basin, New Zealand. *J. Geol. Soc.* 157, 1179–1185. <https://doi.org/10.1144/jgs.157.6.1179>.
- Muir, R.A., Whitehead, B.A., New, T., Stevens, V., Macey, P.H., Groenewald, C.A., Salomon, G., Kahle, B., Hollingsworth, J., Sloan, R.A., 2023. Exceptional scarp preservation in SW Namibia reveals geological controls on large magnitude intraplate seismicity in Southern Africa. *Tectonics* 42. <https://doi.org/10.1029/2022TC007693> e2022TC007693.
- Muirhead, J.D., Kattenhorn, S.A., 2018. Activation of preexisting transverse structures in an evolving magmatic rift in East Africa. *J. Struct. Geol.* 106, 1–18. <https://doi.org/10.1016/j.jsg.2017.11.004>.
- Muirhead, J.D., Wright, L.J.M., Scholz, C.A., 2019. Rift evolution in regions of low magma input in East Africa. *Earth Planet. Sci. Lett.* 506, 332–346. <https://doi.org/10.1016/j.epsl.2018.11.004>.
- Murrell, S.A.F., 1963. A criterion for brittle fracture of rocks and concrete under triaxial stress and the effect of pore pressure on the criterion. In: Fairhurst, C. (Ed.), *Proceedings of the 5th Symposium on Rock Mechanics*. Minneapolis, Minnesota, pp. 563–577.
- Nevitt, J.M., Brooks, B.A., Hardebeck, J.L., Aagaard, B.T., 2023. 2019 M7.1 Ridgecrest earthquake slip distribution controlled by fault geometry inherited from Independence dike swarm. *Nat. Commun.* 14, 1546. <https://doi.org/10.1038/s41467-023-36840-2>.
- Nicol, A., Walsh, J., Berryman, K., Nodder, S., 2005. Growth of a normal fault by the accumulation of slip over millions of years. *J. Struct. Geol.* 27, 327–342. <https://doi.org/10.1016/j.jsg.2004.09.002>.
- Nicol, A., Childs, C., Walsh, J.J., Manzocchi, T., Schöpfer, M.P.J., 2017. Interactions and growth of faults in an outcrop-scale system. *Geol. Soc. Lond., Spec. Publ.* 439, 23–39. <https://doi.org/10.1144/SP439.9>.
- Nixon, C.W., Sanderson, D.J., Dee, S.J., Bull, J.M., Humphreys, R.J., Swanson, M.H., 2014. Fault interactions and reactivation within a normal-fault network at Milne Point, Alaska. *AAPG Bull.* 98, 2081–2107. <https://doi.org/10.1306/04301413177>.
- Norini, G., Carrasco-Núñez, G., Corbo-Camargo, F., Lermo, J., Rojas, J.H., Castro, C., Bonini, M., Montanari, D., Corti, G., Moratti, G., Piccardi, L., Chavez, G., Zuluaga, M. C., Ramirez, M., Cedillo, F., 2019. The structural architecture of the Los Humeros volcanic complex and geothermal field. *J. Volcanol. Geotherm. Res.* 381, 312–329. <https://doi.org/10.1016/j.jvolgeores.2019.06.010>.
- Numelin, T.J., Marone, C., Kirby, E., 2007. Frictional properties of natural fault gouge from a low-angle normal fault, Panamint Valley, California. *Tectonics* 26, 1–14. <https://doi.org/10.1029/2005TC001916>.
- Nutz, A., Ragon, T., Schuster, M., 2022. Cenozoic tectono-sedimentary evolution of the northern Turkana Depression (East African Rift System) and its significance for continental rifts. *Earth Planet. Sci. Lett.* 578, 117285. <https://doi.org/10.1016/j.epsl.2021.117285>.
- Nyblade, A.A., Brazier, R.A., 2002. Precambrian lithospheric controls on the development of the East African rift system. *Geology* 30, 755–758. [https://doi.org/10.1130/0091-7613\(2002\)030<0755:PLCOTD>2.0.CO;2](https://doi.org/10.1130/0091-7613(2002)030<0755:PLCOTD>2.0.CO;2).
- Ogden, C.S., Bastow, I.D., Ebinger, C., Ayele, A., Kounoudis, R., Musila, M., Bendick, R., Mariita, N., Kianji, G., Rooney, T.O., Sullivan, G., Kibret, B., 2023. The development of multiple phases of superposed rifting in the Turkana Depression, East Africa: evidence from receiver functions. *Earth Planet. Sci. Lett.* 609, 118088. <https://doi.org/10.1016/j.epsl.2023.118088>.
- Ojo, O.O., Ohenhen, L.O., Kolawole, F., Johnson, S.G., Chindandali, P.R., Atekwana, E. A., Laó-Dávila, D.A., 2022. Under-displaced normal faults: strain accommodation along an early-stage rift-bounding Fault in the Southern Malawi Rift. *Front. Earth Sci.* 10, 1–19. <https://doi.org/10.3389/feart.2022.846389>.
- Osagiede, E.E., Rotevatn, A., Gawthorpe, R., Kristensen, T.B., Jackson, C.A.L., Marsh, N., 2020. Pre-existing intra-basement shear zones influence growth and geometry of non-colinear normal faults, western Utsira High–Heimdal Terrace, North Sea. *J. Struct. Geol.* 130, 103908. <https://doi.org/10.1016/j.jsg.2019.103908>.
- Osagiede, E.E., Rosenau, M., Rotevatn, A., Gawthorpe, R., Jackson, C.A.L., Rudolf, M., 2021. Influence of zones of pre-existing crustal weakness on strain localization and partitioning during rifting: insights from analog modeling using high-resolution 3D digital image correlation. *Tectonics* 40, 1–30. <https://doi.org/10.1029/2021TC006970>.
- Paton, D.A., 2006. Influence of crustal heterogeneity on normal fault dimensions and evolution: southern South Africa extensional system. *J. Struct. Geol.* 28, 868–886. <https://doi.org/10.1016/j.jsg.2006.01.006>.
- Peace, A., Dempsey, E., Schiffer, C., Welford, J., McCaffrey, K., Imber, J., Phethean, J., 2018a. Evidence for basement reactivation during the opening of the Labrador Sea from the Makkovik Province, Labrador, Canada: insights from field data and numerical models. *Geosciences* 8, 308. <https://doi.org/10.3390/geosciences8080308>.
- Peace, A., McCaffrey, K., Imber, J., van Hunen, J., Hobbs, R., Wilson, R., 2018b. The role of pre-existing structures during rifting, continental breakup and transform system development, offshore West Greenland. *Basin Res.* 30, 373–394. <https://doi.org/10.1111/bre.12257>.
- Petersen, K.D., Schiffer, C., 2016. Wilson cycle passive margins: control of orogenic inheritance on continental breakup. *Gondwana Res.* 39, 131–144. <https://doi.org/10.1016/j.gr.2016.06.012>.
- Petit, C., Déverchère, J., Houdry, F., Sankov, V.A., Melnikova, V.I., Delvaux, D., 1996. Present-day stress field changes along the Baikal rift and tectonic implications. *Tectonics* 15, 1171–1191. <https://doi.org/10.1029/96TC00624>.
- Philippon, M., Willingshofer, E., Sokoutis, D., Corti, G., Sani, F., Bonini, M., Cloetingh, S., 2015. Slip re-orientation in oblique rifts. *Geology* 43, 147–150. <https://doi.org/10.1130/G36208.1>.
- Phillips, T.B., McCaffrey, K.J.W., 2019. Terrane boundary reactivation, barriers to lateral fault propagation and reactivated fabrics: rifting across the Median Batholith Zone, Great South Basin, New Zealand. *Tectonics* 38, 4027–4053. <https://doi.org/10.1029/2019TC005772>.
- Phillips, T.B., Jackson, C.A.L., Bell, R.E., Duffy, O.B., Fossen, H., 2016. Reactivation of intrabasement structures during rifting: a case study from offshore southern Norway. *J. Struct. Geol.* 91, 54–73. <https://doi.org/10.1016/j.jsg.2016.08.008>.
- Phillips, T.B., McCaffrey, K., Magarinos, L., 2022. Influence of variable decoupling between vertically separated fault populations on structural inheritance – The Laminaria High, NW Shelf of Australia. *Basin Res.* 34, 440–456. <https://doi.org/10.1111/bre.12626>.
- Phillips, T.B., Naliboff, J.B., McCaffrey, K.J.W., Pan, S., van Hunen, J., Froemchen, M., 2023. The influence of crustal strength on rift geometry and development – insights from 3D numerical modelling. *Solid Earth* 14, 369–388. <https://doi.org/10.5194/se-14-369-2023>.
- Piqué, A., Laville, E., 1996. The Central Atlantic rifting: reactivation of palaeozoic structures? *J. Geodyn.* 21, 235–255. [https://doi.org/10.1016/0264-3707\(95\)00022-4](https://doi.org/10.1016/0264-3707(95)00022-4).
- Poggi, V., Durrheim, R., Tuluka, G.M., Weatherill, G., Gee, R., Pagani, M., Nyblade, A., Delvaux, D., 2017. Assessing seismic hazard of the East African Rift: a pilot study from GEM and AfricaArray. *Bull. Earthq. Eng.* 15, 4499–4529. <https://doi.org/10.1007/s10518-017-0152-4>.
- Ragon, T., Nutz, A., Schuster, M., Ghienne, J.F., Ruffet, G., Rubino, J.L., 2019. Evolution of the northern Turkana Depression (East African Rift System, Kenya) during the Cenozoic rifting: new insights from the Ekitale Basin (28–25.5 Ma). *Geol. J.* 54, 3468–3488. <https://doi.org/10.1002/gj.3339>.
- Ranalli, G., Yin, Z.M., 1990. Critical stress difference and orientation of faults in rocks with strength anisotropies: the two-dimensional case. *J. Struct. Geol.* 12, 1067–1071. [https://doi.org/10.1016/0191-8141\(90\)90102-5](https://doi.org/10.1016/0191-8141(90)90102-5).
- Reeve, M.T., Bell, R.E., Jackson, C.A.L., 2013. Origin and significance of intra-basement seismic reflections offshore western Norway. *J. Geol. Soc.* 171, 1–4. <https://doi.org/10.1144/jgs2013-020>.
- Reeve, M.T., Bell, R.E., Duffy, O.B., Jackson, C.A.L., Sansom, E., 2015. The growth of non-colinear normal fault systems; what can we learn from 3D seismic reflection data? *J. Struct. Geol.* 70, 141–155. <https://doi.org/10.1016/j.jsg.2014.11.007>.
- Riller, U., Clark, M.D., Daxberger, H., Doman, D., Lenauer, I., Plath, S., Santimano, T., 2017. Fault-slip inversions: their importance in terms of strain, heterogeneity, and kinematics of brittle deformation. *J. Struct. Geol.* 101, B2–B6. <https://doi.org/10.1016/j.jsg.2017.06.013>.
- Rimando, J.M., Peace, A.L., 2021. Reactivation potential of intraplate faults in the Western Quebec Seismic Zone, Eastern Canada. *Earth Space Sci.* 8 <https://doi.org/10.1029/2021EA001825>.
- Ring, U., 1994. The influence of preexisting structure on the evolution of the Cenozoic Malawi rift (East African rift system). *Tectonics* 13, 313–326. <https://doi.org/10.1029/93TC03188>.
- Robertson, E.A.M., Biggs, J., Cashman, K.V., Floyd, M.A., Vye-Brown, C., 2016. Influence of regional tectonics and pre-existing structures on the formation of elliptical calderas in the Kenyan Rift. *Geol. Soc. Spec. Publ.* 43–67. <https://doi.org/10.1144/SP420.12>.
- Roche, V., Childs, C., Madritsch, H., Camanni, G., 2020. Layering and structural inheritance controls on fault zone structure in three dimensions: a case study from the northern Molasse basin, Switzerland. *J. Geol. Soc.* 177, 493–508. <https://doi.org/10.1144/jgs2019-052>.
- Rotevatn, A., Kristensen, T.B., Ksienzyk, A.K., Wemmer, K., Henstra, G.A., Midtkandal, I., Grundvåg, S.A., Andresen, A., 2018. Structural inheritance and rapid rift-length establishment in a multiphase rift: the East Greenland rift system and its Caledonian

- orogenic ancestry. *Tectonics* 37, 1858–1875. <https://doi.org/10.1029/2018TC005018>.
- Rotevatn, A., Jackson, C.A.L., Tvedt, A.B.M., Bell, R.E., Blækkan, I., 2019. How do normal faults grow? *J. Struct. Geol.* 125, 174–184. <https://doi.org/10.1016/j.jsg.2018.08.005>.
- Rowland, J.V., Sibson, R.H., 2004. Structural controls on hydrothermal flow in a segmented rift system, Taupo Volcanic Zone, New Zealand. *Geofluids* 4, 259–283. <https://doi.org/10.1111/j.1468-8123.2004.00091.x>.
- Rowland, J.V., Simmons, S.F., 2012. Hydrologic, magmatic, and tectonic controls on hydrothermal flow, Taupo Volcanic Zone, New Zealand: implications for the formation of epithermal vein deposits. *Econ. Geol.* 107, 427–457. <https://doi.org/10.2113/econgeo.107.3.427>.
- Saalmann, K., Mänttari, I., Nyakecho, C., Isabirye, E., 2016. Age, tectonic evolution and origin of the Aswa Shear Zone in Uganda: activation of an oblique ramp during convergence in the East African Orogen. *J. Afr. Earth Sci.* 117, 303–330. <https://doi.org/10.1016/j.jafrearsci.2016.02.002>.
- Samsu, A., Cruden, A.R., Hall, M., Micklethwaite, S., Denyszyn, S.W., 2019. The influence of basement faults on local extension directions: Insights from potential field geophysics and field observations. *Basin Res.* 31, 782–807. <https://doi.org/10.1111/bre.12344>.
- Samsu, A., Cruden, A.R., Micklethwaite, S., Grose, L., Vollgger, S.A., 2020. Scale matters: the influence of structural inheritance on fracture patterns. *J. Struct. Geol.* 130, 103896. <https://doi.org/10.1016/j.jsg.2019.103896>.
- Samsu, A., Cruden, A.R., Molnar, N.E., Weinberg, R.F., 2021. Inheritance of penetrative basement anisotropies by extension-oblique faults: insights from analogue experiments. *Tectonics* 1–19. <https://doi.org/10.1029/2020tc006596>.
- Sandwell, D., Mellors, R., Tong, X., Wei, M., Wessel, P., 2011. Open radar interferometry software for mapping surface deformation. *EOS Trans. Am. Geophys. Union*. <https://doi.org/10.1029/2011EO280002>.
- Saria, E., Calais, E., Stamps, D.S., Delvaux, D., Hartnady, C.J.H., 2014. Present-day kinematics of the East African Rift. *J. Geophys. Res. Solid Earth* 119, 3584–3600. <https://doi.org/10.1002/2013JB010901>.
- Schiffer, C., Peace, A., Phethean, J., Gernign, L., McCaffrey, K., Petersen, K.D., Foulger, G., 2018. The Jan Mayen microplate complex and the Wilson cycle. *Geol. Soc. Lond., Spec. Publ.* 470. <https://doi.org/10.1144/SP470.2>.
- Schiffer, C., Doré, A.G., Foulger, G.R., Franke, D., Geoffroy, L., Gernign, L., Holdsworth, B., Kuznir, N., Lundin, E., McCaffrey, K., Peace, A.L., Petersen, K.D., Phillips, T.B., Stephenson, R., Stoker, M.S., Welford, J.K., 2020. Structural inheritance in the North Atlantic. *Earth Sci. Rev.* 206, 102975. <https://doi.org/10.1016/j.earscirev.2019.102975>.
- Scholz, C.A., Shillington, D.J., Wright, L.J.M., Accardo, N., Gaherty, J.B., Chindandali, P., 2020. Intrarift fault fabric, segmentation, and basin evolution of the Lake Malawi (Nyasa) Rift, East Africa. *Geosphere* 16, 1293–1311. <https://doi.org/10.1130/GES02228.1>.
- Schumacher, M.E., 2002. Upper Rhine Graben: Role of preexisting structures during rift evolution. *Tectonics* 21. <https://doi.org/10.1029/2001TC900022>, 6–16–17.
- Shaban, S.N., Kolawole, F., Scholz, C.A., 2023. The deep basin and underlying basement structure of the Tanganyika Rift. *Tectonics* 42. <https://doi.org/10.1029/2022TC007726> e2022TC007726.
- Shea, W.T., Kronenberg, A.K., 1993. Strength and anisotropy of foliated rocks with varied mica contents. *J. Struct. Geol.* 15, 1097–1121. [https://doi.org/10.1016/0191-8141\(93\)90158-7](https://doi.org/10.1016/0191-8141(93)90158-7).
- Shillington, D.J., Scholz, C.A., Chindandali, P.R.N., Gaherty, J.B., Accardo, N.J., Onyango, E., Ebinger, C.J., Nyblade, A.A., 2020. Controls on Rift Faulting in the North Basin of the Malawi (Nyasa) Rift, East Africa. *Tectonics* 39. <https://doi.org/10.1029/2019TC005633> e2019TC005633–e2019TC005633.
- Sibson, R.H., 1977. Fault rocks and fault mechanisms. *J. Geol. Soc.* 133, 191–213. <https://doi.org/10.1144/gsjgs.133.3.0191>.
- Sibson, R.H., 1985. A note on local reactivation. *J. Struct. Geol.* 7, 751–754. [https://doi.org/10.1016/0191-8141\(85\)90150-6](https://doi.org/10.1016/0191-8141(85)90150-6).
- Sibson, R.H., 1990. Rupture nucleation on unfavorably oriented faults. *Bull. Seismol. Soc. Am.* 80, 1580–1604. <https://doi.org/10.1785/BSSA08006A1580>.
- Singleton, J.S., Wong, M.S., Johnston, S.M., 2018. The role of calcite-rich metasedimentary mylonites in localizing detachment fault strain and influencing the structural evolution of the Buckskin-Rawhide metamorphic core complex, west-central Arizona. *Lithosphere* 10, 172–193. <https://doi.org/10.1130/L699.1>.
- Smethurst, M.A., 2000. Land-offshore tectonic links in western Norway and the northern North Sea. *J. Geol. Soc.* 157, 769–781. <https://doi.org/10.1144/jgs.157.4.769>.
- Smets, B., Delvaux, D., Ross, K.A., Poppe, S., Kervyn, M., D'Oreye, N., Kervyn, F., 2016. The role of inherited crustal structures and magmatism in the development of rift segments: insights from the Kivu basin, western branch of the East African Rift. *Tectonophysics* 683, 62–76. <https://doi.org/10.1016/j.tecto.2016.06.022>.
- Smith, M., Mosley, P., 1993. Crustal heterogeneity and basement influence on the development of the Kenya Rift, East Africa. *Tectonics* 12, 591–606. <https://doi.org/10.1029/92TC01710>.
- Sokoutis, D., Corti, G., Bonini, M., Pierre Brun, J., Cloetingh, S., Mauduit, T., Manetti, P., 2007. Modelling the extension of heterogeneous hot lithosphere. *Tectonophysics* 444, 63–79. <https://doi.org/10.1016/j.tecto.2007.08.012>.
- Stamps, D.S., Kreemer, C., Fernandes, R., Rajaonarison, T.A., Rambolamanana, G., 2021. Redefining East African Rift System kinematics. *Geology* 49, 150–155. <https://doi.org/10.1130/G47985.1>.
- Stevens, V.L., Sloan, R.A., Chindandali, P.R., Wedmore, L.N.J., Salomon, G.W., Muir, R.A., 2021. The entire crust can be seismogenic: evidence from Southern Malawi. *Tectonics* 40, 1–17. <https://doi.org/10.1029/2020TC006654>.
- Styron, R., Pagani, M., 2020. The GEM global active faults database. *Earthquake Spectra* 36, 160–180. <https://doi.org/10.1177/8755293020944182>.
- Suppe, J., 2014. Fluid overpressures and strength of the sedimentary upper crust. *J. Struct. Geol.* 69, 481–492. <https://doi.org/10.1016/j.jsg.2014.07.009>.
- Sykes, L.R., 1978. Intraplate seismicity, reactivation of preexisting zones of weakness, alkaline magmatism, and other tectonism postdating continental fragmentation. *Rev. Geophys.* 16, 621–688. <https://doi.org/10.1029/RG016i004p00621>.
- Tamas, A., Holdsworth, R.E., Underhill, J.R., Tamas, D.M., Dempsey, E.D., Hardman, K., Bird, A., McCarthy, D., McCaffrey, K.J.W., Selby, D., 2022a. New onshore insights into the role of structural inheritance during Mesozoic opening of the Inner Moray Firth Basin, Scotland. *J. Geol. Soc.* 179. <https://doi.org/10.1144/jgs2021-066>.
- Tamas, A., Holdsworth, R.E., Underhill, J.R., Tamas, D.M., Dempsey, E.D., McCarthy, D.J., McCaffrey, K.J.W., Selby, D., 2022b. Correlating deformation events onshore and offshore in superimposed rift basins: the Lossiemouth Fault Zone, Inner Moray Firth Basin, Scotland. *Basin Res.* 34, 1314–1340. <https://doi.org/10.1111/bre.12661>.
- Theunissen, K., Klerkx, J., Melnikov, A., Mruma, A., 1996. Mechanisms of inheritance of rift faulting in the western branch of the East African Rift, Tanzania. *Tectonics* 15, 776–790. <https://doi.org/10.1029/95TC03685>.
- Thomas, W.A., 2006. Tectonic inheritance at a continental scale. *GSA Today* 16, 4–11.
- TINGAY, M.R.P., Morley, C.K., Hillis, R.R., Meyer, J., 2010a. Present-day stress orientation in Thailand's basins. *J. Struct. Geol.* 32, 235–248. <https://doi.org/10.1016/j.jsg.2009.11.008>.
- TINGAY, M.R.P., Morley, C.K., Hillis, R.R., Meyer, J., 2010b. Present-day stress orientation in Thailand's basins. *J. Struct. Geol.* 32, 235–248. <https://doi.org/10.1016/j.jsg.2009.11.008>.
- Tommasi, A., Vauchez, A., 2001. Continental rifting parallel to ancient collisional belts: an effect of the mechanical anisotropy of the lithospheric mantle. *Earth Planet. Sci. Lett.* 185, 199–210. [https://doi.org/10.1016/S0012-821X\(00\)00350-2](https://doi.org/10.1016/S0012-821X(00)00350-2).
- Tommasi, A., Vauchez, A., 2015. Heterogeneity and anisotropy in the lithospheric mantle. *Tectonophysics* 661, 11–37. <https://doi.org/10.1016/j.tecto.2015.07.026>.
- Tommasi, A., Knoll, M., Vauchez, A., Signorelli, J.W., Thoraval, C., Logé, R., 2009. Structural reactivation in plate tectonics controlled by olivine crystal anisotropy. *Nat. Geosci.* 2, 423–427. <https://doi.org/10.1038/ngeo528>.
- Tranos, M.D., Weber, J.C., Bussey, J., O'Sullivan, P., 2019. Trichonis basin, western central greece: is it an immature basin in the Corinth Rift or a pull-apart in a sinistral rift-trench link? *J. Geol. Soc.* 177, 120–140. <https://doi.org/10.1144/jgs2018-213>.
- Tron, V., Brun, J.P., 1991. Experiments on oblique rifting in brittle-ductile systems. *Tectonophysics* 188, 71–84. [https://doi.org/10.1016/0040-1951\(91\)90315-J](https://doi.org/10.1016/0040-1951(91)90315-J).
- Twiss, R.J., Unruh, J.R., 1998. Analysis of fault slip inversions: do they constrain stress or strain rate? *J. Geophys. Res. Solid Earth* 103, 12205–12222. <https://doi.org/10.1029/98JB00612>.
- Upcott, N.M., Mukasa, R.K., Ebinger, C.J., Karner, G.D., 1996. Along-axis segmentation and isostasy in the Western rift, East Africa. *J. Geophys. Res. Solid Earth* 101, 3247–3268. <https://doi.org/10.1029/95jb01480>.
- Van Hinsbergen, D.J.J., Buitter, S.J.H., Torsvik, T.H., Gaina, C., Webb, S.J., 2011. The formation and evolution of Africa from the Archaean to present: Introduction. *Geol. Soc. Spec. Publ.* 357, 1–8. <https://doi.org/10.1144/SP357.1>.
- Vasconcelos, D.L., Bezerra, F.H.R., Medeiros, W.E., de Castro, D.L., Clausen, O.R., Vital, H., Oliveira, R.G., 2019. Basement fabric controls rift nucleation and postrift basin inversion in the continental margin of NE Brazil. *Tectonophysics* 751, 23–40. <https://doi.org/10.1016/j.tecto.2018.12.019>.
- Vauchez, A., Barruol, G., Tommasi, A., 1997. Why do continents break-up parallel to ancient orogenic belts? *Terra Nova* 9, 62–66. <https://doi.org/10.1111/j.1365-3121.1997.tb00003.x>.
- Versfelt, J., Rosendahl, B.R., 1989. Relationships between pre-rift structure and rift architecture in Lakes Tanganyika and Malawi, East Africa. *Nature* 337, 354–357. <https://doi.org/10.1038/337354a0>.
- Vétel, W., Le Gall, B., Walsh, J.J., 2005. Geometry and growth of an inner rift fault pattern: the Kivu Sogo Fault Belt, Turkana Rift (North Kenya). *J. Struct. Geol.* 27, 2204–2222. <https://doi.org/10.1016/j.jsg.2005.07.003>.
- Vidal, J., Genter, A., 2018. Overview of naturally permeable fractured reservoirs in the central and southern Upper Rhine Graben: insights from geothermal wells. *Geothermics* 74, 57–73. <https://doi.org/10.1016/j.geothermics.2018.02.003>.
- Villamor, P., Nicol, A., Seebeck, H., Rowland, J., Townsend, D., Massiot, C., McNamara, D.D., Milicich, S.D., Ries, W., Alcaraz, S., 2017. Tectonic structure and permeability in the Taupō Rift: new insights from analysis of LiDAR derived DEMs. In: *Proceedings 39th New Zealand Geothermal Workshop*. New Zealand, Rotorua.
- Walsh, J.J., Nicol, A., Childs, C., 2002. An alternative model for the growth of faults. *J. Struct. Geol.* 24, 1669–1675. [https://doi.org/10.1016/S0191-8141\(01\)00165-1](https://doi.org/10.1016/S0191-8141(01)00165-1).
- Wang, K., 2021. If not brittle: ductile, plastic, or viscous? *Seismol. Res. Lett.* <https://doi.org/10.1785/0220200242>.
- Wang, L., Maestrelli, D., Corti, G., Zou, Y., Shen, C., 2021a. Normal fault reactivation during multiphase extension: analogue models and application to the Turkana depression, East Africa. *Tectonophysics* 811, 228870. <https://doi.org/10.1016/j.tecto.2021.228870>.
- Wang, D., Wu, Z., Yang, L., Li, W., He, C., 2021b. Influence of two-phase extension on the fault network and its impact on hydrocarbon migration in the Linnan sag, Bohai Bay Basin, East China. *J. Struct. Geol.* 145, 104289. <https://doi.org/10.1016/j.jsg.2021.104289>.
- Wedmore, L.N.J., Biggs, J., Williams, J.N., Fagereng, Dulanya, Z., Mphepo, F., Mdala, H., 2020a. Active fault scarps in Southern Malawi and their implications for the distribution of strain in incipient continental rifts. *Tectonics* 39. <https://doi.org/10.1029/2019TC005834>.
- Wedmore, L.N.J., Williams, J.N., Biggs, J., Fagereng, Å., Mphepo, F., Dulanya, Z., Willoughby, J., Mdala, H., Adams, B.A., 2020b. Structural inheritance and border fault reactivation during active early-stage rifting along the Thyolo fault, Malawi. *J. Struct. Geol.* 139, 104097. <https://doi.org/10.1016/j.jsg.2020.104097>.

- Wedmore, L.N.J., Biggs, J., Floyd, M., Fagereng, Mdala, H., Chindandali, P., Williams, J. N., Mphepo, F., 2021. Geodetic constraints on cratonic microplates and broad strain during rifting of thick Southern African Lithosphere. *Geophys. Res. Lett.* 48 <https://doi.org/10.1029/2021GL093785>.
- Wedmore, L.N.J., Turner, T., Biggs, J., Williams, J.N., Sichingabula, H.M., Kabumbu, C., Banda, K., 2022. The Luangwa Rift Active Fault Database and fault reactivation along the southwestern branch of the East African Rift. *Solid Earth* 13, 1731–1753. <https://doi.org/10.5194/se-13-1731-2022>.
- Westerhof, A.B.P., Härmä, P., Isabirye, E., Katto, E., Koistinen, T., Kuosmanen, E., Lehto, T., Lehtonen, M.I., Mäkitie, H., Manninen, T., Mänttari, I., Pekkala, Y., Pokki, J., Saalman, K., Virransalo, P., 2014. Geology and geodynamic development of Uganda with explanation of the 1:1,000,000-scale geological map. *Special Paper* 55, 387.
- Wheeler, W.H., Karson, J.A., 1989. Structure and kinematics of the Livingstone Mountains border fault zone, Nyasa (Malawi) Rift, southwestern Tanzania. *J. African Earth Sci. (and the Middle East)* 8, 393–413. [https://doi.org/10.1016/S0899-5362\(89\)80034-X](https://doi.org/10.1016/S0899-5362(89)80034-X).
- Whipp, P.S., Jackson, C.A.L., Gawthorpe, R.L., Dreyer, T., Quinn, D., 2014. Normal fault array evolution above a reactivated rift fabric; a subsurface example from the northern Horda Platform, Norwegian North Sea. *Basin Res.* 26, 523–549. <https://doi.org/10.1111/bre.12050>.
- Wijns, C., Weinberg, R., Gessner, K., Moresi, L., 2005. Mode of crustal extension determined by rheological layering. *Earth Planet. Sci. Lett.* 236, 120–134. <https://doi.org/10.1016/j.epsl.2005.05.030>.
- Williams, J.N., Fagereng, Å., Wedmore, L.N.J., Biggs, J., Mphepo, F., Dulanya, Z., Mdala, H., Blenkinsop, T., 2019. How Do variably striking faults reactivate during rifting? Insights from Southern Malawi. *Geochem. Geophys. Geosyst.* 20, 3588–3607. <https://doi.org/10.1029/2019GC008219>.
- Williams, J.N., Mdala, H., Fagereng, Å., Wedmore, L.N.J., Biggs, J., Dulanya, Z., Chindandali, P., Mphepo, F., 2021. A systems-based approach to parameterise seismic hazard in regions with little historical or instrumental seismicity: active fault and seismogenic source databases for southern Malawi. *Solid Earth* 12, 187–217. <https://doi.org/10.5194/se-12-187-2021>.
- Williams, J.N., Fagereng, Å., Wedmore, L.N.J., Biggs, J., Mdala, H., Mphepo, F., Hodge, M., 2022. Low dissipation of earthquake energy where a fault follows pre-existing weaknesses: field and microstructural observations of Malawi's Bilila-Mtakataka Fault. *Geophys. Res. Lett.* 49, 1–11. <https://doi.org/10.1029/2021GL095286>.
- Wilson, J.T., 1966. Did the Atlantic Close and then Re-open? *Nature* 211, 676–681.
- Wilson, R.W., Holdsworth, R.E., Wild, L.E., McCaffrey, K.J.W., England, R.W., Imber, J., Strachan, R.A., 2010. Basement-influenced rifting and basin development: a reappraisal of post-Caledonian faulting patterns from the North Coast Transfer Zone, Scotland. *Geol. Soc. Lond., Spec. Publ.* 335, 795–826. <https://doi.org/10.1144/SP335.32>.
- Withjack, M., Jamison, W.R., 1986. Deformation produced by oblique rifting. *Tectonophysics* 126, 99–124. [https://doi.org/10.1016/0040-1951\(86\)90222-2](https://doi.org/10.1016/0040-1951(86)90222-2).
- Yale, D.P., 2003. Fault and stress magnitude controls on variations in the orientation of in situ stress. *Geol. Soc. Spec. Publ.* 209, 55–64. <https://doi.org/10.1144/GSL.SP.2003.209.01.06>.
- Yang, H., Quigley, M., King, T., 2021. Surface slip distributions and geometric complexity of intraplate reverse-faulting earthquakes. *GSA Bull.* 133, 1909–1929. <https://doi.org/10.1130/B35809.1>.
- Yardley, B., Gleeson, S., Bruce, S., Banks, D., 2000. Origin of retrograde fluids in metamorphic rocks. *J. Geochem. Explor.* 69, 281–285. [https://doi.org/10.1016/S0375-6742\(00\)00132-1](https://doi.org/10.1016/S0375-6742(00)00132-1).
- Yeomans, C.M., Shail, R.K., Eyre, M., 2020. The importance of tectonic inheritance and reactivation in geothermal energy exploration for EGS resources in SW England. In: *Proceedings World Geothermal Congress 2020, Iceland, Reykjavik*.
- Zang, A., Stephansson, O., 2010. *Stress Field of the Earth's Crust*, 1st ed. Springer Netherlands. <https://doi.org/10.1007/978-1-4020-8444-7>.
- Zhang, J.J., 2019. Abnormal pore pressure mechanisms. In: *Applied Petroleum Geomechanics*. Elsevier, pp. 233–280. <https://doi.org/10.1016/B978-0-12-814814-3.00007-1>.
- Zhang, Y.-Z., Dusseault, M.B., Yassir, N.A., 1994. Effects of rock anisotropy and heterogeneity on stress distributions at selected sites in North America. *Eng. Geol.* 37, 181–197. [https://doi.org/10.1016/0013-7952\(94\)90055-8](https://doi.org/10.1016/0013-7952(94)90055-8).
- Zwaan, F., Schreurs, G., 2017. How oblique extension and structural inheritance influence rift segment interaction: Insights from 4D analog models. *Interpretation* 5, SD119–SD138. <https://doi.org/10.1190/INT-2016-0063.1>.
- Zwaan, F., Schreurs, G., 2020. Rift segment interaction in orthogonal and rotational extension experiments: Implications for the large-scale development of rift systems. *J. Struct. Geol.* 140, 104119. <https://doi.org/10.1016/j.jsg.2020.104119>.
- Zwaan, F., Schreurs, G., 2022. Analogue modeling of continental rifting: an overview. *Continental Rifted Margins* 1, 309–343. <https://doi.org/10.1002/9781119986928.ch6>.
- Zwaan, F., Schreurs, G., Naliboff, J., Buitter, S.J.H., 2016. Insights into the effects of oblique extension on continental rift interaction from 3D analogue and numerical models. *Tectonophysics* 693, 239–260. <https://doi.org/10.1016/j.tecto.2016.02.036>.
- Zwaan, F., Chenin, P., Erratt, D., Manatschal, G., Schreurs, G., 2021a. Complex rift patterns, a result of interacting crustal and mantle weaknesses, or multiphase rifting? Insights from analogue models. *Solid Earth* 12, 1473–1495. <https://doi.org/10.5194/se-12-1473-2021>.
- Zwaan, F., Chenin, P., Erratt, D., Manatschal, G., Schreurs, G., 2021b. Competition between 3D structural inheritance and kinematics during rifting: Insights from analogue models. *Basin Res.* 1–31. <https://doi.org/10.1111/bre.12642>.